

Coding of Touch
in Neurons of the Medicinal Leech
Hirudo medicinalis

Von der Fakultät für Medizin und Gesundheitswissenschaften
der Carl von Ossietzky Universität Oldenburg
zur Erlangung des Grades und Titels
Doktor der Naturwissenschaften (Dr. rer. nat.)
angenommene Dissertation

von Friederice Pirschel
geboren am 02.08.1984
in Wilhelmshaven, Deutschland

Erstgutachterin: Prof. Dr. Jutta Kretzberg

Zweitgutachterin: Prof. Dr. Christine Köppl

Externer Gutachter: Prof. Dr. William B. Kristan

Tag der Disputation: 12.08.2015

Contents

Abbreviations	1
Acknowledgements	2
Summary	3
Zusammenfassung	5
1. Introduction	7
1.1. The medicinal leech: nervous system, coding concepts and local bend behavior	8
1.1.1. The system	8
1.1.2. The behavior	11
1.1.3. The network	14
1.2. The sense of touch	15
1.3. Neuronal coding strategies – an overview	17
2. Aims	20
2.1. Encoding of simple touch stimuli by sensory neurons	20
2.2. Encoding of complex touch stimuli by sensory neurons	21
2.3. Processing of touch stimuli in the local bend network	22
3. Methods	23
3.1. Experiments	23
3.1.1. Preparation	23
3.1.2. Electrophysiological method	24

3.1.3. Stimulation	24
3.1.4. Cell staining	25
3.1.5. Data set	25
3.2. Analysis methods	26
3.2.1. Response features – Sensory neurons	27
3.2.2. Response features – Interneurons	29
3.2.3. Stimulus estimation	29
3.2.3.1. Response feature classes	31
3.2.3.2. Pairwise discrimination	33
3.2.3.3. Classification	33
3.2.3.4. Mutual information	34
3.2.4. Significance tests	34
4. Results	36
4.1. Encoding of simple touch stimuli by sensory neurons	36
4.1.1. Encoding of location	37
4.1.2. Encoding of intensity	41
4.1.3. Encoding of duration	46
4.2. Encoding of complex touch stimuli by sensory neurons	48
4.3. Processing of touch stimuli in the local bend network	53
4.3.1. Influence of touch properties on interneuronal responses	53
4.3.2. Interneuronal response latency	58

4.3.3. Stimulus estimation based on graded response features	60
5. Discussion	65
5.1. Technical limitations	66
5.2. New view on the local bend network	68
5.3. Coding strategies	71
5.3.1. Rate coding versus temporal coding	71
5.3.2. Individual cells versus cell ensembles	72
5.3.3. Separated coding versus multiplexed coding of stimulus properties	73
5.4. Of Worms and Men...	74
6. Publications	76
7. References	96
Contributions of collaborators	106
Curriculum Vitae	107

Figures

Figure 1: The central nervous system of a leech.	10
Figure 2: Receptive field organization and the local bend response.	13
Figure 3: Response features of interneuronal responses to a touch stimulus.	28
Figure 4: Sketch of the stimulus estimation approaches and the estimation process.	31
Figure 5: Influences of touch location on neuronal responses of mechanoreceptors.	38
Figure 6: Estimation results for stimulus location.	39
Figure 7: Influences of touch intensity on neuronal responses of mechanoreceptors.	42
Figure 8: Estimation results for stimulus intensities.	43
Figure 9: Influence of the touch location on intensity discrimination results.	44
Figure 10: Influences of the stimulus duration on neuronal responses of mechanoreceptors.	47
Figure 11: Estimation results for combination of location and intensity.	49
Figure 12: Estimation results for property-dependent cell type feature combinations.	50
Figure 13: Neuronal responses of a left T cell and left P cell to vibrating skin stimulation.	53
Figure 14: Examples of stimulus location and intensity influences on responses of mechanosensory cells and interneurons.	55
Figure 15: Examples of the stimulus influence on amplitude and integral.	56
Figure 16: Connections between cell 157, cell 159 and ipsilateral mechanoreceptors.	57
Figure 17: Examples of stimulus intensity influence on response latencies of INs.	59
Figure 18: Stimulus estimation results for cell 157 response features.	61
Figure 19: Stimulus estimation results for spikelet features of cell 157.	62
Figure 20: Exemplary neuronal responses of several local bend INs to skin stimulation.	64

Tables

Table 1: Varied stimulus properties in the different stimulation protocols.	25
Table 2: Significant changes in response features of the mechanoreceptors due to a location change.	37
Table 3: Significant changes in response features of the mechanoreceptors due to an intensity increase.	41
Table 4: Significant changes in response features of P and T cells due to an duration increase.	46
Table 5: Normalized mutual information of response features with stimulus properties.	52
Table 6: Significant changes in interneuronal response features due to location and intensity changes.	54
Table 7: Normalized mutual information of response features with stimulus properties for cell 157 response features.	60

Abbreviations

A:	Amplitude	PT contra:	Contralateral P cell – T cell
BD:	Burst duration		double recording
BS:	Burst strength	P w/ P:	P cell with P cell combined
C:	(Spike) count	P w/ T:	P cell with T cell combined
CNS:	Central nervous system	RA:	Rapidly adapting
Dur:	Duration	RC:	Relative (spike) count
EPSP:	Excitatory postsynaptic potential	RD:	Response duration
FA1:	Fast adapting type 1	RI:	Relative 1 st interspike interval
FA2:	Fast adapting type 2	RL:	Relative latency
I:	1 st interspike interval	S:	Slope
In:	Integral	SA1:	Slowly adapting type 1
IN(s):	Interneuron(s)	SA2:	Slowly adapting type 2
Int:	Intensity	SC:	Summed (spike) count
ISI:	Interspike interval	SEM:	Standard error of the mean
L:	Latency	SN(s):	Sensory neuron(s)
LBI:	Local bend interneuron	Sp:	Spikelet count
Loc:	Location	STD:	Standard deviation
MN(s):	Motor neuron(s)	T cell:	Touch cell
N cell:	Noxious cell	T-T:	T cell double recording
N-P:	N cell – P cell double recording	T w/ P:	T cell with P cell combined
		T w/ T:	T cell with T cell combined
P cell:	Pressure cell	<u>Units:</u>	
PBS:	Phosphate buffered saline	g:	Gram
PC:	Pacinian	M:	Molar
PFA:	Paraformaldehyde	min:	Minute
P-P:	P cell double recording	mM:	Millimolar
PSP:	Postsynaptic potential	mN:	Millinewton
P-T:	P cell – T cell double recording	ms:	Millisecond
		mV:	Millivolt
PT ipsi:	Ipsilateral P cell – T cell double recording	nA:	Nanoampere
		sec:	Second
		µm:	Micrometer

Acknowledgements

I have heard “the journey is the reward”. Considering that I am still on the journey – I am not able to appraise that completely. But this intermediate goal – or reward – is worth to say thanks.

I would like to thank Prof. Dr. Jutta Kretzberg for this part of scientific journey that she spent with me. Jutta, thank you for discussions, joint projects and all that made this study possible.

Great thanks to Prof. Dr. William B. Kristan and Prof. Dr. Christine Köppl as well as apl. Prof. Dr Karin Dedek for enriching discussions and their support.

I would like to thank my colleagues – actual and former – Lena, Go, Leon and Gerrit in particular. Thanks for laughing, supporting, discussing and keeping it real.

It is only a study, but in reality, it is always a lot of personality in this scientific journey. Because of that, great, great thanks owe to Nadine, Beate and Anne: I am so glad to have you and your lovely families in my life. Thanks for your support!

A big thank you to all of my friends – in the hope that you feel addressed without reading your names! – you made hard times easier for me.

Special thanks and honor to my lovely family, my loving parents and my great siblings: To make this journey with you is truly a reward.

Summary

A fundamental question in neuroscience is how neurons code and process sensory information so that precise behavioral responses arise. Briefly, the goal is to “crack” the code of the neuronal information processing.

In this thesis, a small neuronal network of the leech was investigated in order to reveal the neuronal coding strategies of its extremely precise behavior. The leech possesses one of the smallest neuronal systems with about 10,000 neurons in total, located in a segmented ventral nerve cord with units (ganglia) consisting of about 400 neurons. In response to a touch of the skin, this animal produces a local bend away from the touch with contraction and elongation of muscles. The location accuracy of this behavior is comparable to the human fingertip. Fascinating in this network is the small number of neurons required for this behavior. Three types of mechanosensory neurons are located at the first stage of the neuronal network and code the information about the tactile stimulus: touch (T) cells, pressure (P) cells and noxious (N) cells. A number of studies examined the same behavior and cells involved (Kristan, 1982; Lockery and Kristan, 1990; Lockery and Sejnowski, 1992; Lewis and Kristan, 1998; Zoccolan and Torre, 2002; Baca et al., 2005; Thomson and Kristan, 2006), but still gaps have to be filled between the coding mechanisms and information processing at different network layers.

The first part of this study aimed at investigating the neuronal responses of the mechanosensory cell types to individual touch properties (location, intensity and duration). Based on characteristic response features (e.g., spike count, latency, interspike intervals, etc.) it was analyzed which feature led to the best stimulus estimation performance – i.e., which feature conveyed the most reliable information about the underlying touch property. Thomson and Kristan (2006) found a discrepancy between the encoding (theoretical estimation of the touch location based on neuronal responses elicited by a touch stimulus) and decoding (behavioral location estimation based on simulating natural cell responses induced by intracellular current stimulation) of one cell type – the P cells. However, results of the present thesis revealed that this discrepancy most likely arose from the fact that, in the decoding experiments of Thomson and Kristan (2006), the T cells were not stimulated. This highly sensitive cell type showed extremely accurate responses which allowed precise stimulus estimations. The results show evidence for multiscale coding mechanisms: the location was accurately preserved by a fast

temporal code, while the intensity was conveyed by a rate code – both were represented by cell ensembles rather than single cells. The touch duration could be best estimated based on slow temporal features.

In the second part of this study, it was analyzed how more complex stimuli – combinations of two touch properties: intensity combined with duration and location with intensity - were encoded by these cell types. Linking response features and cell types, location and intensity combinations were almost perfectly estimated. The findings indicated that this neuronal system can encode touch stimuli with a small cell ensemble by use of multiplexing: information of touch properties exists in each cell response (of T and P cells) but more reliable stimulus images were conveyed by a combination of cell types at different time scales (e.g., relative first spike latency vs. summed spike count).

The third part of the study focused on the processing of sensory information in the next stage of the local bend network: the interneurons (see Lockery and Kristan, 1990b). The connections between local bend interneurons and the aforementioned mechanosensory cells as well as their responses to different touch properties were analyzed. Furthermore, stimulus estimation approaches were used for characterizing graded interneuronal responses. The results suggested a more complex local bend network than initially thought: in particular T cells had an influence on the interneurons and also N cells could be involved in the behavior, since they were synaptically linked to the examined interneurons. Significantly different response characteristics among interneuron types to tactile stimulation suggested specialized filter properties like coincidence detection or diverse integration processes.

This thesis provides for the first time a comprehensive picture of coding mechanisms of the leech mechanosensory cells and insights into the processing of sensory information by interneurons of this network. Moreover, despite the simplicity of the neuronal system, the results suggest fundamental coding strategies in somatosensation.

Zusammenfassung

Eine grundlegende Frage der Neurowissenschaften ist es, zu verstehen wie Nervenzellen sensorische Informationen codieren und verarbeiten, so dass ein präzises Verhalten entsteht. Kurz gesagt, Ziel ist es die neuronale Kommunikation zu “knacken”.

In der vorliegenden Arbeit wurde ein kleines neuronales Netzwerk des Blutegels untersucht, mit dem Ziel die Codierungsstrategien für sein präzises Verhalten zu definieren. Der Blutegel besitzt eines der kleinsten neuronalen Systeme mit $\sim 10'000$ Nervenzellen, welche in Untereinheiten (Ganglien) von ~ 400 Nervenzellen in einem segmentierten Strickleiternervensystem untergebracht sind. Eine Berührung der Haut löst bei dem Tier ein lokales Wegbiegen (“Local bend”) des Hautmuskelschlauches aus. Die Genauigkeit dieses Verhaltens ist vergleichbar mit der Zweipunktdiskrimination der menschlichen Fingerspitze. Faszinierend an diesem System ist die kleine Anzahl an Nervenzellen, die für dieses Verhalten benötigt werden. Drei Typen von Mechanorezeptoren codieren auf erster Netzwerkebene Informationen über die Berührung: Touch/“Tast” (T)-Zellen, Pressure/“Druck” (P)-Zellen und Noxious/“Schmerz” (N)-Zellen. In mehreren Studien wurde dieses Verhalten und diese Zellen untersucht (Kristan, 1982; Lockery und Kristan, 1990; Lockery und Sejnowski, 1992; Lewis und Kristan, 1998; Zoccolan und Torre, 2002; Baca et al., 2005; Thomson und Kristan, 2006), aber es gab Lücken in Bezug auf Codierungsmechanismen und Informationsverarbeitung der einzelnen Netzwerkschichten.

Ziel des ersten Teils dieser Studie war es, die neuronalen Antworten der Mechanorezeptoren auf einzelne Druckeigenschaften (Ort, Intensität, Dauer) zu untersuchen. Basierend auf charakteristischen Antwortmerkmalen (z.B. Anzahl der Spikes, Antwortlatenz oder Intervalle zwischen den Spikes) wurde analysiert, welches Merkmal die beste Stimulusschätzung ermöglichte – welches Merkmal also die zuverlässigste Information über die Druckeigenschaft lieferte. Thomson und Kristan (2006) fanden in ihrer Studie, basierend auf neuronalen Antworten eines Zelltypes – den P-Zellen –, eine Diskrepanz zwischen Codierung (theoretische Schätzung des Druckortes basierend auf Antwortmerkmalen der Nervenzellen bei unterschiedlichen Druckorten) und Decodierung (verhaltensbezogene Druckortschätzung basierend auf der Simulation von natürlichen Zellantworten ausgelöst durch Strominjektion in die Zellen). Ergebnisse der vorliegenden Arbeit lassen darauf schließen, dass diese Diskrepanz aus der fehlenden

Stimulation der T-Zellen in den Decodierungsexperimenten folgte. Dieser hochsensitive Zelltyp zeigte extrem genaue Antworten, die eine ausgesprochen präzise Schätzung des Druckortes ermöglichten. Die Resultate dieser Studie liefern Belege für die Nutzung multipler Codierungsmechanismen: der Druckort war höchst exakt enthalten in einem schnellen zeitlichen Code, während die Intensität in einen Ratencode übersetzt wurde – unter Nutzung mehrerer Zellen anstelle einer einzelnen. Die Druckdauer konnte am besten aus langsamen Antwortmerkmalen herausgelesen werden.

Die zweite Studie beschäftigt sich damit wie komplexere Stimulationen – Kombinationen von Druckeigenschaften: Intensität mit Dauer und Ort mit Intensität – durch die Mechanorezeptoren codiert wurden. Eine Verbindung von Antwortmerkmalen und Zelltypen ermöglichte eine fast perfekte Rekonstruktion von Ort-Intensitäts-Kombinationen. Die Ergebnisse lassen auf einen spezialisierten Codierungsmechanismus unter Nutzung von Multiplexing schließen: Informationen über den Druckreiz waren in allen Antworten (von T- und P-Zellen) enthalten, aber ein zuverlässiges Bild wurde erst durch mehrere Zellen und unterschiedliche Zeitskalen (z.B.: Zeit zwischen den ersten Spikes vs. Anzahl der Spikes) überliefert.

Als drittes wird die Informationsverarbeitung der nächsten Netzwerkschicht der Interneurone (siehe: Lockery und Kristan, 1990b) betrachtet. Es wurden Verbindungen zwischen den am Verhalten beteiligten Interneuronen und den Mechanorezeptoren sowie ihre Antworten auf die Druckeigenschaften untersucht. Außerdem wurden mit Hilfe der theoretischen Stimulusschätzung die graduierten Antworten der Interneurone charakterisiert. Die Ergebnisse deuten auf ein komplexeres “Local-bend“-Netzwerk hin als vorher angenommen: die T-Zellen hatten einen Einfluss auf die Interneurone und auch N-Zellen könnten am Verhalten beteiligt sein, da sie ebenfalls synaptische Verbindungen zu den untersuchten Interneurontypen besitzen. Die signifikant unterschiedlichen Antworten der Interneurontypen deuten auf spezialisierte Filtereigenschaften wie Koinzidenzdetektion oder verschiedene Integrationsprozesse hin.

Diese Arbeit liefert zum ersten Mal ein umfassendes Bild zu den Codierungsmechanismen der Mechanorezeptoren des Blutegels und gibt Einblicke in die Verarbeitung auf dem Level von nachgeschalteten Nervenzellen. Zudem weisen die Ergebnisse, trotz der Einfachheit des Systems, auf grundlegende somatosensorische Codierungsstrategien hin.

1. Introduction

Earliest thoughts about the communication of nerve and muscle cells involving electric currents were obtained in the late 18th century by Luigi Galvani, who shaped the term “animal electricity” (see Piccolino, 1997). About 50 years later, the action potential (or “spike”) was initially described as “negative variations” with a directional movement of electricity by Emil du Bois-Reymond (Du Bois-Reymond, 1849; Pearce, 2001). Adrian and Zotterman characterized in the early 20th century the first idea of neuronal coding, when they claimed that the spike count is the decisive factor for stimulus interpretation (Adrian, 1926; Adrian and Zotterman, 1926a, b).

Since then, scientists attempted to interpret this “language” of nerve cells and a number of hypotheses about neuronal coding strategies were added to the pure rate coding approach of Adrian and Zotterman. For instance, Perkel et al. (1967) stated that the temporal arrangement of spikes is not arbitrary but dependent on the stimulus and carries important information.

In the last few decades the knowledge about structures of neuronal networks and neuronal pathways (Engel et al., 2001; Bullmore and Sporns, 2009) have grown enormously. New coding mechanisms were investigated in all sensory systems of various animal models. Besides the above-mentioned debate on rate versus temporal coding (Theunissen and Miller, 1995), coding by individual cells versus cell ensembles were examined (Sakurai, 1996; Pouget et al., 2000) as well as coding of separated stimulus properties versus multiplexed coding of several stimulus properties (Panzeri et al., 2010).

Examinations of these hypotheses require good experimental configurations in which the link between stimulus and behavior can be monitored. And at best, general insights obtained in one system should be transferred to other animals or systems.

In this study, a small neuronal network of the leech *Hirudo medicinalis* with a tight connection between sensory inputs and behavioral outputs was used, in order to test the aforementioned coding hypotheses. Like other invertebrates – the possibly most famous example is the sea slug *Aplysia* with which Eric R. Kandel investigated the neuronal principles of learning (for reviews Kandel, 2001; Kandel et al., 2014) – the nervous system of the leech has several advantages for neuroscientific studies:

- small and easily accessible,
- individually identifiable neurons,
- relatively simple neuronal networks.

The presence of all neuronal cell types in one ganglion makes it possible to observe behavioral responses with only one segment (Kristan et al., 2005; Baca et al., 2005). The leech produces such a locally limited behavior in response to a touch of the skin that could be of a broader scientific relevance because of its remarkable precision and its dependence on various stimulus properties (see 1.1.). These advantages make the leech an ideal model organism for investigating the sense of touch; with the glabrous skin as the sensory organ (see 1.2.).

1.1. The medicinal leech: nervous system, coding concepts and local bend behavior

1.1.1. The system

The medicinal leech *Hirudo medicinalis* possesses one of the smallest neuronal systems with ~ 10,000 neurons in total (Kristan et al., 2005). Its rigorously segmented structure, typical for annelids, is shown in Figure 1. The central nervous system (CNS) is located in the ventral nerve cord, surrounded by the ventral sinus (Fig. 1B) and consists of 21 midbody ganglia plus an anterior and a posterior brain in the sucker region (Fig. 1A). The suckers comprise fused segments and the corresponding ganglia form the brains: four segments form the anterior sucker with the brain and the seven last segments merge into the tail sucker and the posterior brain (Kristan et al., 2005).

The brains coordinate behaviors like swimming, crawling and feeding (Kristan et al., 2005; Puhl and Mesce, 2010) although they have different and sometimes counteracting functions. The anterior brain, for instance, has inhibitory effects on swimming, whereas the posterior brain prolongs swim episodes and counteracts the inhibitory effect of the anterior brain (Brodfuehrer and Friesen, 1986; Brodfuehrer et al., 1993). Brains and ganglia in the nerve cord are connected through a pair of large lateral connectives and a

third smaller connective, the Faivre's Nerve (Kristan et al., 2005). These three interganglionic connectives (Fig. 1A, B) accommodate axons from interneurons and ensure the communication between the segments (Kristan et al., 2005). Each segment comprises five circumferential annuli. The ganglion of the segment is placed under the middle annulus, which also contains sensory end organs, called sensilla (Blackshaw et al., 1982). The sensilla contains different receptors: light-sensitive receptors as well as ciliated mechanosensitive neurons (Kristan et al., 2005). The cilia of the mechanosensitive neurons react to small water movements, which is important for swim triggering (Kristan et al., 2005).

A huge experimental advantage of the nervous system of the leech is its iterative structure: the segmental ganglia are uniformly structured with each other containing about 400 neurons, except ganglia no. 5 and 6 which contain more neurons to control reproductive organs (Zipser, 1979; Kristan et al., 2005). Additionally, all possible types of neurons, sensory and motor neurons (SNs and MNs) as well as interneurons (INs), exist in each ganglion. The neurons of the leech are monopolar: the soma only exhibit one process (Kristan et al., 2005). Synaptic links proceed on fine branches, which emerge from subdivision of the main process. These fine branches lay subjacent in the ganglion, so called the neuropil, in between the ventral and dorsal layers of cell somata (Kristan et al., 2005). Figure 1C shows the ventral side of one segmental ganglion. Six giant glial cells surround the neurons and form the characteristic structure of cell clusters (Fig. 1C; Kristan et al., 2005). Processes from sensory and motor neurons leave the ganglion through the roots and end up in the skin respectively in the muscle layer (Blackshaw, 1981; Blackshaw et al., 1982; Kristan et al., 2005).

The leech possesses three types of mechanosensory cells: the touch (T) cells, the pressure (P) cells and the noxious (N) cells (Nicholls and Baylor, 1968). The characteristic modalities of these sensory neurons were defined by Nicholls and Baylor (1968). They described the cells in detail based on shape, position, physiological properties and their responses to tactile stimulation. They found that each segmental ganglion contains six T cells, four P cells and four N cells (Fig. 1C). The cell types can be clearly distinguished

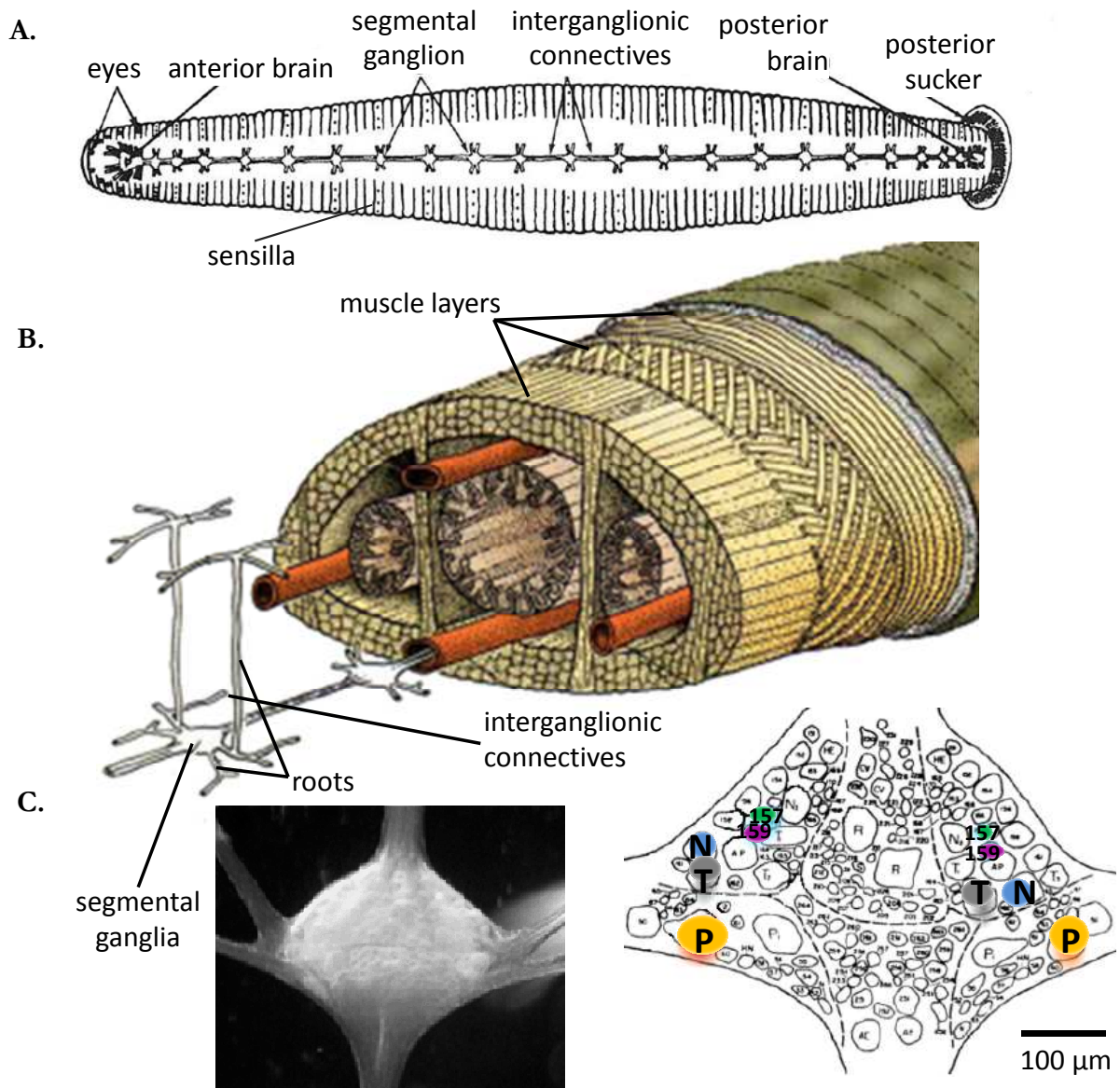


Figure 1: The central nervous system of a leech. **A.** Sketch of the ventral nerve cord of a leech with 21 midbody or segmental ganglia and an anterior and posterior brain. Fused segments form the brains and suckers. The interganglionic connectives connect ganglia in adjacent segments. Each segment comprises of five circumferential annuli. The dots in the middle annulus mark the places of a sensory end organ, called sensilla. Modified from: Kristan et al., 2005. **B.** Cross section of a leech. Ganglia are connected with each other via connectives and each segmental ganglion sends also roots into the skin. The leech body is formed by (from outside): skin followed by layers of circular, oblique and longitudinal muscles. The ends of the dorsoventral muscles are fixed in the longitudinal muscle layer. The ventral nerve cord is surrounded by the ventral sinus (in red brown). Additionally the leech possesses a lateral and dorsal sinus. Modified from: Nicholls et al., 2001, "From Neuron to Brain", p. 294. **C.** Picture (left) and sketch (right) of a segmental ganglion with connectives, roots and cell bodies. Circular edges inside the ganglion contour the somata. Exemplarily, some of the sensory neurons in the sketch are labeled: Pressure ("P") cells in orange, touch ("T") cells in grey, noxious ("N") cells in blue, cell 157 in green and cell 159 in magenta. Dashed lines illustrate the edges of the giant glial cells which form characteristic clusters of neurons in the ganglion. Modified from: Lockery and Kristan, 1990b.

based on the previously mentioned characteristics (Nicholls and Baylor, 1968). The receptive fields of the cells are also robust and distinctly definable: the skin areas where the cells respond to tactile stimulation are equal over several preparations and segments (Nicholls and Baylor, 1968). The receptive fields overlap strongly in anterior-posterior as well as in lateral directions, so that fields of one cell type cover the whole circumference of a segment (Fig. 2A; Nicholls and Baylor, 1968; Yau, 1976; Lewis and Kristan, 1998c). The sensitivity of each cell is highest in the receptive field center and decreases with distance from the center. That is due to the density of nerve endings which the cells develop as receptors on the skin (Nicholls and Baylor, 1968; Blackshaw, 1981; Blackshaw et al., 1982). Because of this structure (Nicholls and Baylor, 1968; Blackshaw, 1981; Blackshaw et al., 1982), the cell soma can also be regarded as an afferent and the nerve endings in the skin as receptors (see 1.2).

The classical concept for touch coding that resulted from the study of Nicholls and Baylor in 1968 was the following: “Each of the three groups of sensory cells responds to a different mechanical stimulus applied to the skin of the ipsilateral body wall. On each side of a ganglion three cells respond to a light touch (the T cells), two to maintained pressure (the P cells), and two to more severe noxious stimuli such as pinching or squeezing (the N cells). The time course of adaptation is characteristic for each type of cell.” (Nicholls and Baylor, 1968, p. 755). Hence, the idea was that the three cell types encode different intensity ranges of touch stimuli. Carlton and McVean (1995) defined more accurate intensity ranges in which each cell type should respond and concluded that T cells are responsible for coding of contact information, whereas P cells mainly respond to local pressure peaks. They also suggested that T cells encode the velocity of skin deformation. N cells have, because of their high pressure thresholds, only little importance for exploration of the environment (Carlton and McVean, 1995).

1.1.2. The behavior

Previous studies on the coding of tactile stimuli by the sensory neurons focused mainly on a behavioral response: the local bend response (see Fig. 2B, C). During the behavior, the leech bends away from the touch (Stuart, 1970; Kristan, 1982; Lockery and Kristan,

1990a, b; Lockery and Sejnowski, 1992; Lewis and Kristan, 1998a, b; Zoccolan and Torre, 2002b; Baca et al., 2005; Thomson and Kristan, 2006) and the magnitude depends on the touch intensity and duration (Baca et al., 2005). The discrimination ability of intensities is better for low touch intensities than for high intensities and additionally improves with longer stimulus durations (Baca et al. 2005). But how these two properties, intensity and duration, are encoded by the mechanoreceptors was unknown.

Interestingly, the local bending behavior of the leech is extremely precise (Baca et al. 2005, Thomson and Kristan, 2006). The animal is able to discriminate behaviorally touch locations that are only 9° of the body circumference apart (Thomson and Kristan, 2006), which means a distance of $500\ \mu\text{m}$ for a typical animal with a circumference of 2 cm.

Thomson and Kristan (2006) investigated how two P cells with ventral receptive fields (Fig. 2A) respond to touch stimuli with an intensity of 200 mN ($\sim 20\ \text{g}$) at different locations. They performed encoding experiments, in which they touched the skin and recorded the neuronal responses of two ventral P cells simultaneously, as well as decoding experiments, in which they stimulated the P cells by current pulses and analyzed elicited muscle movements. They tested the discrimination performance of location distances by means of stimulus estimation and found that the latency difference of the first spikes of two P cells is the best encoder of touch locations (Thomson and Kristan, 2006). With this response feature a distance of 4° ($\sim 222\ \mu\text{m}$ - for a typical leech with 2 cm circumference) could be reliably discriminated, whereas the spike count difference reached a value of 13° ($\sim 722\ \mu\text{m}$) (Thomson and Kristan, 2006). However, the decoding experiments gave a different picture: better results were obtained for the spike count difference with 14° ($\sim 778\ \mu\text{m}$) location distances to be discriminated than for latency differences with 25° ($\sim 1.34\ \text{mm}$) distances (Thomson and Kristan, 2006). Based on these results the authors stated that the “count difference is encoded coarsely and decoded precisely, whereas latency difference is encoded precisely and decoded coarsely” (Thomson and Kristan, 2006, p. 8014). The discrepancy might be explained in connection with T cells being more involved in decoding (Thomson and Kristan, 2006) of behavioral responses than initially thought (Kristan, 1982; Lewis and Kristan, 1998; Zoccolan and Torre, 2002b).

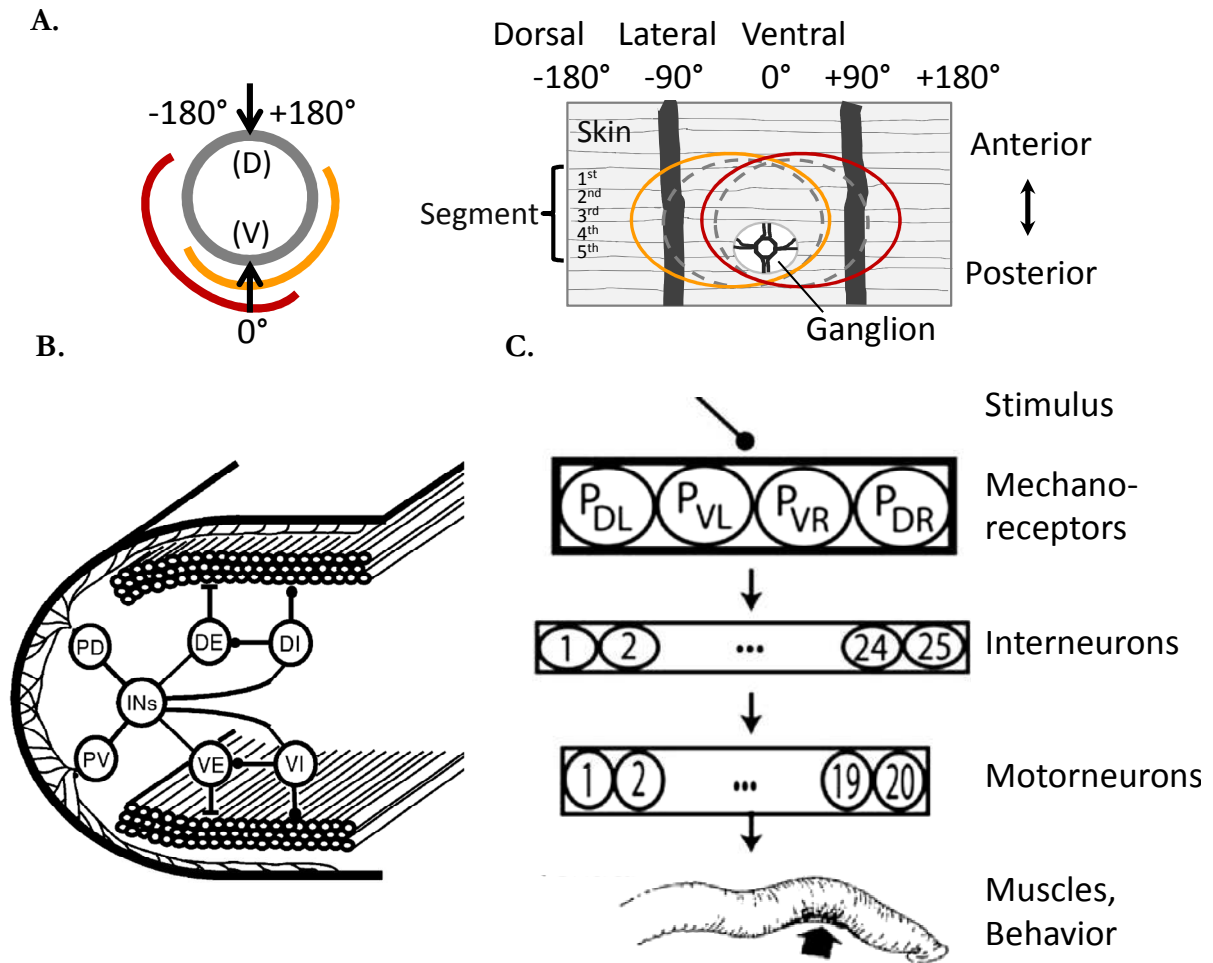


Figure 2: Receptive field organization and the local bend response. **A.** Sketch of the receptive field organization of ventral P cells (in orange and red) and ventral T cells (in grey). The overlap of the fields is exemplarily shown for a circular form (left) and in a sketch of a semi-intact preparation consisting of about three segments, taking the body circumference as 360° (right). 1st to 5th mark the annuli of one segment. The skin was stimulated at the 3rd annulus around 0° . **B.** The local bend circuit (simplified). PD = P cell with dorsal receptive field; PV = P cell with ventral receptive field; INs = Interneurons; VE, VI and DE, DI mark excitatory (E) or inhibitory (I) ventral (V) or dorsal (D) motor neurons. From: Kristan et al., 2005. **C.** The assumed neuronal network for the local bend response. Touching the skin leads to a locally limited bend away from the touch. See Introduction for detailed description. Modified from: Thomson and Kristan, 2006 and Kristan et al., 2005.

Earlier studies showed that T cells are able to elicit the behavior but not so effectively as P cells (Nicholls and Baylor, 1968; Kristan, 1982; Lewis and Kristan, 1998c; Zoccolan and Torre, 2002b), and whether N cells could also play a role remains unsolved (Kristan et al., 2005). As a result, P cells have been regarded as the main trigger for the local bend response and suggested neuronal networks for this behavior included only the P cells (Fig. 2B, C).

1.1.3. The network

The next level of the neuronal network is formed by interneurons (INs) (Figs. 1C, 2B, C) - the largest group of neurons in the leech central nervous system. This cell type sends its processes through the connectives into adjacent ganglia, possesses no direct peripheral connections and processes information from sensory neurons onto motor neurons (Kristan et al., 2005). Several INs are identified and known to be involved in behaviors of the leech: crawling (Eisenhart et al., 2000), swimming (Friesen et al., 1978; Weeks, 1982a, b, c; Friesen, 1985; Brodfuehrer and Friesen, 1986a, b), shortening (Shaw and Kristan, 1995), local bending (Lockery and Kristan, 1990a, b), feeding (Zhang et al., 2000), reproduction (Zipser, 1979) and heartbeat (Thompson and Stent, 1976; Calabrese, 1980). Swimming, crawling, feeding and heartbeat are rhythmic behaviors driven with more complex neuronal networks containing central pattern generators and feedback mechanisms (Shaw and Kristan, 1997; Wilson and Kleinhaus, 2000; Friesen and Kristan, 2007; Puhl and Mesce, 2010), whereas shortening and local bending are reflexive and episodic behaviors with simpler underlying networks (Lockery et al., 1985; Lockery and Kristan, 1990a, b; Lewis and Kristan 1998a, b, c).

In several studies, INs that are involved in the local bend behavior were described and used to evaluate a computational neuronal network model (Lockery et al., 1989; Lockery and Kristan, 1990a, b; Lockery and Kristan, 1991; Lockery and Sejnowski, 1992; Lockery and Sejnowski, 1993a, b; Lewis and Kristan, 1998a, b, c). Nine different INs (eight paired and one unpaired) and their connections were physiologically identified by current stimulation of P cells (Lockery and Kristan, 1990b). It was found that most of these INs receive inputs from ventral as well as dorsal P cells, indicating that the INs are not specialized in only one local bend direction (Fig. 2B). They are activated by a wider range of touch locations mediated by the corresponding mechanoreceptors (Lockery and Kristan, 1990b). The INs send synaptic connections on motor neurons (MNs) that elicit the contraction or elongation of the muscles during the local bend (Lockery and Kristan, 1990a, b). The underlying neuronal network for this behavior (Fig. 2C) was suggested with the optimization of a computational neuronal network model (Lockery et al., 1989; Lockery and Sejnowski, 1992; Lockery and Sejnowski, 1993a, b; Lewis and Kristan,

1998a). The consequential network includes 4 P cells sending their information to about 25 INs which are connected with 8 MNs (Lockery et al., 1989; Lockery and Kristan, 1990b; Lockery and Sejnowski, 1992; Lockery and Sejnowski, 1993a, b; Lewis and Kristan, 1998a). The proposed computational network was purely feedforward containing only excitatory connections (Lockery et al., 1989; Lockery and Sejnowski, 1992; Lockery and Sejnowski, 1993a, b; Lewis and Kristan, 1998a), assuming that inhibitory effects on the muscles are modulated by inhibitory motor neurons and not by inhibitory connections (Kristan et al., 2005; Fig. 2B).

Inhibitory connections were found in lateral connections of mechanosensory cells: P cells and N cells have such connections on T cells (Burgin and Szczupak, 2003) and P cells form inhibitory polysynaptic chemical connections on other cells of the same type (Baltzley et al., 2010). This lateral inhibition on sensory cell level might play a role in localization of the local bend response (Baltzley et al., 2010). Additionally, lateral inhibition among INs of the local bend network was also found (Baca et al., 2008). These results suggest that the local bend network may use balanced excitation and inhibition for gain control with a circuit that is more likely to be feedforward inhibitory than purely excitatory (Baca et al., 2008). This generalized inhibition means that the motor neurons “normally receive a significant level of inhibition that strongly reduces the excitation triggered by the stimulus” (Baca et al., 2008, p. 258).

1.2. The sense of touch

After delineating the leech mechanoreceptors and fundamental ideas about the coding of touch stimuli by these neurons, some facts about the sense of touch in humans and primates should be summarized. Submodalities like shape, texture, motion, grip control, vibration, temperature as well as nociception are encoded by human skin receptors (see: Saal et al., 2014). The glabrous skin of primates contains four types of mechanoreceptors. Slowly adapting type 1 (SA1) afferents end in Merkel cells (about 100 per cm² skin of the fingertip), which are sensitive to static touch and transmit information about the surface or form of an object (Johnson, 2001; Johansson and Flanagan, 2009). This afferent type

shows strong responses to stimulus onset and decreased – or adapted – responses in the sustained phase of the stimulus (Bensmaia, 2008). The slowly adapting type 2 (SA2) afferents finish in Ruffini corpuscles, which innervate the skin less densely than the other mechanoreceptors (Johnson, 2001; Johansson and Flanagan, 2009). This receptor is sensitive to static touch and responds to stretching of the skin (Johnson, 2001; Johansson and Flanagan, 2009).

Rapidly or fast adapting type 1 (RA or FA1) afferents terminate in Meissner corpuscles (about 150 per cm² skin of the fingertip), which are not sensitive to static touch but to movement and vibration (Johnson, 2001; Johansson and Flanagan, 2009). The FA1 afferents respond to transient parts of the stimulus (Bensmaia, 2008) and thus one of the most important functions of these afferents would be the stabilization and control of the grip (Johnson, 2001; Johansson and Flanagan, 2009). Pacinian or fast adapting type 2 (PC or FA2) afferents end in Pacinian corpuscles, which are extremely sensitive to mechanical transients and vibration (Johnson, 2001; Johansson and Flanagan, 2009). Additionally, free nerve endings in the skin transmit information about temperature and nociception (Dykes, 1975). Despite their functional specializations, the different afferents are activated by various stimulations and are involved in several overlapping and multiplexed encoding tasks (Hollins et al., 2002; Bensmaia, 2008; Johansson and Flanagan, 2009; Harvey et al., 2013; Zeveke et al., 2013; Saal et al., 2014).

For human tactile afferents, the relative timing of the first spikes provide information about fingertip force and object shapes (Johansson and Briznieks, 2004). This information is mainly transmitted by FA1 afferents (Johansson and Briznieks, 2004), which also respond to the contact and release of objects (Johansson and Flanagan, 2009). In contrast, intensity perception was suggested to be encoded mainly in weighted firing rates of the three main mechanoreceptive afferents (Muniak et al., 2007; Bensmaia, 2008). Luna et al. (2005) suggested that information for vibrotactile discrimination is most likely to be coded by the firing rate, computed as a weighted spike count in a time window. However, they concluded that temporal properties may play a role for coding by cell ensembles (Luna et al., 2005). A recent study of Harvey et al. (2013) showed that the information about amplitude and frequency of a tactile stimulus are multiplexed in the primate somatosensory cortex. These studies indicate a complex picture of tactile sensation, where

submodalities were not assigned to one mechanosensory type but rather combinations of multiple afferent types are involved in the coding of several submodalities (Saal et al., 2014).

1.3. Neuronal coding strategies – an overview

A suitable stimulation generally evokes a pattern of action potentials in a neuron. After breakthrough discoveries in the late 18th and early 19th century by Luigi Galvani, Giovanni Aldini, Alexander von Humboldt and Emil du Bois-Reymond (Piccolino, 1997; Parent, 2004; Kettenmann, 1997; Du Bois-Reymond, 1843; Pearce, 2001), stimulus-evoked action potentials were found in different sensory systems. Hypotheses about neuronal coding strategies were first described by Adrian and colleagues in the early 20th century (Adrian, 1926; Adrian and Zotterman, 1926a, b; Adrian and Matthews, 1927a, b; 1928). They found, in different animals, correlations between the intensity of a tactile stimulus and the discharge frequency in mechanoreceptors (Adrian, 1926; Adrian and Zotterman, 1926a, b). They also reported that firing rates in the retina increased with light intensity (Adrian and Matthews, 1927a, b; 1928), and described adaptive processes with long or very strong stimuli (Adrian, 1926; Adrian and Zotterman, 1926a, b; Adrian and Matthews, 1927a, b; 1928). In the retina, they also found that the “nerve reaction time” depends on the strength of the stimulus (Adrian and Matthews, 1927a, b; 1928).

These detailed observations from the early 20th century raise crucial points in the debate about neuronal coding: a single stimulus affects several features of a neuronal response and different stimulus properties could affect the same response features. For instance, a rising light intensity or an increasing light area affects the frequency of action potentials as well as the response latencies of the first spikes (or “nerve reaction time”) (Adrian and Matthews, 1927a, b, 1928).

Hence, the questions are: which response features (e.g., spike rate or response latency) carry more or major information about the stimulus? Is a combination of response features the key to sensory encoding? Or is it the combination of cells and cell types?

When one considers the neuron response as a spike train like a Morse code with its own rules, the question of neuronal coding could be simplified to a question like: Is the number of signals more informative than the time of or between these signals or vice versa? For a Morse code, we know that all three features are important to understand (decode) the message: the number of signals, the duration of signals as well as the time between signals. For neuronal spike trains, however, the solution is not so simple at all. First, we have to know to which stimulation – or to which exact stimulus property – the neuron responds: What information should be transferred? Second, how many neurons are affected by the stimulus: So, what is the amount of the transferred information? And we should be aware of the next stage of the information processing: Is the receiving neuron able to decode the features which were used by the sending neuron?

In the last decades, a number of studies focused on these questions and described various types of neuronal code across systems (for a review see: deCharms and Zador, 2000). Gawne and colleagues (1996) investigated the visual system in monkeys and recorded responses of striate cortical complex cells to a set of stimuli that varied in orientation and contrast. They found that the latency and strength (spikes per second) of neuronal responses were influenced differently by the stimulus properties. The latency was strongly influenced by the stimulus contrast, whereas the response strength reflected the stimulus orientation (Gawne et al., 1996). From these observations, they attributed different response features to defined stimulus properties and stated “a more general possibility: the response strength encodes information about the localized features in a scene, whereas temporal variation carries information that is used to help solve the binding problem” (Gawne et al., 1996, p. 1356). However, Shadlen and Newsome (1998) concluded, based on their results about neuronal integration mechanisms, that cortical neurons unlikely transmit information through timing of their spikes. They suggested instead information coding by spike rates of populations of neurons (Shadlen and Newsome, 1998).

In contrast, another approach pointed out that temporal coding might be more important when coding by cell ensembles is considered (Theunissen and Miller, 1995). Panzeri, Petersen and colleagues found that stimulus locations are encoded by the first

poststimulus spikes of a population of neurons in the rat somatosensory cortex (Panzeri et al., 2001; Petersen et al., 2001; Petersen et al., 2002a; Petersen et al., 2002b). And Foffani et al. (2004) suggested that the spike timing is a general property of the rat primary somatosensory cortex and not only used by highly specialized brain regions. Moreover, studies of Di Lorenzo and colleagues verified that in the nucleus tractus solitarius of rats, not only the spike count conveys information about taste stimuli (Di Lorenzo and Victor, 2003, 2007; Di Lorenzo et al., 2009): broadly tuned cells are able to represent a clear image of the taste domain using temporal characteristics of their responses (Di Lorenzo et al., 2009).

Reich and colleagues (2001) showed that, in the primate visual system, information about the contrast is encoded by a temporal – mainly latency – code, supporting the hypothesis of Gawne et al. (1996). They emphasized that “temporal structure of neurons’ responses may extend the dynamic range for contrast encoding” (Reich et al., 2001, p. 1039) and that “information about static features of the stimulus (...) can be multiplexed into the temporal structure of the response” (Reich et al., 2001, p. 1047).

In addition to these studies, evidence for multiplexed encoding was also found in other sensory systems. For instance, in recordings from the anterior piriform cortex in awake, behaving mice, the information about the odor identity and the impact (“value”) was found to be conveyed simultaneously by the neuronal firing pattern (Gire et al., 2013).

Thus, evidence for multiplexing in neuronal responses was found at various different stages of processing (see for review Panzeri et al., 2010 and: Huk, 2012; King and Walker, 2012; Meister et al., 2013; Harvey et al., 2013; Akam and Kullmann, 2014; Saal et al., 2014). The underlying idea is that the neuronal code transmits complementary information through different response features (spike count, latency etc.) that use different temporal scales: “Multiplexing increases the encoding capacity of neural responses, enables disambiguation of stimuli that cannot be discriminated at a single response timescale, and makes sensory representations stable to the presence of variability in the sensory world” (Panzeri et al., 2010, p. 111).

2. Aims

Coding of sensory stimuli is as complex and variable as the studied systems or animals. Regarding neuronal responses, however, the variability and complexity seem to be finite: A limited number of characteristics are qualified to carry information about the stimulus. My aim was to find definite coherences between stimulus properties and spike patterns in one system – may it be ever so simple, but also complex enough to answer questions about fundamental principles of neuronal coding. In order to keep the experimental design as succinct as possible, the relatively simple neuronal system of the leech was used (see 1.1.), where only a few stages of information processing exist between stimulus and behavior.

2.1. Encoding of simple touch stimuli by sensory neurons

Thomson and Kristan (2006) extensively investigated encoding and decoding of touch locations by P cells of the leech. They used a touch stimulus of 200 mN and changed the touch locations in 3° steps (Thomson and Kristan, 2006). Results of the encoding experiments showed coherences between touch location and neuronal response features (Thomson and Kristan, 2006). They found that latency and spike count differences of cell pairs led to different touch location estimations in encoding and decoding experiments: P cells stimulated with specific current pulses could not trigger local bend behaviors with the same precision as touch stimuli applied to the skin (Thomson and Kristan, 2006). To solve this discrepancy, I introduced new aspects into the study (see *Methods* for details):

1. The responses of all three mechanosensory cell types, innervating the ventral area of the skin, were investigated.
2. The list of response features were extended by adding interspike intervals, properties of spike bursts, and combinations of response features.
3. The touch stimulus varied in location, intensity and duration.

It was shown that touch intensity and duration shape the magnitude of the local bend behavior of the leech (Baca et al. 2005), but the encoding of these properties by mechanosensory cells have not been studied so far. Hence, the aim of my study was to investigate how all three mechanosensory cell types respond to a wide range of touch stimuli. I analyzed the neuronal responses using various different stimulus estimation approaches (see 3.2. for details) for defining and studying coding strategies in this small neuronal network. The first part of the study aims to:

- Description of response patterns of all three types of sensory neurons to different stimulus properties
- Identification of coding strategies for single touch properties by means of different stimulus estimation approaches

2.2. Encoding of complex touch stimuli by sensory neurons

Studies of Lewis and Kristan (1998c) and Baca et al. (2005) revealed that the local bend response depends on touch location, intensity and duration. In order to complement these investigations of coding strategies, I examined how combinations of these properties are encoded by the sensory neurons. The aims are:

- Analysis of spike patterns related to combined stimulus properties
- Characterization of coding strategies for complex stimuli

Results of the first two parts of this study are mainly contained in the article “Multiplexed Encoding of Stimulus Properties by Leech Mechanosensory Cells” submitted on 5th May 2015 to the Journal of Neuroscience (JN-RM-1753-15) as well as the Frontiers Research article “Encoding of Tactile Stimuli by Mechanoreceptors and Interneurons of the Leech” (see *Publications* for details).

2.3. Processing of touch stimuli in the local bend network

The coding of touch properties in local bend INs is still not well understood. Lewis (1999) described the receptive fields of local bend INs based on the computational model of the local bend network (Lockery et al., 1989; Lockery and Kristan, 1990a, b; Lockery and Kristan, 1991; Lockery and Sejnowski, 1992; Lockery and Sejnowski, 1993a, b; Lewis and Kristan, 1998a, b, c). To investigate how INs respond to tactile stimuli, I focused on processing of input from all sensory cell types in mainly two local bend INs (cell 157 and 159; see Fig 1C; Lockery and Kristan, 1990b). The mechanoreceptors were stimulated by touch on the skin or current injection and evoked interneuronal responses were analyzed with stimulus estimation approaches (see 3.2. for details) so as to test the assumed neuronal network experimentally. The aims are:

- Characterization of responses of specific local bend INs
- Analysis of connections between sensory neurons and the INs
- Drawing of conclusions from stimulus estimation methods about processing of information in local bend INs

These results are contained in the manuscript “Decoding of Tactile Stimulus Parameters by Interneurons of the Local Bend Network” (planned submission to the Journal of Neurophysiology in June 2015) and the Frontiers Research article “Encoding of Tactile Stimuli by Mechanoreceptors and Interneurons of the Leech” (see *Publications* for details).

3. Methods

3.1. Experiments

3.1.1. Preparation

For this study, adult medicinal leeches *Hirudo medicinalis* from Biebertaler Leech Breeding Farm (Biebertal, Germany) were used. The leeches weighed 1 - 2 g (circumference average 1.96 cm) and were kept in tanks with Ocean Sea Salt 1:1000 diluted with purified water at room temperature. Animals were anesthetized with ice-cold saline (Muller et al., 1981) before and during dissection. Experiments were done at room temperature. In total, 112 preparations were used. The body-wall preparation (Fig. 2A) consisted of mid-body segments 9 to 11 with corresponding ganglia. Innervations of segment 10 remained unscathed. The body-wall was flattened and pinned out, with the epidermis upwards, in a plastic Petri dish, which was coated with a silicone elastomere (Sylgard; Dow Corning Corporation, Midland, MI, USA). In the area of 5th annulus (counted from anterior) of 10th segment, a hole was cut into the skin to provide access to the ganglion. The skin was stimulated at the middle annulus (3rd annulus of segment 10, Fig. 2A), which was identified by location of the sensilla (Blackshaw et al., 1982).

The ventral midline of each preparation was defined as 0°. Touch locations to the left are denoted as negative and to the right as positive numbers of degrees (Fig. 2A). While stimulating the skin mechanically, intracellular recordings (described below) from all three types of sensory cells and two types of interneurons (see *Introduction*) were performed. The mechanosensory cells of *Hirudo medicinalis* have been well-studied and are easily identifiable based on their location in the ganglion, their size and electrical properties (Nicholls and Baylor, 1968). Results and descriptions of Lockery and Kristan (1990b) were utilized for the identification of the local bend INs.

3.1.2. Electrophysiological method

Intracellular recordings were performed from one to three cells at the same time. Sharp glass micropipettes with resistances between 20 and 40 M Ω , filled with 3 M potassium-acetate, were used. Micropipettes contained a filament and had an outer diameter of 1 mm. The glass electrodes were pulled with the micropipette puller model P-97 from Sutter Instruments Co. (Novato, CA, USA).

The experimental rig consisted of three mechanical micromanipulators type MX-1 (Narishige Group, Japan), and three amplifiers (model SEC-05X and BA1S) from NPI electronic (Tamm, Germany). Data were acquired by an interface BNC-2090 with NI PCI-6036E board from National Instruments (Austin, TX, USA). The touch location was controlled by a motorized micromanipulator type DC-3K with controller type MS 314 (Märzhäuser Wetzlar GmbH & Co. KG, Germany). Neuronal responses were recorded (sample rate 10 kHz) with Matlab-based custom-developed software (MathWorks, Version R2009a, Natick, MA, USA) using the Matlab Data Acquisition Toolbox (MathWorks, Natick, MA, USA). The software was developed 2005 and revised 2010 in the group of Prof. Dr. Jutta Kretzberg, University of Oldenburg, Germany. In the years 2010 to 2014, I reworked consistently parts of the software.

3.1.3. Stimulation

For applying touch stimuli onto the skin, a Dual-Mode Lever Arm System (Aurora Scientific, Ontario, Canada, Model 300B) with a poker tip size of 1 mm² was used (see Baca et al., 2005; Thomson and Kristan, 2006). The stimulus was varied in intensity (5 to 200 mN) and location (-20° to +20°, relative to ventral midline, in 5° steps, for the estimations). Touch lasted 200 ms (see Thomson and Kristan, 2005; Lewis and Kristan, 1998) except for the duration encoding experiments, in which stimulus durations of 50, 200 and 500 ms were combined with intensities of 20 and 60 mN at 0° (Table 1). All combinations of stimulus properties were presented 10 – 15 times in pseudo-randomized order.

3.1.4. Cell staining

In order to visualize cell morphologies and points of contact, interneurons and mechanosensory cells were filled through sharp glass electrodes with either 10 mM Alexa-dyes (Invitrogen, Karlsruhe, Germany) and/or 2% Neurobiotin (Vector Labs, Peterborough, UK) in 200 mM KCl. Positive (for Neurobiotin) or negative (for Alexa) currents (2-4nA, 500 ms, 1Hz, 30-60 min) were injected and the ganglion was fixated afterwards in 4% PFA (Sigma, Muenchen, Germany) for up to 1 hour. After washing with 0.1 M PBS (6 x 10 min), the ganglion was incubated overnight at 4°C in 1:1000 Streptavidin (Vector Labs)/PBS/0.5% Triton-X. Next, the ganglion was washed again (6 x 10 min) in PBS and embedded with VectaShield (Vector Labs) on a microscope slide for confocal microscopy. Multiple cell fillings with Alexa-dyes and Neurobiotin (Fig. 16, p. 57) were kindly provided for illustration purposes by Dr. Gerrit Hilgen.

3.1.5. Data set

The numbers of cells used for the statistical evaluation can be found in tables 2, 3, 4 (sensory neurons; p. 37/41/46) and table 6 (interneurons; p. 54).

Stimulus duration was estimated based on 12 P cell and 11 T cell single cell recordings.

The data set for the low intensities consists of 12 P cell and 7 T cell double recordings.

Table 1: Varied stimulus properties in the different stimulation protocols used for stimulus estimation (see Pirschel and Kretzberg, 2015, submitted). Details on analyzed property combinations see also Results 4.2.

Encoding task	Location [°]	Intensity [mN]	Duration [ms]
Location	-20 to +20 in 5° steps	10, 50, N cells: 100	200
Intensities low	0	10, 20, 30, 40, 50	200
Intensities high	0	10, 20, 50, 70, 100	200
Duration	0	60	50, 200, 500
Duration & Intensity	0	20, 60	50, 200, 500
Location & Intensity	-20 to +20 in 10° steps	10, 20, 50	200

For the high intensities the data set involves 5 P cell, 8 T cell, 11 P-T and 7 N-P double recordings. The location estimation by sensory neurons bases on 5 T cell double recordings and 5 P cell double recordings. To approach the full mechanosensory cell ensemble, additionally pooled data of these P and T cell double recordings were used for the estimation of location-intensity combinations (Table 1). For this purpose, features of the 5 P cell double recordings were randomly combined across preparations with the 5 T cell double recordings. Tests revealed that the results of these pooled groups (consisting of 5 pairs each) did not show significant differences ($p < 0.05$, Wilcoxon rank sum test). For testing connections between cell 157 and the mechanoreceptors, 29 double recordings were included in this study: 5 ipsi- and 5 contralateral P cells (for definition see Lockery and Kristan, 1990b), 3 ipsi- and 6 contralateral N cells and 4 ipsi-, 6 contralateral T cells. For cell 159 only 1 ipsilateral combination for each mechanosensory cell type was considered.

The data set for the location estimation consisted of cells 157 (from 6 experiments) which were stimulated at locations -20° to $+20^\circ$ in 5° steps with 50 mN. The results for the intensity estimation were based on 7 cells 157 which were stimulated with intensities between 10 and 50 mN at location 0° .

3.2. Analysis methods

The spike detection was done by the custom-developed software which was also used for data acquisition (see 3.1.2.). The parameters, threshold (in mV), time window (in ms) and artifact window (default value 0.5 ms) were manually set. Spikes were traced when: the membrane potential exceeded the threshold and fell again by half of the peak within the time window. The detection continued in a new interval after the time window in which a spike was determined. Fast artifacts could occur at the end or beginning of current stimuli due to invalid capacity compensations of the electrodes. On that account, no spike was detected when the membrane potential decrease happened during the artifact window. The spike time was defined as the time of the maximum spike amplitude. For further data analyses, I developed in 2010-2014 software which is customized to the tactile stimulation

protocols and enables the analysis of neuronal responses to different stimulus properties and their combinations.

To compare encoding performances of the response features, three approaches that complement each other were utilized. The pairwise discrimination (Thomson and Kristan, 2006; see chapter 3.2.3.2.) was used to estimate the minimum difference between touch locations and intensities. The classification approach (see chapter 3.2.3.3.) was used to quantify how well all experimentally tested stimuli could be classified based on a specific neuronal response feature. To confirm stimulus estimation results, mutual information (see chapter 3.2.3.4.) between stimulus properties and response features was computed.

3.2.1. Response features – Sensory neurons

A cell pair denotes two simultaneously recorded cells. Relative features are computed as values of the left cell minus the right cell. Neuronal responses of the sensory neurons were quantified by the following response features:

- | | |
|---|--|
| A. Spike count: | total number of spikes elicited by a single cell during the stimulation period. |
| B. Relative spike count: | difference of spike counts of a cell pair. |
| C. Summed spike count: | sum of spike counts of a cell pair. |
| D. Latency: | time [ms] between stimulus onset and first spike of one cell. |
| E. Relative latency: | time difference [ms] of the first spikes of a cell pair. |
| F. First interspike interval (1 st ISI): | time difference [ms] between the first and second spike of one cell. |
| G. Relative 1 st ISI: | time difference [ms] of the 1 st ISIs of a cell pair. |
| H. Response duration: | time difference [ms] between the first spike and the last spike of the elicited neuronal response. |
| I. Burst strength: | number of spikes in a burst of one cell. |

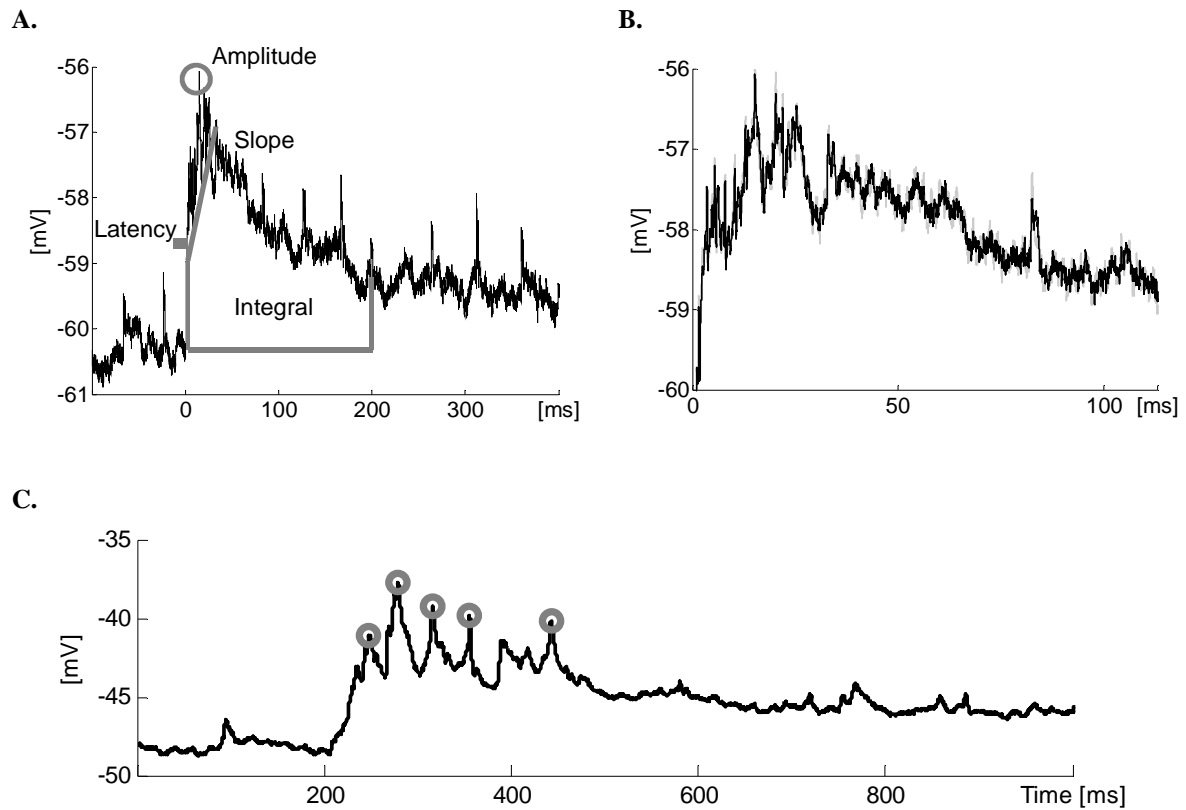


Figure 3: Response features of interneuronal responses to a touch stimulus. **A.** Sketch of the analyzed response features (see text). Touch stimulus from 0 to 200 ms. **B.** Filtered (black) and unfiltered (grey) response part (0 to 100 ms) plotted together. **C.** Detected spikelets with threshold 2 mV and detection window of 15 ms. Touch stimulus from 200 to 400 ms.

J. Burst duration: time difference [ms] between first and last spike in a burst of one cell.

Responses of all mechanoreceptor types were tested for occurrence of bursts. Bursts were identified based on the distribution of interspike intervals. If this distribution was bimodal, a threshold was defined separating burst interspike intervals from longer ISIs (see Oswald et al., 2007). Since only T cells were found to generate bursts (see Figs. 5A, 7A; Baltzley et al., 2010) and showed bimodal distributions of ISIs, results for burst features were only presented for this cell type.

3.2.2. Response features – Interneurons

The INs respond to inputs from the sensory neurons with graded postsynaptic potentials (PSPs) in their somata (Fig. 3). The resting potential of the cell, which is used for the definition of the response features, was computed as the mean of the potential 0 to 1 sec before the stimulation starts. The starting point of a graded interneuronal response was defined as the time point where the membrane potential changed from the resting potential by \pm two-fold standard deviation. In order to avoid the detection of noise-induced, short potential peaks, reference values for latency and maximal amplitude were averaged over a time window of 5 ms. Time windows for slope and integral depended on potential shape and stimulation time. Thus, the interneuronal responses were quantified by the following features:

K. Latency:	time [ms] between stimulus onset and starting point of the interneuronal response.
L. Slope:	increase/ decrease of the signal from start of the response to start time plus 30 ms.
M. Integral:	area under the graded signal from start of response to start time plus 200 ms.
N. Maximal amplitude:	potential difference [mV] between the cell's resting potential and the maximum value of the response.
O. Spikelets:	Detection features: threshold of 2 mV and 15 ms time window (see 3.1.6.). Definition of spikelet features was like spike features - A., D., and F. - of sensory neurons (see 3.2.1.).

3.2.3. Stimulus estimation

The idea of stimulus estimation is to calculate how well the underlying, or presented, stimulus can be predicted based on neuronal responses. This method should provide an insight into potential encoding strategies which may be used by the neuronal system.

Here, I used two different estimation approaches that based on the maximum likelihood method (Aldrich, 1997) with a “leave one out” validation (Quiñ Quiroga and Panzeri, 2009). Moreover, the mutual information (see 3.2.3.4) was computed to verify the consistence of the estimation results.

Basically, the maximum likelihood method predicts the presented stimulus that most likely elicited the neuronal response. The neuronal responses were “separated” into response features (e.g., spike count, response latency), and the presented stimulus was described by its properties (e.g., touch location). The estimation was expected to reveal specific response features as encoder for the presented stimulus property. The “leave one out” validation was used for the definitions of test data and training data: each trial was used separately as test trial, while the remaining trials comprised the training data set. For the training data set, it was known which stimulus elicited the response. This knowledge provided the basis for the estimation. At the next step, the test trial was assigned to the stimulus (= predicted stimulus), based on the training data which elicited its response feature value most probable. The results related the predicted stimulus with the presented stimulus. For instance, 100% correct estimation means that all predicted stimuli matched the presented stimuli. In the special case that several stimuli elicited the test value with the same probability, the test trial was assigned to each of them to equal parts. This procedure was performed for all response features of all cells and their combinations.

Based on these ideas, I used two different estimation approaches: a pairwise discrimination (see Thomson and Kristan, 2006) and a classification. Main difference of these approaches was the number of tested stimuli. The pairwise discrimination compared two stimuli and provided an insight into the discriminability threshold of stimulus property differences. These results were also comparable to results from the Thomson and Kristan study (2006). In contrast, multiple values of a stimulus property were compared in the classification (e.g., at 9 locations between -20° and $+20^\circ$ with differences of 5°). Results of this approach indicated how well property amounts could be distinguished from others.

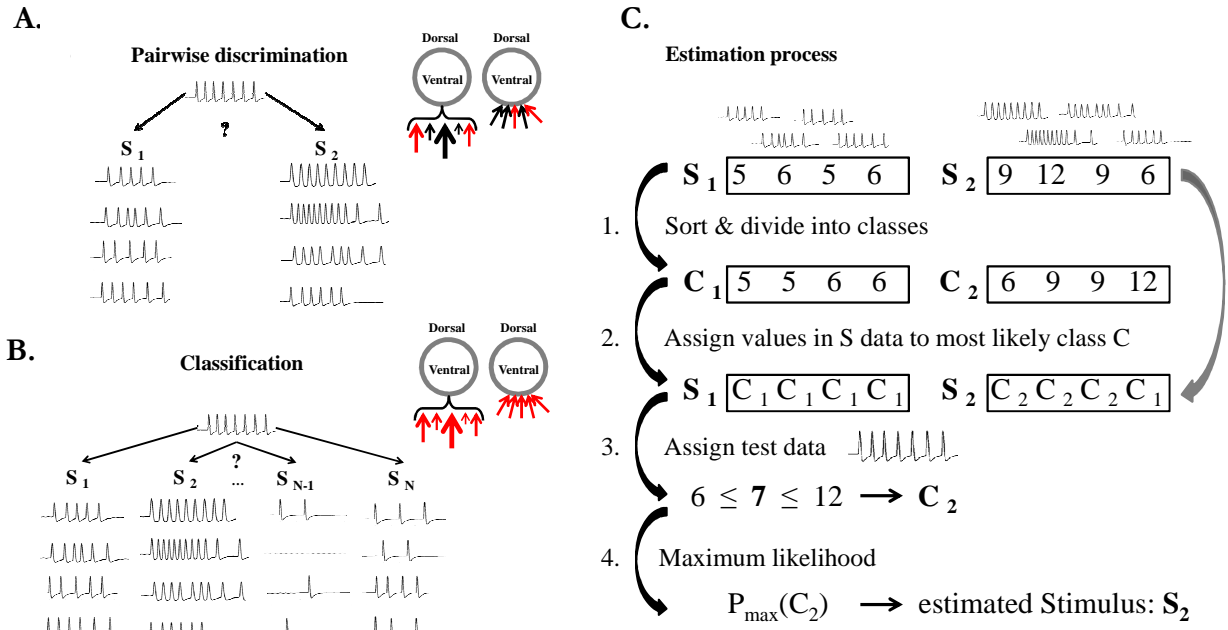


Figure 4: Sketch of the stimulus estimation approaches and the estimation process (see text). **A.** Pairwise discrimination task: the stimulus is estimated based on response features evoked by two different stimuli. Red arrows indicate exemplarily the estimated stimulus intensities (left) or locations (right) in one iteration of the discrimination task. **B.** Classification task: the stimulus is estimated based on response features evoked by a set of N stimuli. Red arrows indicate exemplarily classified stimulus intensities (left) or locations (right). **C.** Sketch of the stimulus estimation process. S = Training data set elicited by stimulus number N ; C = Response feature rank class. Top: examples of neuronal responses for two stimulus conditions and their spike counts. 1. Absolute values of spike counts in S were sorted and divided into response feature classes C (n = number of stimulus conditions). 2. Each value in S was assigned to the most probable response feature class C . 3. The most probable response feature class of the test trial was determined based on the borders of the classes. 4. The most probable stimulus class was defined based on the response feature class of the test trial.

3.2.3.1. Response feature classes

Response feature classes are used for stimulus estimation. Variations in statistical properties of the response features, however, caused difficulties for the analysis of response classifications: the spike count had only integer numbers < 20 , while the latency and interspike intervals were continuous variables and the relative features encompassed also negative numbers.

A definition of classes based on absolute values, for instance, could lead to varied class numbers higher or lower than the number of presented stimuli: when fewer classes than the stimuli were defined, the values in one response feature class could be elicited by two (or more) different stimuli and vice versa. This systematic error biases the results:

continuous variables, e.g., the latency, have more often greater numbers of classes with this method, while the spike counts are more likely to be divided into fewer groups than stimuli. These problems were solved by setting the number of classes equal to the number of presented stimuli and by using ranks rather than absolute values:

1. For each response feature, based on the training data set $S_{\{1,\dots,N\}}$, the rank classes $C_{\{1,\dots,N\}}$ ($N =$ number of presented stimuli) were determined. The absolute values of S were first sorted and then divided into equally sized classes C (Fig. 4C, step 1). For feature combinations, this step was made for both features, so that two training data sets and two corresponding sets of rank classes exist.
2. The absolute values of the (unsorted) training data set S were assigned according to its rank to the most likely class C (Fig. 4C, step 2). If more than one class contained the same response feature value (e.g., a spike count of 6; Fig. 4C), this value was assigned to the class with the highest number of occurrences (maximum likelihood; Fig. 4C, step 2: the spike count of 6 in S_2 was assigned to C_2). If two or more classes were equally probable to elicit the specific value, one of them was chosen by chance. Outputs are new training data sets containing ranks rather than absolute values (Fig. 4C, 3rd row: $C_1 = 1$; $C_2 = 2$ as rank values).

For feature combinations, these training data sets were summed, so that the result was one training data set S consisting of summed rank values.

For example, a combination of spike counts (SC) and latencies (L):

$SC_1 = [1; 1; 2; 1; 2]$; $L_1 = [2; 2; 1; 1; 1]$; $SC_1 \& L_1 = [3; 3; 3; 2; 3]$, and so on.

This combined training data set ($SC_{\{1,\dots,N\}} \& L_{\{1,\dots,N\}}$) could be used for further analysis in the same way as for single feature response classes.

3. In the same way, the test trial was assigned to the most probable response feature class C (Fig. 4C, step 3). If more than one class contained the same response feature value: see procedure in step 2.
4. The determined class C of the test trial was then assigned to the stimulus which evoked this class C most probably (Fig. 4C, step 4).

Finally, a confusion matrix (Quiñ Quiroga and Panzeri, 2009) was calculated, showing how well presented stimulus and predicted stimulus match. The more entries are in the diagonal, the better is the stimulus estimation (Quiñ Quiroga and Panzeri, 2009).

This procedure was used for all response features A.-H. (sensory neurons) and K.-N. (interneurons) individually and in all possible pairwise combinations for all cell types. For T cells, burst strength (I.) in combination with burst duration (J.) and with relative latency (E.) as a feature pair were additionally analyzed.

3.2.3.2. Pairwise discrimination

The pairwise discrimination (Fig. 4A) deals with the question how well two stimuli can be discriminated based on specific response features. This approach reveals the minimum differences between intensities or locations, which can be discriminated using the neuronal responses. Results are presented as mean values with standard errors of the means (SEM) and fitted with a logistic function. Chance level of pairwise discrimination was 0.5 and discrimination threshold was defined as 0.75, which corresponded to 75% correct estimation (Johnson and Philips, 1981; Thomson and Kristan, 2006).

3.2.3.3. Classification

The idea of the classification approach is to quantify how well a set of N stimuli can be estimated based on a specific response feature (Fig. 4B). The test trial was assigned to values of the complete stimulus set. Results are given in % correct and displayed in boxplots (see *Results*), in which black dots mark the median values and box edges the 25th and 75th percentiles. Whiskers show minimum and maximum data values, which were not considered as outliers. Outliers are plotted as individual points and defined as:

$$x > q_3 + 1.5(q_3 - q_1) \quad \text{or} \quad x < q_1 - 1.5(q_3 - q_1),$$

where q_1 is the 25th and q_3 the 75th percentile (standard Matlab boxplot function). Since in our data set all stimuli were presented equally often, the chance level for this method was defined as $100/N$ %. With the classification approach, the stimulus properties location, intensity and duration (see Table 1) were analyzed, as well as the combination of stimulus properties. Three durations (50, 200 and 500 ms) were combined with two intensities (20 and 60 mN) and furthermore, three locations ($-20^\circ / 0^\circ / +20^\circ$) with two

intensities (10 / 50 mN). Additional experiments were performed with up to three intensities (10 / 20 / 50 mN) and five locations (-20° / -10° / 0° / +10° / +20°).

3.2.3.4. Mutual information

Furthermore, the mutual information (Cover and Thomas, 2006; Quian Quiroga and Panzeri, 2009) of all possible pairs of response features with stimulus properties in bits was computed:

$$I(X, Y) = \sum_{x,y} p(x, y) \log_2 \left(\frac{p(x,y)}{p(x)p(y)} \right),$$

where X denotes the stimulus property and Y the observed neuronal response feature. $p(x, y)$ is the joint probability distribution function of X and Y ; $p(x)$ and $p(y)$ are the marginal probability distribution of X and Y , respectively. Numbers of repetitions and stimuli have influences on the maximal information for each response feature. To allow a comparison of results, the values in the corresponding tables are normalized by the maximal information.

3.2.4. Significance tests

Significant influences of stimulus properties on neuronal response features were identified with the Kruskal-Wallis significance test (Gibbons, 1985; Hollander and Wolfe, 1999), a non-parametric version of the one-way analysis of variance (ANOVA). This test compares medians of independent samples from two or more groups. Unless stated otherwise, the significance level for the test was $p < 0.001$. A significance level of $p < 0.05$ was used for the features of the N cells, because of the low firing rate of this cell type. The value for $p < 0.05$ was regarded as “significant” and $p < 0.001$ as “highly significant”.

Significant differences between classification results were tested with the Wilcoxon rank sum test (equivalent to a Mann-Whitney U-test; see: Gibbons, 1985; Hollander and Wolfe, 1999), where null hypothesis is that two independent data sets are from identical

distributions with equal medians ($p < 0.05$ “significant”; $p < 0.001$ “highly significant”). For pairwise discrimination, a one tailed t-test with $p < 0.05$ was applied to define which discrimination results were significantly above the performance threshold of 0.75 (75% correct).

The Kolmogorov-Smirnov test was used to investigate significant membrane potential changes of interneurons in response to spikes of mechanosensory cells. The null hypothesis was that the data sets were from the same continuous distribution ($p < 0.05$). All tests were performed with the Matlab Statistics Toolbox (Matlab version 7.8.0 (R2009a), MathWorks, Natick, MA, USA).

4. Results

The three mechanosensory cell types of the leech are generally well defined and described (see *Introduction*). What is missing is a systematical investigation of their ability to respond to different touch properties and a broad overview of changes in their response features. Moreover, it is mostly unknown how the sensory responses are processed in the postsynaptic INs. The results presented here provide a detailed description of the coding strategies of the mechanosensory cell types to simple and more complex tactile stimulations. A description of these findings is also given in the submitted manuscript (see *Publications*). In addition, the study provided first insights into the mechanisms of the next network level and unveiled a new view on the local bend network.

4.1. Encoding of simple touch stimuli by sensory neurons

This study gives for the first time a detailed insight into the response characteristics of all three types of mechanoreceptors to a broad range of tactile stimuli. The touch location, the intensity as well as the duration was varied. Furthermore, the analysis of the neuronal responses combines three complementary approaches (see *Methods*): a pairwise discrimination, a classification and the mutual information between stimulus properties and response features. These methods revealed fundamental principles of coding strategies for the different touch properties.

Distinctly different spiking patterns were generated by each of the cell types in response to a touch stimulus. P cells responded in a sustained way with spikes of large amplitudes, while T cells generated small and fast spikes in a phasic manner (Figs. 5A, 7A, 10A). Remarkably, T cells showed on- and off-bursts in response to the touch (Figs. 5A, 7A, 10A; see Baltzley et al., 2010). Typical attributes of N cell spikes were a long duration combined with a large afterhyperpolarization (Figs. 5A, 7A). This cell type generated noticeably less spikes than the other two cell types in response to the stimuli used here (Figs. 5, 7).

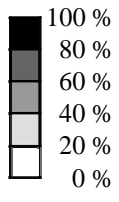
4.1.1. Encoding of location

The touch location affected the P cell responses (Fig. 5A, C): The response latency increased significantly with increasing distance to the center of receptive field, whereas the spike count significantly decreased (Table 2). The T cell response features showed similar dependencies (Fig. 5A, B). Both cell types showed a small variance across trials in latencies compared to spike counts (Fig. 5B, C). The variation of T cell latencies over trials at each touch location was even in the range of 1 ms (Fig. 5B). Instead, the 1st ISI of both cell types was less strongly influenced by the touch location (Table 2). The results for the P cells are in line with the study of Thomson and Kristan (2006) even though stimuli of lower intensities were used here. Responses of the third cell type, the N cells, suggest the same effects of touch location changes (Table 2), although for this cell type higher touch intensities were needed. N cells generated only one spike for intensities around 100 mN (see Fig. 7B), which made the analysis of a location influence on interspike intervals unfeasible.

To illustrate the encoding performance of P and T cell response features, two different stimulus estimation approaches were used (Fig. 6). From all response features (see *Methods*) and possible combinations, the relative response latency gained the highest values for the classification, the pairwise discrimination as well as for the mutual information (Fig. 6, Table 5) (see Pirschel and Kretzberg, 2013; Kretzberg et al., 2015). For a stimulus of 50 mN, this feature results are significantly above the remaining features

Table 2: Significant changes in response features of the mechanoreceptors due to a location change (see Pirschel and Kretzberg, 2015, submitted). The location is changed away from the center of the receptive field ($p < 0.001$ for P and T cells; (*) $p < 0.05$ for N cells, Kruskal-Wallis test). Percentages of cells showing significant changes are color-coded, exact numbers of cells are given as 'significant / total' cell numbers.

	Spike count [decrease]			Latency [increase]			1 st ISI [increase]		
	10	50	100	10	50	100	10	50	100
[mN]	10	50	100	10	50	100	10	50	100
T cells	9 / 10	10 / 10	-	10 / 10	10 / 10	-	8 / 10	7 / 10	-
P cells	10 / 10	10 / 10	-	8 / 10	10 / 10	-	1 / 10	5 / 10	-
N cells (*)	-	-	7 / 8	-	-	5 / 8	-	-	-



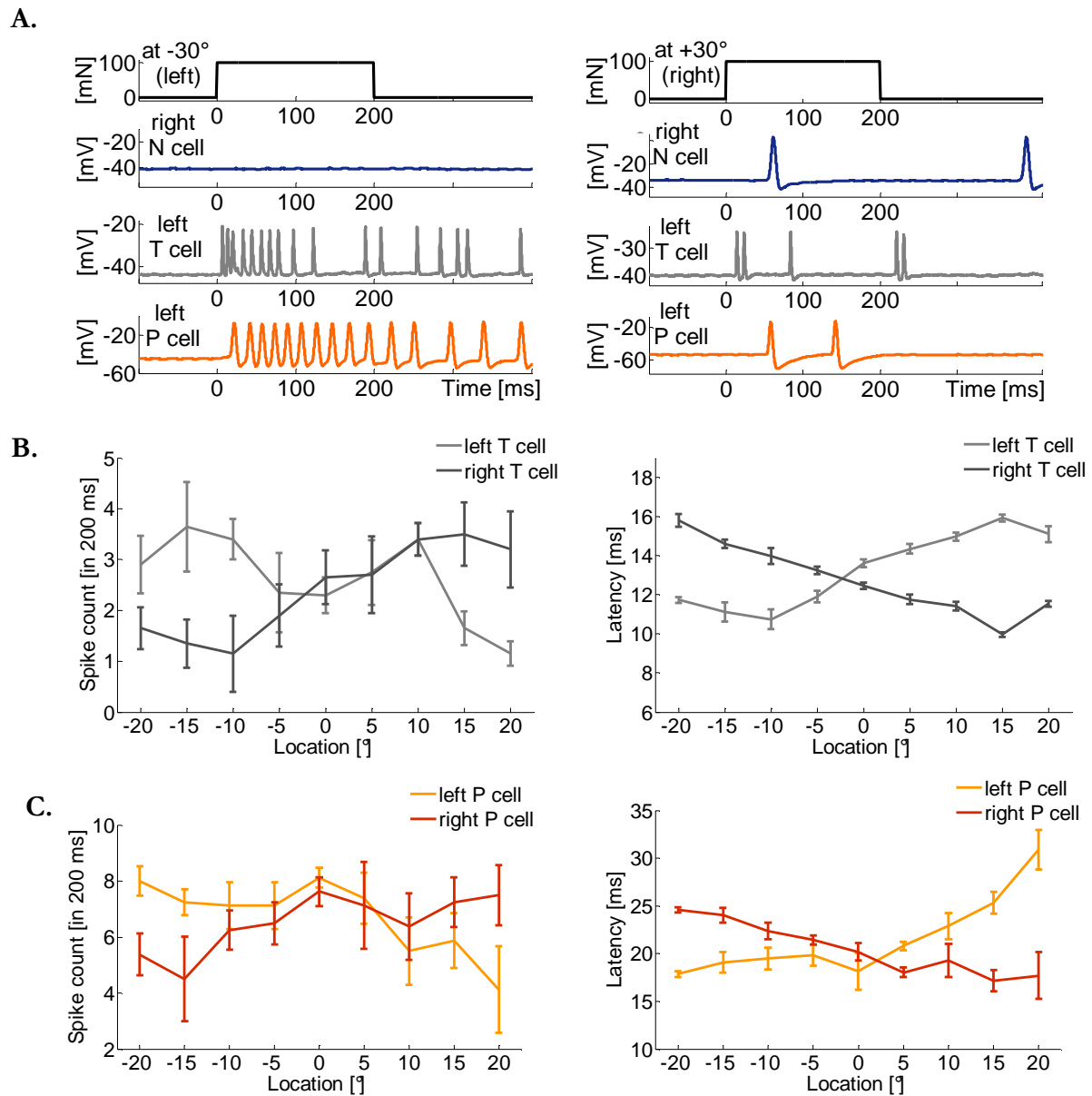


Figure 5: Influences of touch location on neuronal responses of mechanoreceptors (see Pirschel and Kretzberg, 2015, submitted). **A.** Representative responses of a right N cell (blue), left T cell (grey) and left P cell (orange) to a touch stimulus of 100 mN for 200 ms at -30° (left) and $+30^\circ$ (right). **B.** Spike count and latency (mean and STD) of a T cell double recording for a stimulus of 50 mN. **C.** Spike count and latency (mean and STD) of a P cell double recording for a stimulus of 50 mN.

or feature combinations for P cells (Fig. 6D) ($p < 0.05$, Wilcoxon rank sum test; P cells: 13 of 22 cases with $p < 0.001$). Sole exception is the feature combination of relative spike count with relative latency (RC & RL) showing only a slightly lower performance by tendency ($p = 0.0986$). The same applies for the relative latencies of T cells for the 10 mN stimulus (Fig. 6C) ($p < 0.05$, Wilcoxon rank sum test; T cells: 15 of 27 cases with $p < 0.001$). However, two features – the response latency and the relative 1st ISI – for a 50 mN stimulus were not significantly different from the relative latency of this cell type

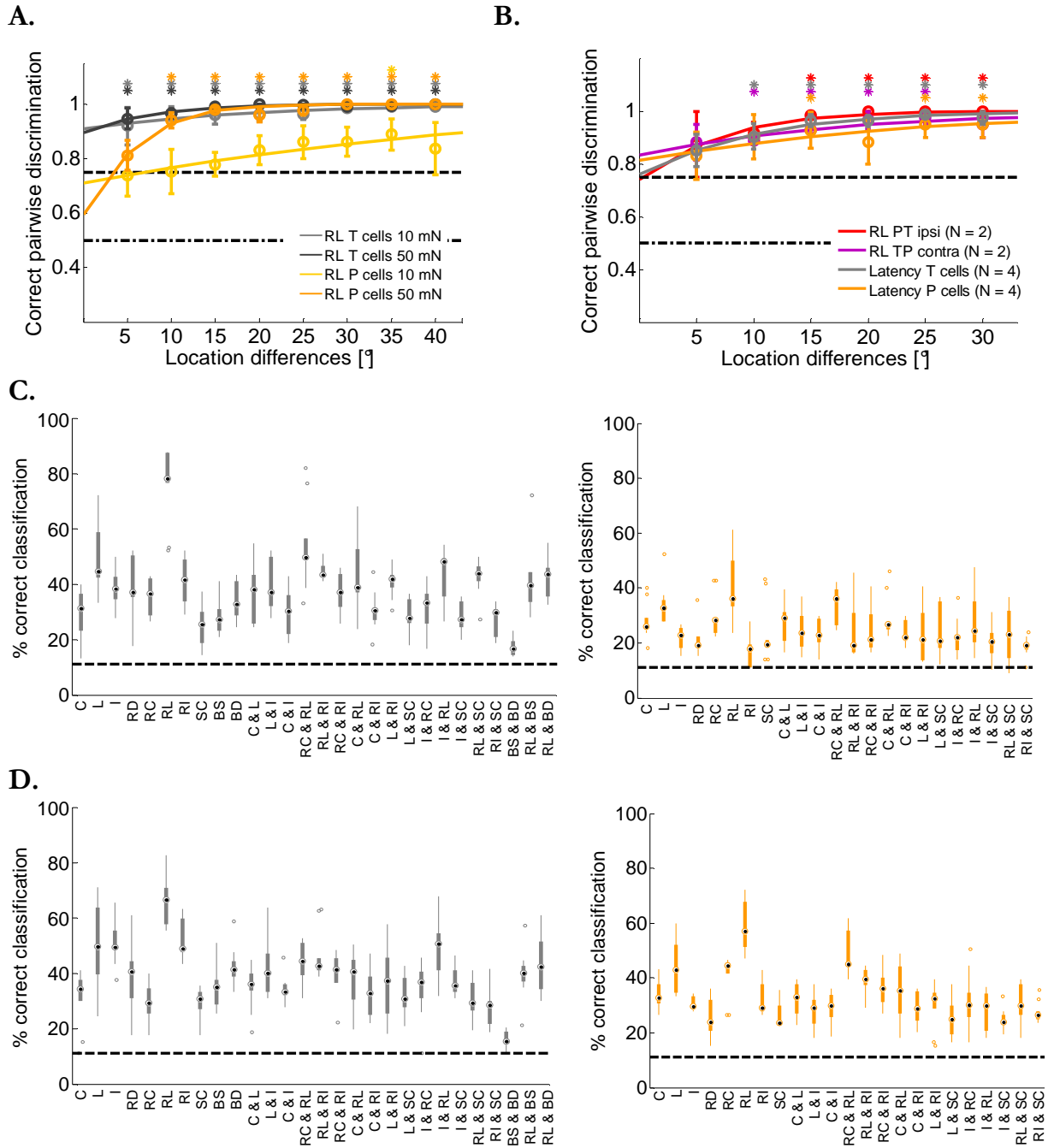


Figure 6: Estimation results for stimulus location (see Pirschel and Kretzberg, 2015, submitted). **A.** Pairwise discrimination results for location differences between 5° and 40°, around 0°, for the relative latency (RL) of T and P cells at two touch intensities (# of cells, see Table 2, stimulus presentations = 10). Black dashed lines show chance level and 75% threshold. Asterisks indicate mean values which are significantly ($p < 0.05$, t -test) above threshold. **B.** Pairwise discrimination results for location differences between 5° and 30°, around 0°, for T-P cell recordings for 50 mN (stimulus presentations = 10). Ipsi = ipsilateral; contra = contralateral. Black dashed lines show chance level and 75% threshold. Asterisks indicate mean values which are significantly ($p < 0.05$, t -test) above threshold. **C.** Classification result for 9 locations for 10 mN stimulus intensity. T cell features in grey, P cells features in orange. Black dashed line show chance level and black dots mark the median values (see Methods). Response features: C = spike count; L = latency; I = 1st ISI; RD = response duration; RC = relative spike count; RL = relative latency; RI = relative 1st ISI; SC = summed count; BS = burst strength; BD = burst duration. Asterisks: $p < 0.05$, Wilcoxon rank sum test. **D.** Data correspond to C for a stimulus intensity of 50 mN.

(Fig. 6D) ($p = 0.0586$ and $p = 0.0556$, Wilcoxon rank sum test). Overall, combinations of features did not improve the estimation for any of the methods tested (Fig. 6C, D).

For P cells, the relative latency discriminated touch location differences of 10° significantly above threshold (stimulus intensity 50 mN; Fig. 6A). This means a distance of about 0.6 mm for an average leech (circumference 2 cm) and is in the range of the behavioral discrimination threshold measured by Thomson and Kristan (2006). Additionally, the estimation performance of T-P cell combination features was analyzed (Fig. 6B). The small data set indicated that location estimation was not improved by a combination across cell types. Neither ipsilateral nor contralateral T-P cell pairs yielded better results than the latencies of single T and P cells (Fig. 6B).

The findings revealed two interesting aspects. First, the location encoding performance depended on the stimulus intensity: The relative P cell latency for a stimulus of 50 mN allowed significantly better stimulus estimations than this feature at 10 mN (Fig. 6A, C). Second, T cells showed distinctly better results for the same tasks than P cells: The relative T cell latency allowed a discrimination of location differences smaller than 5° even for the low intensity of 10 mN and led to the significantly best estimation of the nine possible touch locations ($p < 0.05$, Wilcoxon rank sum test) (Fig. 6A, C). Moreover, the mutual information of relative T cell latencies and location was higher than for any other response feature (Table 5). These findings for P cells could be explained by more precise response latencies – and consequently more precise relative latencies – for higher touch intensities (see Table 2): averaging over many cells showed an increasing accuracy of latencies for ascending intensity values (see Fig. 7C).

The touch location was most precisely encoded by a temporal ensemble code – the relative latency of the first spikes of a cell pair of the same type. Additionally, the encoding performance was influenced by the touch intensity – for different cell types varyingly strong – which may indicate different specializations of cell types.

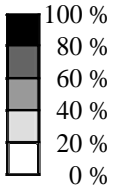
4.1.2. Encoding of intensity

The traditional hypothesis for intensity encoding is that the mechanosensory cell types respond to separated touch intensity ranges (Nicholls and Baylor, 1968). As a result the cell type itself encodes the stimulus intensity. Surprisingly, here all three types of mechanosensory cells responded to strongly overlapping intensity ranges (50 – 200 mN; Fig. 7) (see Pirschel and Kretzberg, 2013): P cells were already activated by a light touch of 5 mN, while T cells spike counts did not completely saturate for stimulus intensities around 200 mN and N cells show spikes reliably around 100 mN (Fig. 7). Generally, stimulus intensity significantly affected the spike counts and latencies of P and T cells (Table 3). This effect was more salient at lower intensities and attenuates for higher intensities (Table 3). The T cell latency was strikingly precise – independent of the touch intensity and number of cells in the data set (Fig. 7C). N cells are known to be the leech's nociceptors (Kristan et al., 2005) and their impact on encoding touch stimuli at the intensity ranges tested is presumably very low. Although N cells responded to the stimulus intensities up to 200 mN with a low spike number (Fig. 7), none of the analyzed N cell response features were found to depend significantly on touch intensity (Table 3).

These results seem to contradict to a certain extent the hypothesis that the activated cell type itself is the intensity encoder. To test if the intensity is encoded in a response feature, the aforementioned approaches were utilized. The feature which led to the best performance was generally the spike count (Fig. 8) (see Pirschel and Kretzberg, 2011; 2012 and 2013). Nevertheless, the analysis outcome for this property was not so obvious:

Table 3: Significant changes in response features of the mechanoreceptors due to an intensity increase ($p < 0.001$, Kruskal-Wallis test) (see Pirschel and Kretzberg, 2015, submitted). Percentages of cells showing significant changes are color-coded, exact numbers of cells are given as 'significant / total' cell numbers. Low intensities are < 50 mN; Medium (med) intensities 50 to 100 mN; High intensities 100 up to 200 mN.

Intensity	Spike count [increase]			Latency [decrease]			1 st ISI [decrease]		
	low	med	high	low	med	high	low	med	high
T cells	21/ 33	10/ 26	3/ 7	25/ 33	14/ 26	5/ 7	12/ 33	8/ 26	2/ 7
P cells	36/ 42	14/ 23	3/ 6	38/ 42	9/ 23	1/ 6	20/ 42	8/ 23	1/ 6
N cells	-	1/ 27	0/ 4	-	0/ 27	0/ 4	-	0/ 27	0/ 4



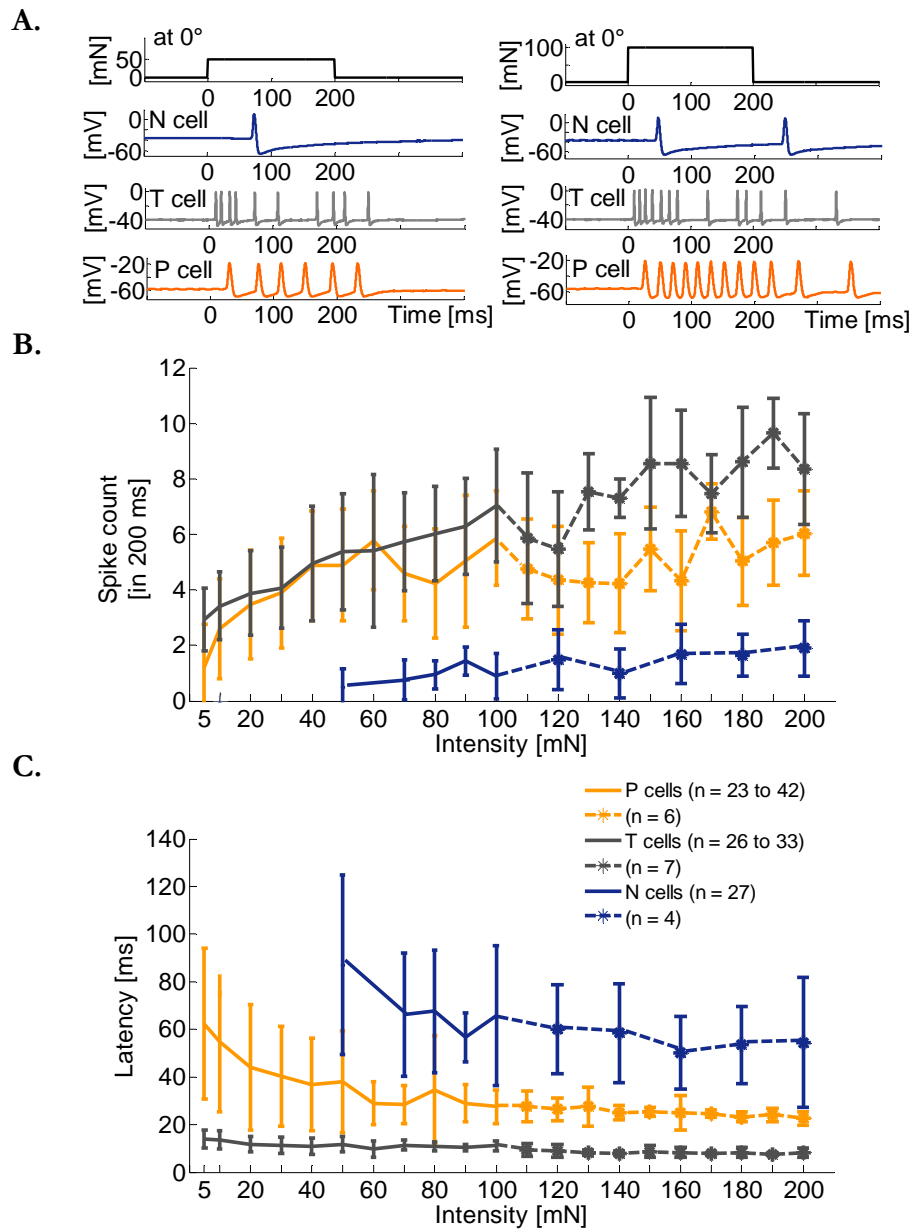


Figure 7: Influences of touch intensity on neuronal responses of mechanoreceptors (Pirschel and Kretzberg, 2015, submitted). **A.** Representative responses of a right N cell (blue), left T cell (grey) and P cell (orange) to a touch stimulus of 50 mN (left) and 100 mN (right) for 200 ms at 0°. **B.** Spike count (mean and STD) for P cells (orange), T cells (blue) for intensities of 5 to 200 mN. **C.** Latency (mean and STD) for the same cells and conditions like B.

similar results for response latencies and spike counts of T and P cells were revealed in both estimation approaches (Fig. 8). The same applies to the mutual information between these features and the touch intensity (Table 5). Slightly better results were found for the summed spike count of cell pairs (Fig. 8). Overall, intensity estimation results were not as statistically clear as the location estimation results for the intensity range tested here.

The summed spike count of T and P cells tended to give the best estimations (Fig. 8): with approximately 70% correct estimations of five intensities and a significant pairwise discrimination of 30 mN intensity differences (Fig. 8). Especially relative spike counts

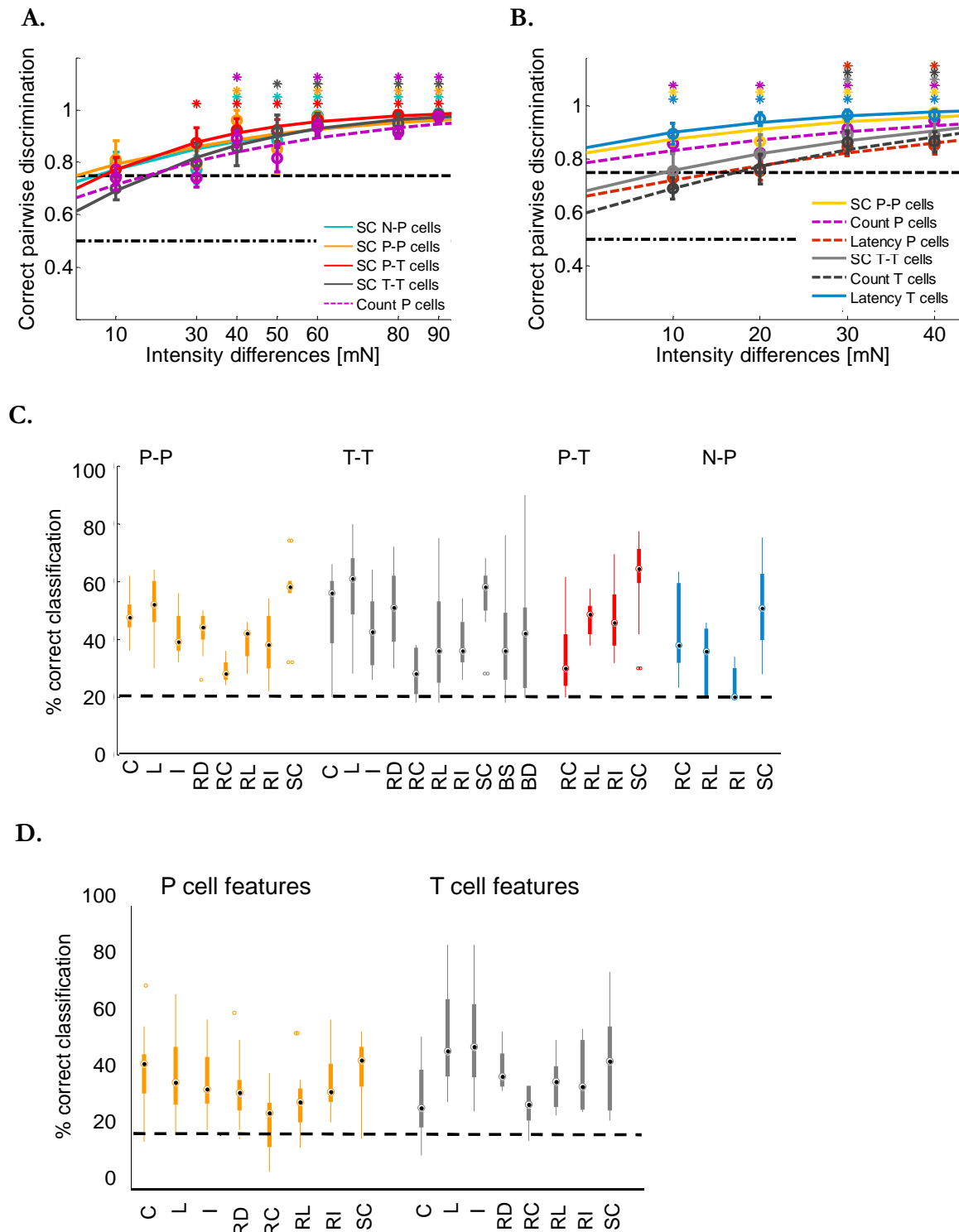


Figure 8: Estimation results for stimulus intensities (see Pirschel and Kretzberg, 2015, submitted). **A.** Pairwise discrimination of intensity differences between 10 and 90 mN, compared to the 10 mN stimulus. $N = 5$ PP; 8 TT; 11 PT; 7 NP cell double recordings. Black dashed lines show chance level and 75% threshold. Asterisks indicate mean values which are significantly ($p < 0.05$, t -test) above threshold. Response features: see Abbreviations. **B.** Pairwise discrimination of intensity differences between 10 and 40 mN, compared to the 10 mN stimulus. $N = 12$ PP and 7 TT cell double recordings. **C.** Classification results. 5 intensities between 10 and 100 mN at 0° . Same cells as in A. Black dashed line show chance level and black dots mark the median values (see Methods). Response features: see Abbreviations. **D.** Classification results. 5 intensities between 10 and 50 mN at 0° . Same cells as in B. Black dashed line show chance level and black dots mark the median values (see Methods). Response features: see Abbreviations.

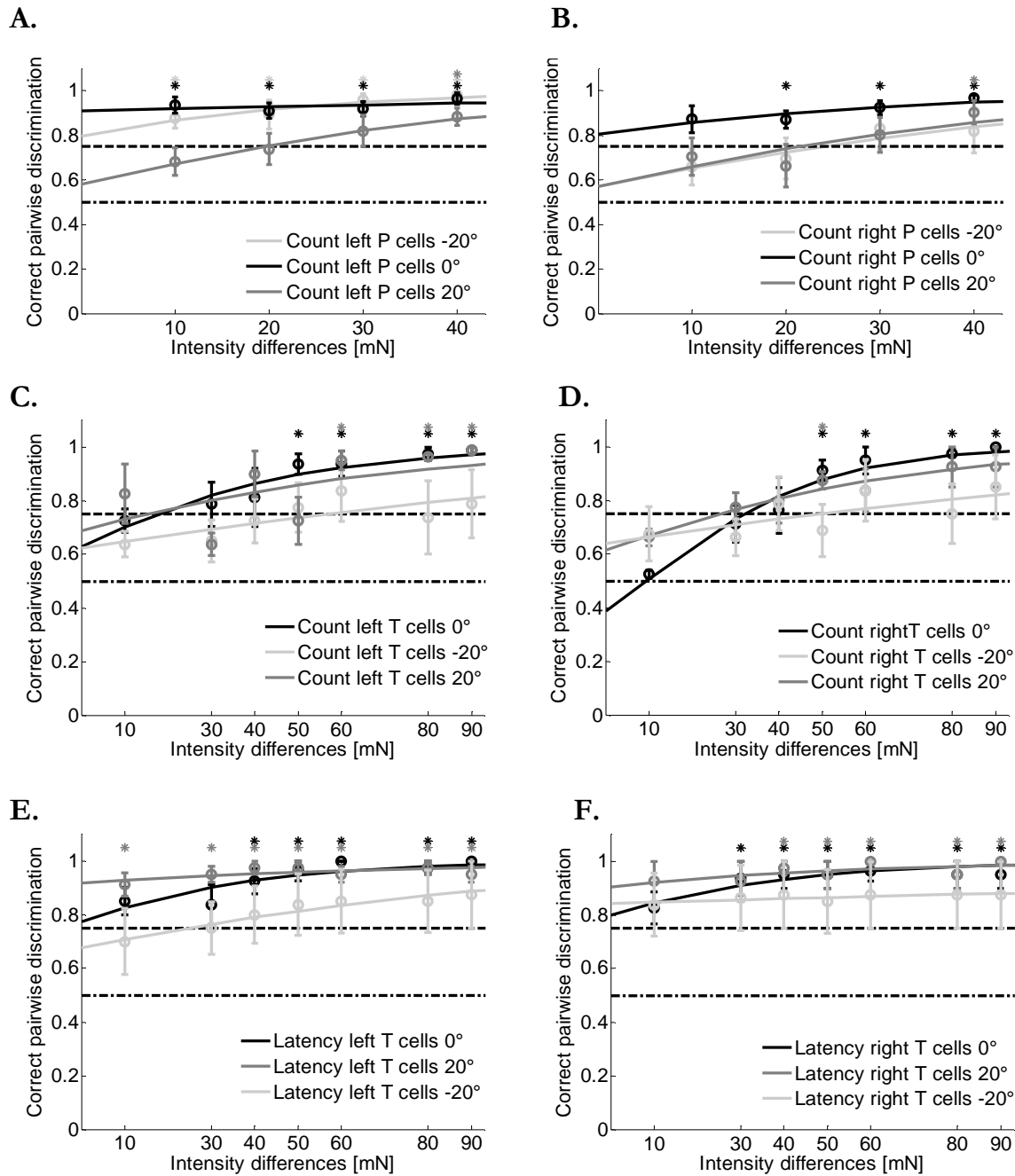


Figure 9: Influence of the touch location on intensity discrimination results. Black dashed lines show chance level and 75% threshold. Asterisks indicate mean values which are significantly ($p < 0.05$, t -test) above threshold. **A.** Discrimination of intensity differences between 10 and 40 mN, compared to the 10 mN stimulus, for 5 left P cells and **B.** for 5 right P cell recordings. **C.** Discrimination of intensity differences between 10 and 90 mN, compared to the 10 mN stimulus. Spike count of 4 left T cells and **D.** for spike count of 4 right T cells. **E.** Discrimination of intensity differences between 10 and 90 mN, compared to the 10 mN stimulus. Latency of 4 left T cells and **F.** for latency of 4 right T cells.

and relative latencies lagged behind this feature. Acceptable classification values could also be yielded by T cell burst features, in particular the burst duration (Fig. 8C). Downstream neurons might be able to evaluate T cell bursts, which makes it an

interesting feature for further investigations on the level of interneurons. Addition of N cell spike counts was less effective than it was hypothesized. For higher intensities (200 mN and higher), where N cells could be more active, a summation of spike counts of this cell type might have a greater impact.

A larger data set of P and T cells stimulated with a range of lower intensities showed qualitatively the same results regarding the best performing features (Fig. 8B, D) (see Pirschel and Kretzberg, 2012). However, with this data set intensity differences of 10 mN could be discriminated above threshold based on the summed spike count of two P cells (Fig. 8B). Notably, response latencies of single T cells showed good estimation performances (Fig. 8B). This feature is highly significantly influenced by the touch intensity (Table 3) as well as the location (Table 2). Since it counts on owing to the precision of the first T cell spikes, this feature may reflect even small intensity changes. But it is yet questionable whether postsynaptic cells could use absolute response latencies of single cells without any reference point (e.g., spike of another cell, etc.).

It was shown that the encoding of the touch location was intensity-dependent (see Pirschel and Kretzberg, 2012). Since the touch intensities also influenced the responses of the sensory neurons to locations, the estimation of intensity differences was tested with varied locations (Fig. 9). However, the estimation at 0° works quite well for P and T cells. The results at preferred stimulation locations (more to the center of the receptive fields) did not show a reliable tendency to better or worse performances. Conceivably, this effect may be more prominent for stimulus locations with a larger distance (e.g., -40° vs. +40°) or at higher intensities. The location indeed affected the absolute spike count of the cells (see Table 2), but likely not the relations between spike counts at different intensities. For instance, low touch intensities elicited low spike counts at preferred locations as well as at peripheral locations. This held true for high intensities. Absolute spike counts were lower at peripheral locations for all touch intensities related to preferred locations (Fig. 5).

In conclusion, the summed spike count was the most suitable response feature for intensity encoding, which suggest a rate code based on a population of cells for this property. For a faster – but coarser - encoding of intensity, it may be feasible to use the onset bursts of T cells.

4.1.3. Encoding of duration

The third stimulus property investigated was the touch duration. This property mainly affected spike counts and periods of spike occurrence, defined as response duration. This is not surprising, since all cell types show no spontaneous activity in the absence of stimulation. For a 60 mN stimulus, the spike counts and the response duration significantly increased with stimulus duration in all P and T cells ($p < 0.001$, Kruskal-Wallis test) (Table 4, Fig. 10A, B) (see Pirschel and Kretzberg, 2011). The same applied for the lower intensity, except for spike counts of T cells: only 5 of 10 T cell spike counts showed a significant increase depending on the stimulus duration ($p < 0.001$, Kruskal-Wallis test) (Table 4, Fig. 10A). Besides the absolute values of features, the variance of these features also increased with longer touch durations (Fig. 10B). It seems that spikes occurred more unreliably after some time of constant stimulation (see Figs. 5A, 7A, 10A).

For the estimation of response duration, the spike count yielded the best results, slightly better than the response duration (Fig. 10B). Accordingly, the highest mutual information with duration was reached by the spike count of P cells (Table 5). Thus, the touch duration was represented in slow encoding features, the total spike count and the response duration. Conceivably, the characteristic spiking pattern of T cells (Figs. 5A, 7A, and 10A) with bursts at the beginning and at the end of stimulus could be used by downstream neurons to detect the start and end time of a touch.

Table 4: Significant changes in response features of P and T cells due to an duration increase ($p < 0.001$, Kruskal-Wallis test). Percentages of cells showing significant changes are color-coded, exact numbers of cells are given as 'significant / total' cell numbers.

	Spike count [increase]		Response Duration [increase]	
	20 mN	60 mN	20 mN	60 mN
T cells	5/ 10	10/ 10	10/ 10	10/ 10
P cells	11/ 12	12/ 12	12/ 12	12/ 12

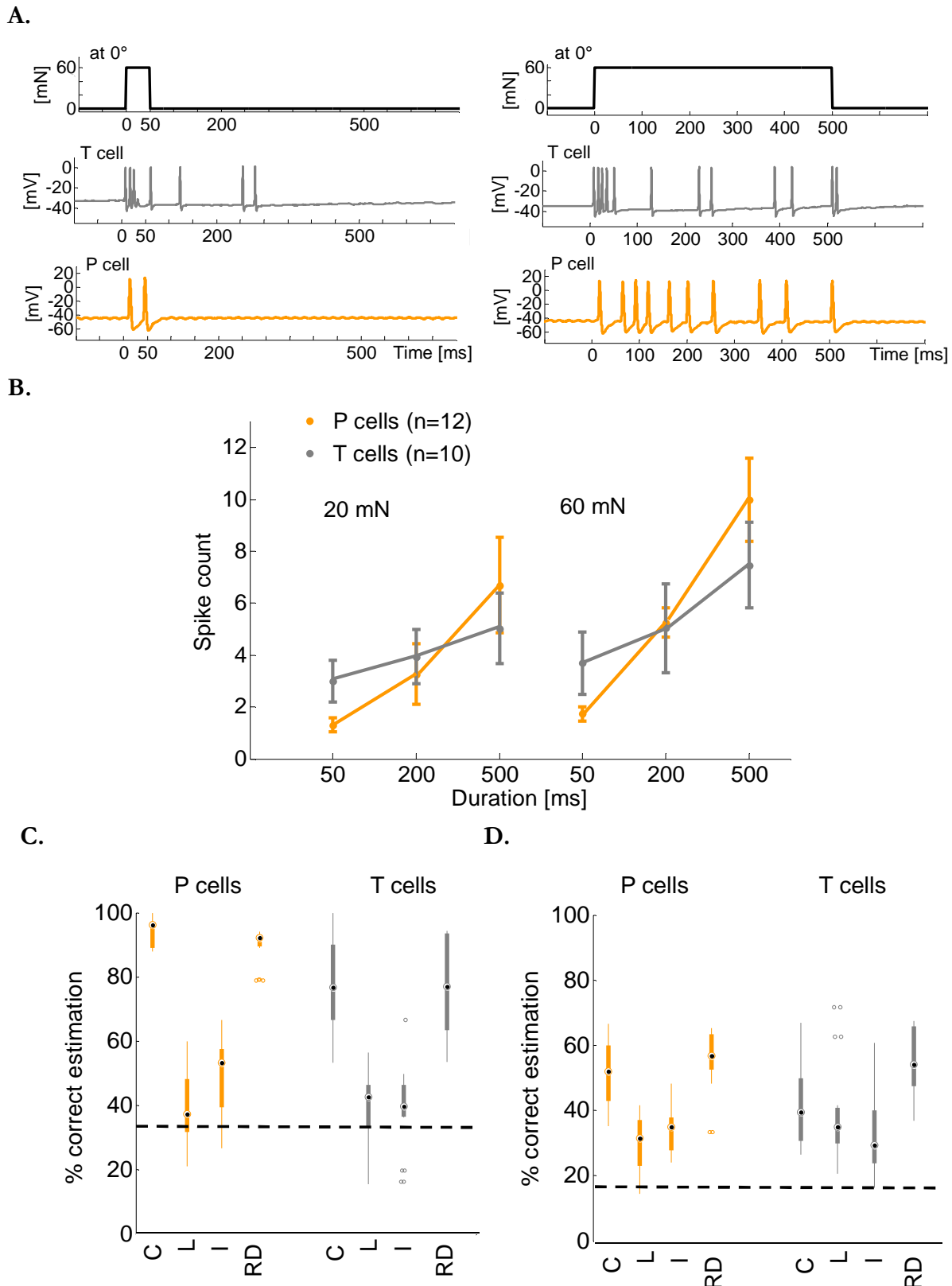


Figure 10: Influences of the stimulus duration on neuronal responses of mechanoreceptors (see Pirschel and Kretzberg, 2015, submitted). **A.** Representative responses of a T cell (grey) and P cell (orange) to a touch stimulus of 60 mN for 50 ms (left) and 500 ms (right) at 0° . **B.** Spike count (mean and STD) for P cells (orange) and T cells (grey) for stimuli of 20 and 60 mN with 50, 200 and 500 ms duration at 0° stimulus location. **C.** Classification results for 60 mN stimulus intensity with three durations (Table 1). Black dashed line show chance level and black dots mark the median values (see Methods). Response features: see Abbreviations. P cell features (orange), T cell features (grey). **D.** Classification results for two intensities with three durations (Table 1). Legend as in B.

4.2. Encoding of complex touch stimuli by sensory neurons

The magnitude of the local bend behavior depends on various stimulus properties (Baca et al., 2006). Since estimation of the individual touch properties revealed specific response features as good encoders, the question here is how more complex stimuli could be read out from neuronal responses. The results of encoding of single stimulus properties revealed considerable ambiguity: As was shown for single cell responses, touch intensity affected the same features as did the touch location. Shifting the touch towards the receptive field center led to a decreasing latency and an increasing spike count, just as an increase of touch intensity at the same touch location. Moreover, a longer duration affected the spike count similar to a rising intensity.

The best encoder for intensity as well as duration was found to be the spike count (see *Results 4.1.*). However, combination of two intensities with three durations (Table 1) can be estimated best from response duration (T cells RD vs. C: $p = 0.0535$; Wilcoxon rank sum test) (Fig. 10D). Accordingly, the highest mutual information with the combination of intensity and duration was reached by this feature (Table 5). The response duration may gain relevance with task complexity when spike counts represent additional stimulus properties. Baca and colleagues (2005) found that longer stimulus durations (200 vs. 500 ms) led to significantly larger local bend responses with the same stimulus intensities (Baca et al., 2005). Here, spike counts are strongly influenced by touch intensities and durations, which may indicate, in line with findings by Baca et al. (2005), that spike counts and response durations behaviorally affect the strength of muscle responses.

For the estimation of individual stimulus properties of location and intensity, two different ensemble codes were identified: a temporal feature – the relative latency of two cells of the same type – was found to be the best encoder for touch location. Touch intensity was encoded best by a spike count code – the summed spike count of cell pairs. For different intensity-location combinations (Table 1, Fig. 11), best estimations were obtained by the relative latency of T cells and the summed spike count of P cells (Fig. 11A, C, E; Table 5). Even for more difficult tasks (5 locations and 3 intensities, Fig. 11D), the results were above chance level.

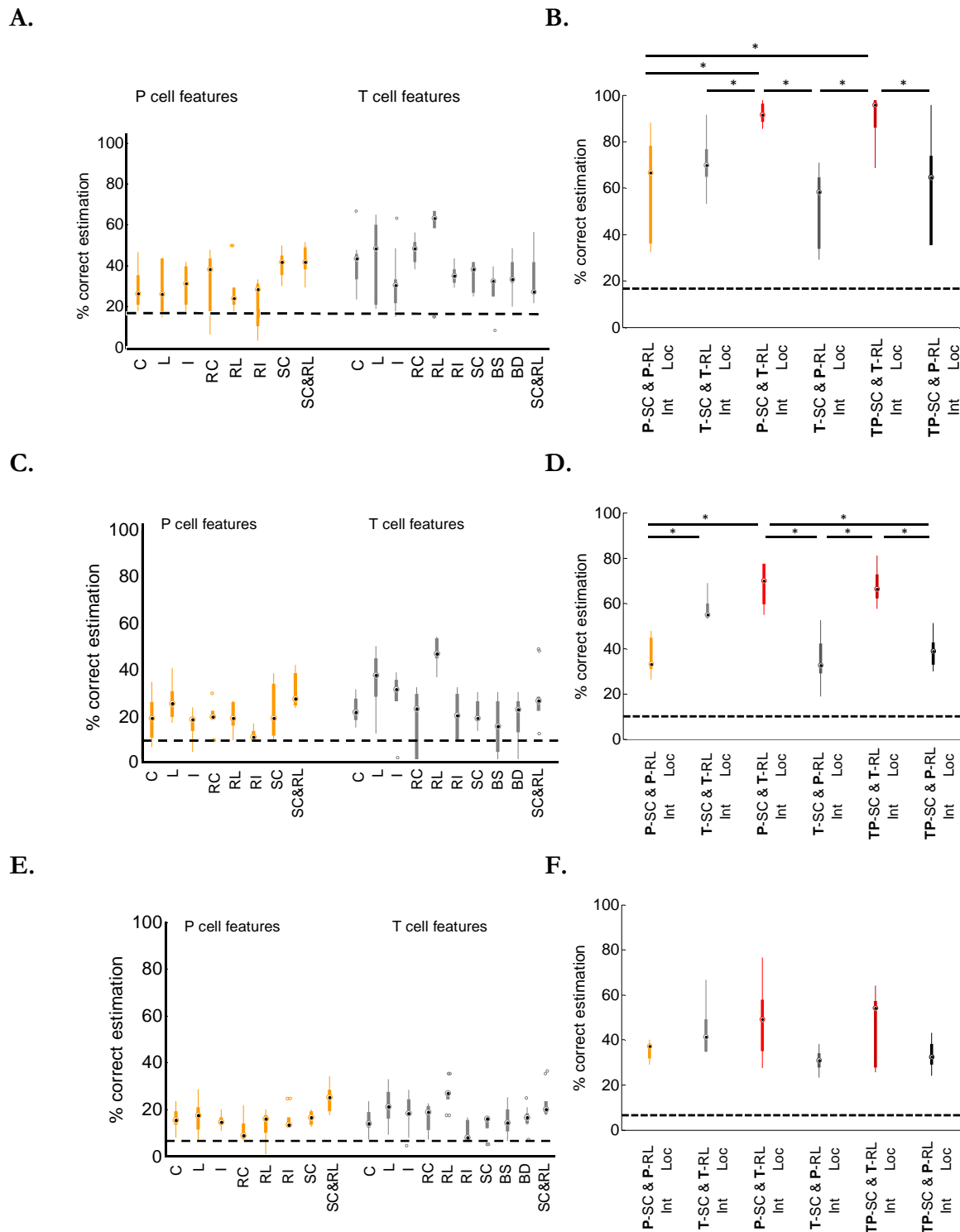


Figure 11: Estimation results for combination of location and intensity (modified, Pirschel and Kretzberg, 2015, submitted). Response features: see Abbreviations. Black dashed lines show chance level. P cell pairs (orange); T cell pairs (grey); pooled data of P cell summed spike count (SC) and T cell relative latency (RL) (red), T cell SC and P cell RL (dark grey); SC of P cell plus T cell pooled data (counts of 4 mechanoreceptors) with RL of T cells (dark red) and RL of P cells (blue). Asterisks indicate a significant difference ($p < 0.05$, Wilcoxon rank sum test). **A.** 1st property combination 3 locations with 2 intensities ($[-20 \mid 0 \mid 20]$ with $[10, 50 \text{ mN}]$). Chance level: 16.6%. **B.** Results for SC for intensity estimation (Int) and RL for location estimation (Loc). Location-intensity combination as in A. **C.** 2nd property combination 5 locations with 2 intensities ($[-20 \mid -10 \mid 0 \mid +10 \mid 20]$ with $[10, 20 \text{ mN}]$). Chance level: 10%. **D.** Results for SC for Int estimation and RL for Loc estimation. Location-intensity combination as in C. **E.** 3rd property combination 5 locations with 3 intensities ($[-20 \mid -10 \mid 0 \mid +10 \mid 20]$ with $[10, 20, 50 \text{ mN}]$). Chance level: 6.6%. **F.** Results for SC for Int estimation and RL for Loc estimation. Location-intensity combination as in E.

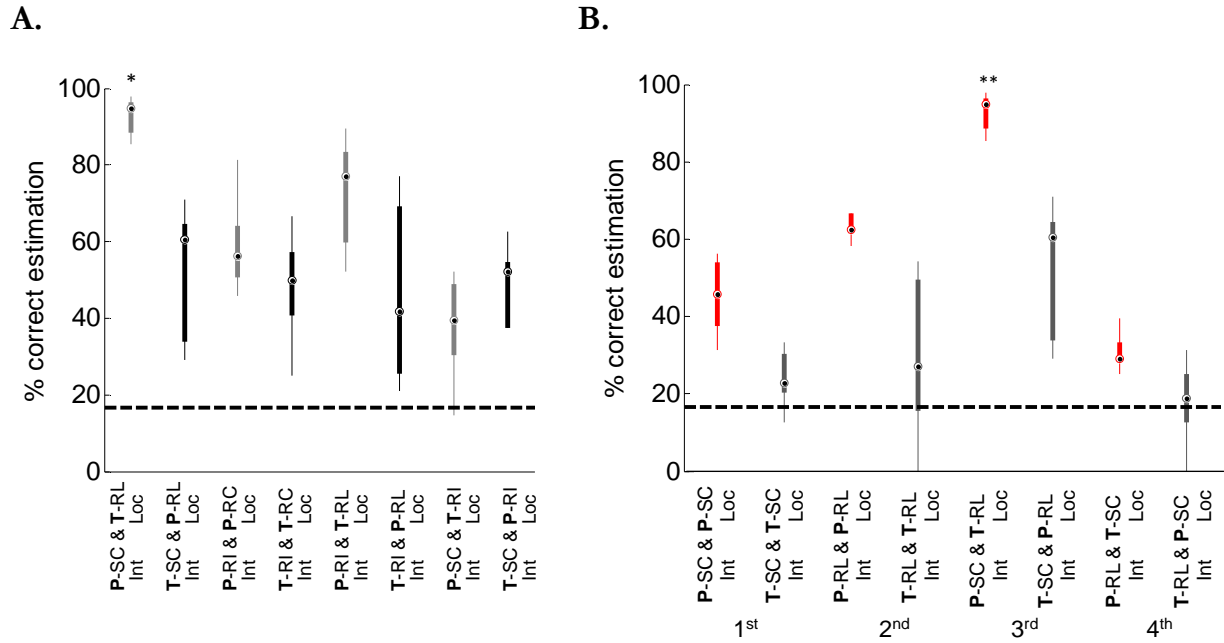


Figure 12: Estimation results for property-dependent cell type feature combinations. Response features: see Abbreviations. Black dashed lines show chance level. One asterisk: significant difference ($p < 0.05$, Wilcoxon rank sum test); Two asterisks: highly significant difference ($p < 0.001$, Wilcoxon rank sum test) – to all other feature combinations. **A.** Results for different feature combinations for the property combination 3 locations with 2 intensities ($[-20 | 0 | 20]$ with $[10, 50 \text{ mN}]$), 3rd case as in B. details see text. SC = summed spike count; RL = relative latency; RC = relative spike count; RI = relative 1st ISI; Int = Intensity; Loc = Location. **B.** Results for combinations of the features SC and RL. Location-intensity combination as in A. Description of case 1st – 4th see text.

However, a feature combination of summed spike count and relative latency did not improve the estimation for the combination of 3 locations and 2 intensities (Fig. 11A, C). Remarkably, this feature combination gained better results for more difficult tasks (Fig. 11C and E): for 5 locations and 3 intensities (Fig. 11E), the P cell feature combination performed significantly better than individual features ($p < 0.05$, Wilcoxon rank sum test), and the relative T cell latencies did not yield significantly better results than summed spike count and relative latencies (T cells: RL vs. RL&SC_{1.Combi} $p = 0.025$; RL vs. RL&SC_{2.Combi} $p = 0.004$; RL vs. RL&SC_{3.Combi} $p = 0.209$; Wilcoxon rank sum test; Fig. 11A, C, E).

Based on the analysis results of the individual stimulus properties, a property-dependent cell type feature combination was tested (Fig. 11B, D, and F). For this analysis, a pooled data set containing 5 P cell and 5 T cell double recordings was used (see *Methods*), because simultaneous recordings from 4 sensory neurons was unfeasible due to technically

limitations. Outcomes from this pooled data set were very consistent across preparations. Features of T cells and P cells were teamed to investigate if the stimulus estimation of a location-intensity combination can be improved by the integration of several cell types. First, results of all possible combinations of the response features summed spike count and relative latency as well as relative spike count and relative first ISI were analyzed (Fig. 12A). In this task the feature combination of summed spike count with relative latency led to the significantly best result (Fig. 12A).

Second, in order to find the best performance for this feature team, the following four sets for all possible cell pairings (P w/ P, T w/ T, P w/ T and T w/ P) were tested (Fig. 12B):

1st: Summed spike count for intensity and location encoding,

2nd: Relative latency for intensity and location encoding,

3rd: Summed spike count for intensity encoding and relative latency for location encoding,

4th: Relative latency for intensity and summed spike count for location encoding.

The best estimation results were achieved, for all cell type combinations, by the 3rd case: summed spike count for intensity encoding and relative latency for location encoding (Fig. 12B). Furthermore, for this set the best performance was reached by a combination of summed spike counts of P cells and relative latencies of T cells (Fig. 11B, D, and F) (see Kretzberg et al., 2015). This combination of cell type and feature classified six different stimuli almost perfectly (median 90% correct, Fig. 11B) and also led to the best performances in tasks involving more locations and intensities (Fig. 11D, E). These results were not improved by adding the spike counts of two P and two T cells (summed counts of 4 mechanoreceptors). This extended to more difficult tasks with 5 locations and several intensities (Fig. 11B, D, and F).

In summary, the first spike times of a cell pair reflected best the touch location. This feature makes an extremely fast and precise encoding of the location possible. The stimulus intensity could be best estimated by a rate code. On the one hand, P and T cells seem to be specialized in encoding preferred stimulus properties: Summed spike counts of P cells encode best stimulus intensity, while relative latencies of T cells encode the

touch location. On the other hand, the neuronal responses of both cell types contain information about all three stimulus properties (Fig. 11). These results suggest that multiplexing of sensory information may be used by this small and simple system to code complex stimuli in a highly precise manner.

For instance, relevant for the leech behavior might be vibrating or moving stimuli, which were not investigated in this study. However, an individual example with such a stimulation is shown in Figure 13. The trace accidentally arose due to technical problems: the poker tip vibrated just above the skin at a location of -10° . Unfortunately the signal of the poker was not recorded, but still the T cell and P cell recording leaves an impression of how the cells would respond to vibrating stimuli.

Table 5: Normalized mutual information of response features with stimulus properties (see Pirschel and Kretzberg, 2015, submitted). Bold numbers indicate the highest normalized mutual information. Sum = Summed; Rel = Relative; Resp = Response; Dur = Duration. Stimulus properties for the combined encoding tasks see Table 1.

Location					
Int [mN]	Cells	Count	Latency	Sum Count	Rel Latency
10	T	0.35 ± 0.12	0.49 ± 0.15	0.30 ± 0.11	0.73 ± 0.12
10	P	0.35 ± 0.07	0.36 ± 0.07	0.25 ± 0.07	0.45 ± 0.12
50	T	0.33 ± 0.04	0.51 ± 0.16	0.28 ± 0.08	0.61 ± 0.09
50	P	0.36 ± 0.04	0.49 ± 0.10	0.33 ± 0.06	0.62 ± 0.09
Intensity					
Loc [°]	Cells	Count	Latency	Sum Count	Rel Latency
0	T	0.44 ± 0.15	0.46 ± 0.16	0.48 ± 0.15	0.28 ± 0.17
0	P	0.40 ± 0.09	0.39 ± 0.12	0.47 ± 0.11	0.25 ± 0.11
0	N-P	-	-	0.41 ± 0.13	0.23 ± 0.17
0	P-T	-	-	0.52 ± 0.18	0.38 ± 0.11
Duration					
Int [mN]	Cells	Count	Latency	1 st ISI	Resp Dur
60	T	0.60 ± 0.24	0.11 ± 0.15	0.12 ± 0.12	0.59 ± 0.17
60	P	0.84 ± 0.11	0.10 ± 0.08	0.18 ± 0.09	0.72 ± 0.12
Duration & Intensity					
	Cells	Count	Latency	1 st ISI	Resp Dur
3 & 2	T	0.42 ± 0.13	0.34 ± 0.21	0.32 ± 0.13	0.49 ± 0.12
3 & 2	P	0.50 ± 0.07	0.30 ± 0.7	0.32 ± 0.09	0.53 ± 0.05
Location & Intensity					
	Cells	Count	Latency	Sum Count	Rel Latency
3 & 2	T	0.38 ± 0.14	0.56 ± 0.07	0.36 ± 0.11	0.71 ± 0.08
3 & 2	P	0.53 ± 0.14	0.49 ± 0.15	0.52 ± 0.13	0.52 ± 0.20

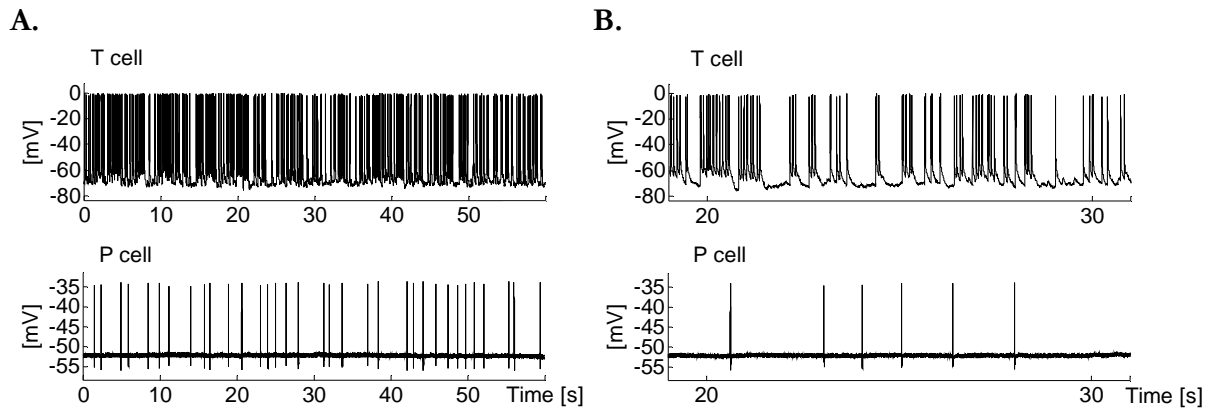


Figure 13: Neuronal responses of a left T cell and left P cell to vibrating skin stimulation (see Results 4.2) at -10° . **A.** Complete trace of 60 sec stimulation. **B.** Magnification of the time 20 to 30 sec trace in A.

4.3. Processing of touch stimuli in the local bend network

The aims of the third study were to analyze connections of INs of the local bend network and mechanosensory cells as well as to characterize the responses of these INs to tactile stimulation. Whereas some details were known about the involved INs and their connections to P cells (Lockery and Kristan, 1990b), no experimental data existed with tactile stimulation of local bend INs so far. Here, the data are mainly from cell 157, whose graded responses were also analyzed by means of the stimulus estimation approaches (see 3.2. for details), and to a minor degree from cell 159 (see Fig 1C; Lockery and Kristan 1990b). For characterization of the graded responses, the response features integral and amplitude, the slope as well as latency were used (see *Methods*). In the last section, a smattering of responses from cell 161 and 162 are shown.

4.3.1 Influence of touch properties on interneuronal responses

All recorded cells 157 showed strong correlations between the interneuronal response features and the touch location (Table 6; Figs. 14, 15, 18). Like the mechanoreceptors, the cell 157 seems to have a spatially structured receptive field, showing greater responses at stimulus locations nearer to the receptive field center (Figs. 14, 15). Apparently, the receptive field of cell 157 covers a larger area (Fig. 15A, B) than the fields of the

mechanosensory cells which overspan about 180° (Nicholls and Baylor, 1968; Yau, 1976; Blackshaw, 1981; Blackshaw et al., 1982; Lewis and Kristan, 1998c): cell 157 responded over a range of 140° with still increasing responses, which indicates a receptive field of about 280° or broader. This could be explained by the inputs from several mechanosensory cells processed by the IN (connections of INs-P cells: Lockery and Kristan, 1990b). The touch intensity, in particular lower intensities in the range of 10 to 50 mN, also affected significantly the interneuronal response features (Table 6).

Compared to cell 157, the response shape of cell 159 seems to be more influenced by T cells (Fig. 14). The response of this cell type clearly reflected the phasic response patterns of T cells to tactile stimulation (Fig. 14B). Additionally, the response lasted longer than in cell 157 (Fig. 14B). Cell 159 also showed a spatially structured receptive field (Table 6; Fig. 15E, F). Qualitative differences in receptive fields between cell 159 and 157 could not be analyzed here owing to the lack of recordings.

In addition to excitatory postsynaptic potentials (EPSPs) in response to mechanosensory cell spikes, both IN types showed fast membrane fluctuations of small amplitudes called spikelets (Fig. 3; Epsztein et al., 2010). The spikelet frequency depended on the membrane potential. After penetration of the cell membrane, the INs were depolarized

Table 6: Significant changes in interneuronal response features due to location and intensity changes. Location changed towards the center of the receptive field of the mechanoreceptors ($p < 0.05$, Kruskal-Wallis test). Only if the cell features show clear dependencies (increase or decrease), they were stated as "significant". Low intensities: $< 50\text{mN}$; High intensities: up to 100mN . Exact numbers of cells are given as 'significant/total' cell numbers.

cell 157

Location	Intensity	Amplitude [increase]	Latency [decrease]	Integral [increase]	Slope [increase]
9 Locs	50 mN	8/ 8	6/ 8	8/ 8	8/ 8
	70 mN	7/ 7	7/ 7	7/ 7	7/ 7
0°	5 Ints low	8/ 11	6/ 11	9/ 11	7/ 11
	5 Ints high	5/ 10	2/ 10	7/ 10	4/ 10

cell 159

Location	Intensity	Amplitude [increase]	Latency [decrease]	Integral [increase]	Slope [increase]
9 Loc	50 mN	1 / 1	1 / 1	1 / 1	1 / 1
	70 mN	2 / 2	2 / 2	2 / 2	2 / 2

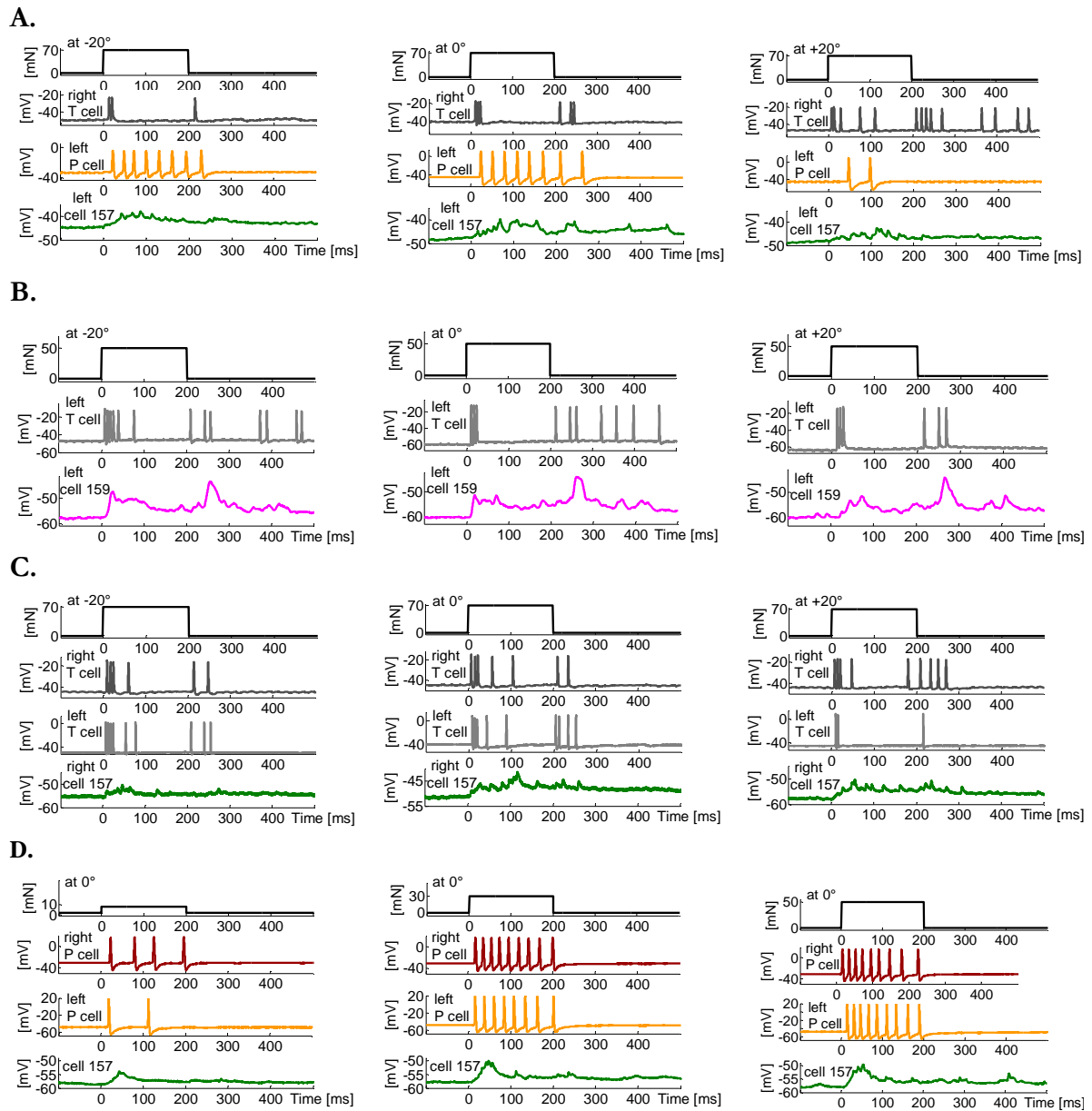


Figure 14: Examples of stimulus location and intensity influences on responses of mechanosensory cells and interneurons. **A.** Representative responses of a right T cell (grey), left P cell (orange) and left cell 157 (green) to a touch stimulus of 70 mN for 200 ms at -20° (left), 0° and $+20^\circ$ (right). **B.** Representative responses of a left T cell (grey) and left cell 159 (magenta) to a touch stimulus of 50 mN for 200 ms at -20° (left), 0° and $+20^\circ$ (right). **C.** Representative responses of a right T cell (dark grey), left T cell (light grey) and right cell 157 (green) to a touch stimulus of 70 mN for 200 ms at -20° (left), 0° and $+20^\circ$ (right). **D.** Representative responses of a right P cell (orange), left P cell (red) and cell 157 (green) to a touch stimulus of 10 mN (left), 30 mN and 50 mN (right) for 200 ms at 0° .

here around -20 to -30 mV membrane potential and showed frequent spontaneous spikelets. This effect was also described by Lockery and Kristan (1990b). When their membrane potentials were more hyperpolarized, the INs showed the spikelets considerably less frequent (Fig. 14). Connections between the mechanoreceptors and cell

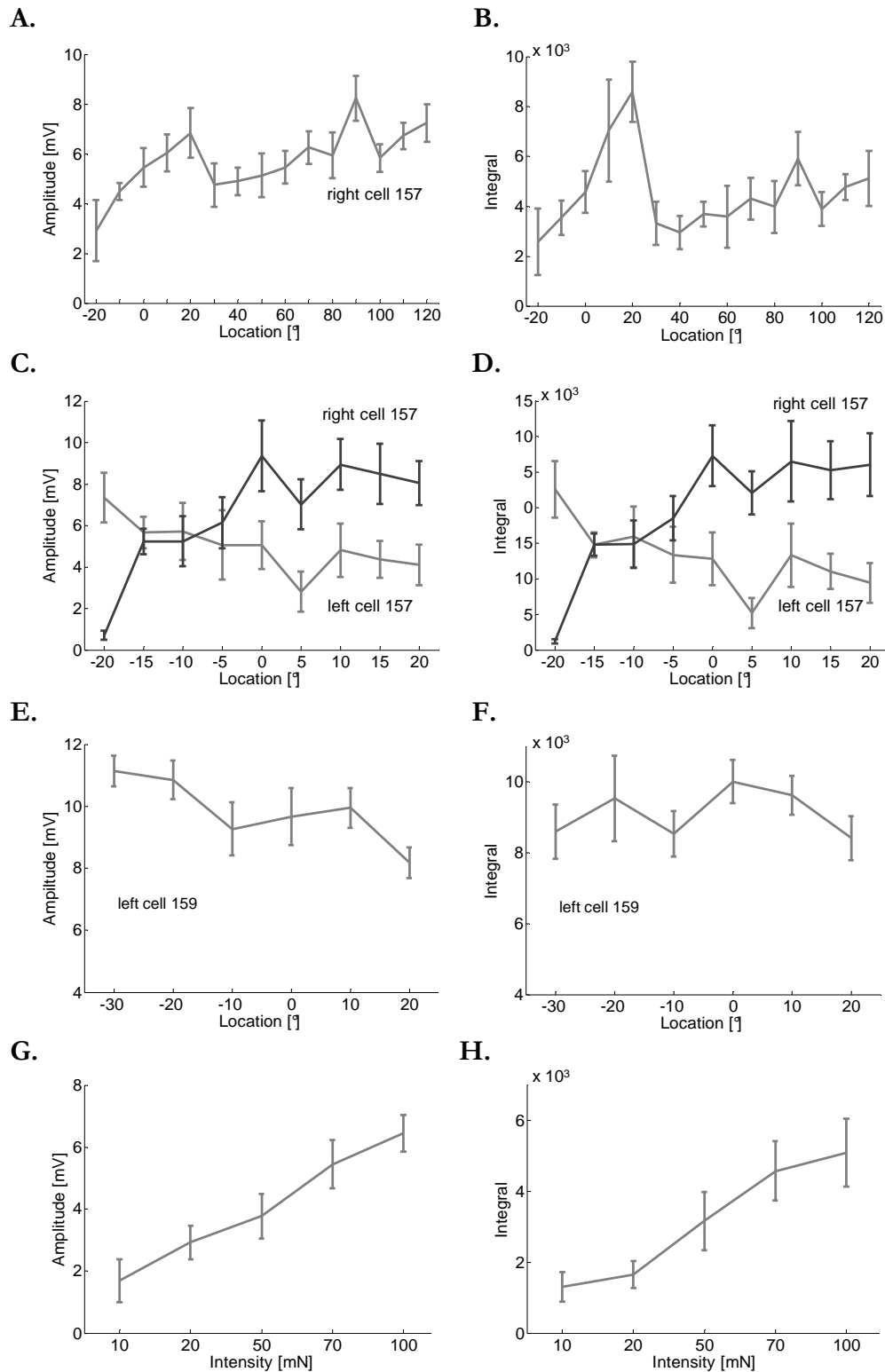


Figure 15: Examples of the stimulus influence on amplitude and integral (mean and STD). **A.** Amplitude in mV of a right cell 157 stimulated with 70 mN at locations: -20° to $+120^{\circ}$. **B.** Integral of the same cell as in A. **C.** Amplitude in mV of a left cell 157 (light grey) and a right cell 157 (dark grey) stimulated with 70 mN at locations: -20° to $+20^{\circ}$. **D.** Integral of the same cells as in C. **E.** Amplitude in mV of a left cell 159 stimulated with 70 mN at locations: -30° to $+20^{\circ}$. **F.** Integral of the same cell as in E. **G.** Amplitude in mV for a cell 157 stimulated at 0° with intensities between 10 and 100 mN **H.** Integral for the same cell as in G.

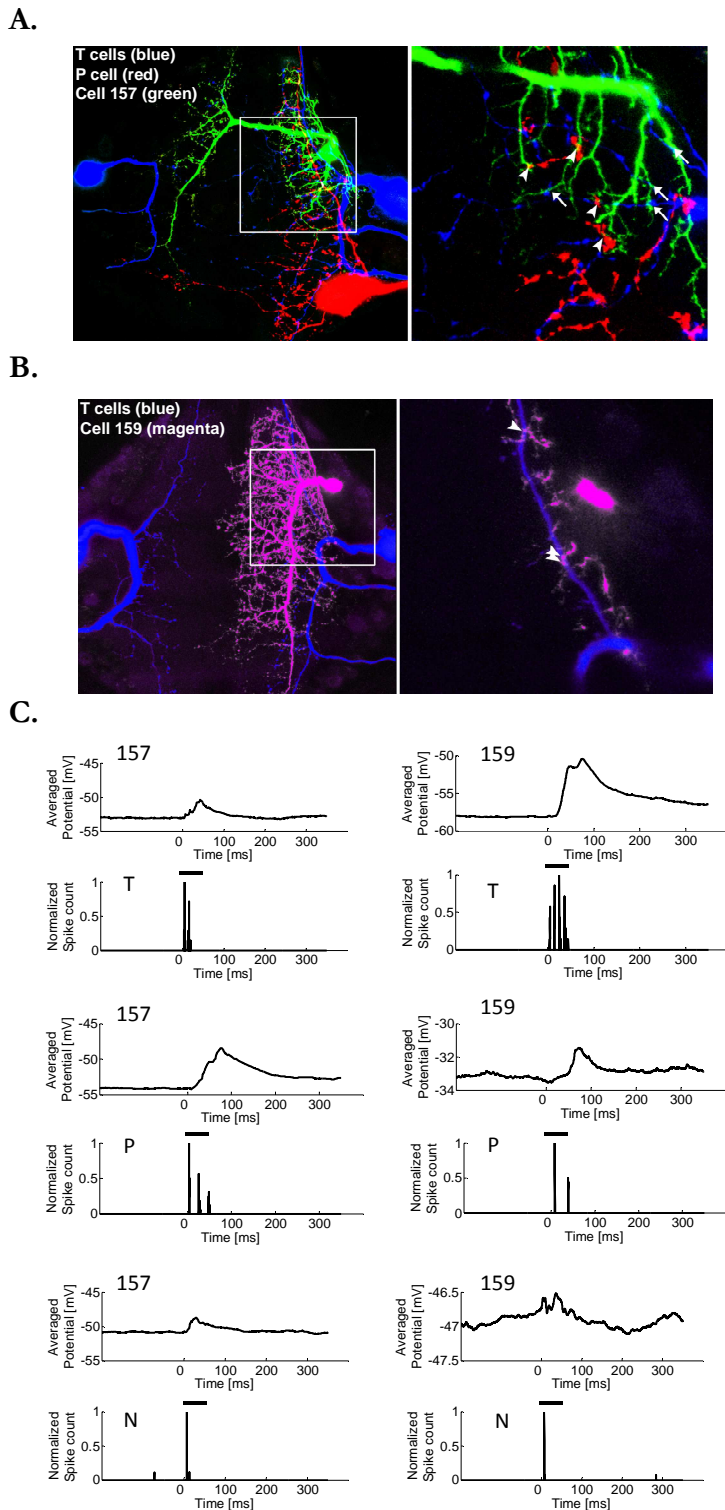


Figure 16: Connections between cell 157 and ipsilateral mechanoreceptors. **A.** Cell staining of T cells (blue), P cell (red), cell 157 (green). Magnification (right): Arrowheads indicate putative P cell input sites, arrows putative T cell input sites. From Gerrit Hilgen. **B.** Cell stainings of T cells (blue), cell 159 (magenta). Arrowheads indicate putative T cell input sites. From Gerrit Hilgen. **C.** Double recordings of mechanoreceptors - cell 157 (left), cell 159 (right). The mechanoreceptors were stimulated by current (black bar, see Methods) and IN responses were recorded simultaneously. First row: INs paired with T cells; Second row: IN with P cells; Third row: IN with N cells.

157 as well as cell 159 were analyzed by cell staining and intracellular double recordings with current stimulations of the mechanoreceptors (see *Methods*). Dr. Gerrit Hilgen obtained the cell staining, and kindly provided them for illustration purposes.

P cell, T cell as well as N cell spikes significantly changed the interneuronal membrane potential of all recorded cells 157 (see *Methods*; $p < 0.05$, Kolmogorov-Smirnov test) (Fig. 16). Connections of T and P cells to cell 157 were visualized by cell staining (Fig. 16A). The analysis showed points of contact of P cell (red) and T cell (blue) to cell 157 (green). Higher magnifications of a subset of confocal microscope layers (Fig. 16A) showed putative P cell (arrowheads) and T cell (arrows) input sites (Fig. 16A) to cell 157 (green).

To test whether all INs

respond similarly to mechanosensory cell inputs, recordings from cell 159 were performed. This IN is located near cell 157 (Lockery and Kristan, 1990b) but showed distinctly different response shapes to the same tactile stimulation (see Fig. 14). The shape of interneuronal responses, electrophysiological recordings (Fig. 16C) and cell staining (Fig. 16B) suggest also a synaptic coupling of cell 159 and T cells (see Pirschel et al., 2015), while the effect of N cells spikes in the 159 soma is less strong than in 157 (Fig. 16C).

All three types of mechanosensory cells influenced the investigated INs and cell staining suggests monosynaptic connections from mechanoreceptors to cells 157 and 159.

4.3.2 Interneuronal response latency

For the latency computation, the threshold was defined by the resting potential of the cell plus/minus its two-fold standard deviation (see *Methods*). The latency of the graded interneuronal responses was strongly influenced by fluctuations of the resting potential: appearances of spikelets, for instance, biased the definition of the threshold and so the latency. Also influences by network activity cannot be ruled out, which made the interneuronal response latency the most unstable feature.

Nevertheless, the response latency of cells 157 and 159 showed significant changes to touch location alteration and less strongly to intensity changes (Table 6, Fig. 17). Interestingly, for tactile stimulations, the response latency of cell 157 was faster than the first P cell spikes and more in the range of the latencies of T cells (Fig. 17), which indicates that the initiation or slope of the cell 157 response could be triggered by T cells rather than by P cells. Cell 159 showed also a short latency which suggests – besides its response pattern (4.3.1., Fig. 14) – a direct connection from T to cell 159 (Figs. 15 and 17).

Figure 18A shows the latency of a right cell 157 and a simultaneously recorded left P cell. The P cell did not generate spikes to stimuli at locations over $+30^\circ$ which were outside of the receptive field (Fig. 18A).

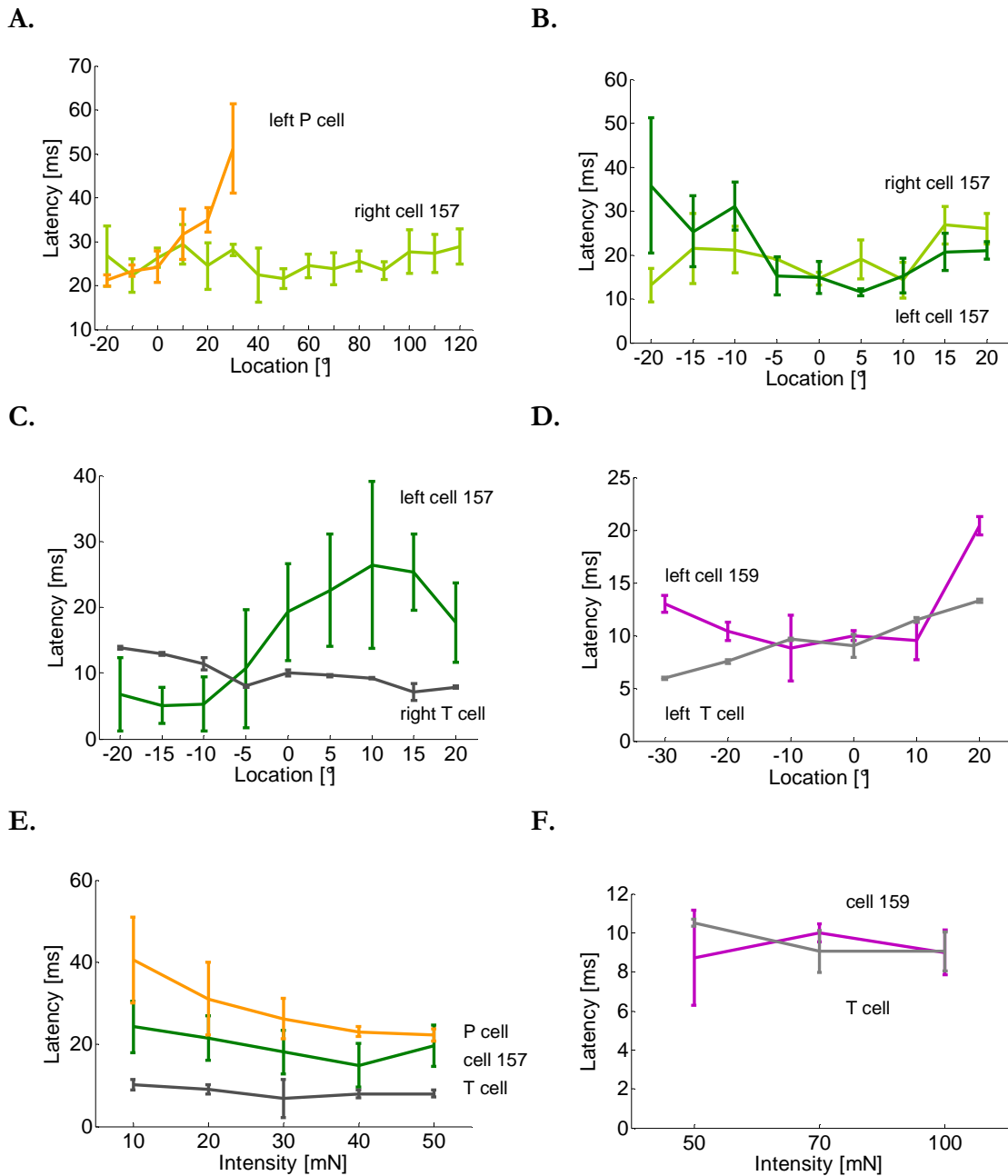


Figure 17: Examples of stimulus intensity influence on response latencies of INs. **A.** Latency in ms (mean and STD) of a right cell 157 (dark green) and a simultaneously recorded left P cell (orange), stimulated with 70 mN at locations between -20° to $+120^{\circ}$. **B.** Latency in ms (mean and STD) of a left cell 157 (green) and a right cell 157 (dark green) stimulated with 70 mN at locations between -20° to $+20^{\circ}$. **C.** Latency in ms (mean and STD) of a left cell 157 (green) and a right T cell (grey), stimulated with 70 mN at locations between -20° to $+20^{\circ}$. **D.** Latency in ms (mean and STD) of a left cell 159 (magenta) and left T cell (light grey), stimulated with 70 mN at locations between -30° to $+20^{\circ}$. **E.** Latency in ms (mean and STD) of simultaneously recorded cell 157, T cell (grey) and P cell (orange) for intensities of 10 to 50 mN at location 0° . **F.** Latency in ms (mean and STD) for a double recording of a cell 159 (magenta) and a T cell (grey), stimulated at 0° with intensities 50, 70 and 100 mN.

4.3.3. Stimulus estimation based on graded response features

The aforementioned estimation approaches (see *Methods*) were used to investigate how the response features (amplitude, integral, latency and slope) of the graded interneuronal responses of cell 157 encoded touch properties (Fig. 18). Additionally, the encoding ability of spikelets (Fig. 19) was tested.

Surprisingly, even smallest touch location differences of 5° could be discriminated significantly above threshold (Fig. 18A) (see Pirschel et al., 2015). For the pairwise discrimination of touch locations (Fig. 18A) equally good results were yielded by the amplitude and the integral as well as a combination of these features. The same combination and the integral were also the best encoders for intensity differences (Fig. 18C). However, the response feature which led to the best classification results – for location as well as intensity estimation – was the integral (Fig. 18B, D). Intuitively, this is not surprising, since the integral depends on both amplitude and slope of the interneuronal response and may reflect hence its shape most reliably. Combinations of response features or spikelet features (Fig. 19) did not improve the estimation. Accordingly, the highest mutual information with the touch location or with the intensity was also reached by the integral (Table 7). Only for high intensities, the amplitude and the combination of amplitude with integral yielded slightly higher values than the integral. Additionally, the intensity estimation performance of two left cells 157 at different locations was also analyzed (Fig. 18E). The intensity discrimination seems to be more precise when the location was closer to the receptive field center of the cells, in this case -20° .

Table 7: Normalized mutual information of response features with stimulus properties for cell 157 response features. *Ampl* = Amplitude; *A & In* = Amplitude - integral combination. Low intensities: Intensities < 50mN; High intensities: up to 100 mN.

Location	Intensity	Ampl	Latency	Integral	Slope	A & In
9 Locs	50 mN	0.46 ± 0.12	0.26 ± 0.04	0.48 ± 0.08	0.33 ± 0.09	0.46 ± 0.1
0°	5 Ints low	0.18 ± 0.11	0.14 ± 0.06	0.24 ± 0.13	0.19 ± 0.09	0.23 ± 0.11
0°	5 Ints high	0.23 ± 0.18	0.15 ± 0.13	0.22 ± 0.14	0.20 ± 0.14	0.24 ± 0.17

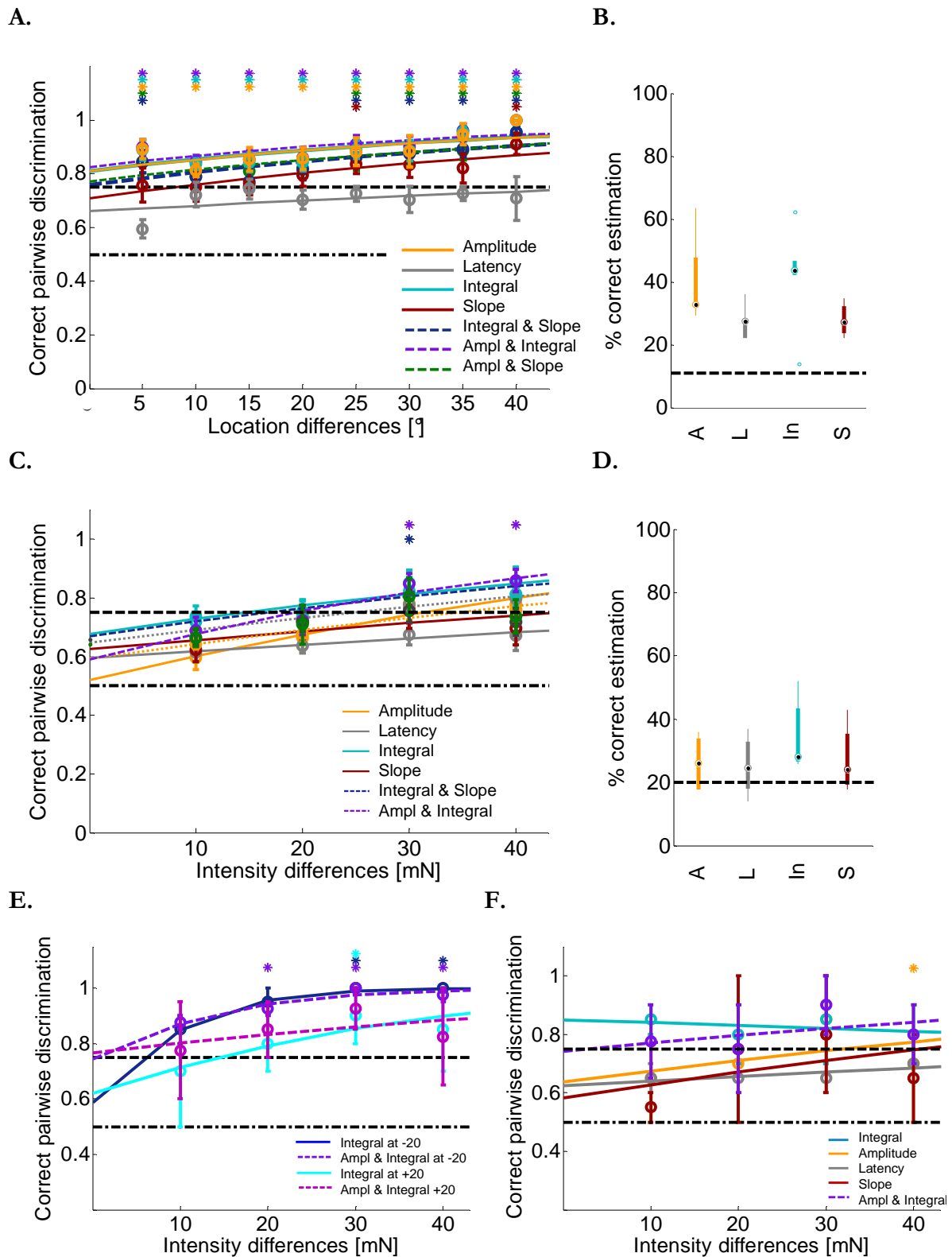


Figure 18: Stimulus estimation results for cell 157 response features. **A.** Pairwise discrimination for location differences 5° to 40° , stimulation center 0° , for 50 mN ($n = 6$). Black dashed lines show chance level and 75% threshold. Asterisks indicate mean values which are significantly ($p < 0.05$, t -test) above threshold. **B.** Classification of 9 locations for 50 mN. Black dashed line show chance level and black dots mark median values. A = Amplitude; L = Latency; In = Integral; S = Slope. **C.** Pairwise discrimination for intensity differences between 10 and 40 mN, at 0° ($n = 7$). **D.** Classification of 5 intensities between 10 and 50 mN at 0° . **E.** Pairwise discrimination of intensity differences at -20° and $+20^\circ$ of cells 157 ($n = 2$, both left). **F.** Pairwise discrimination of intensity differences at 0° for the same cells as in E.

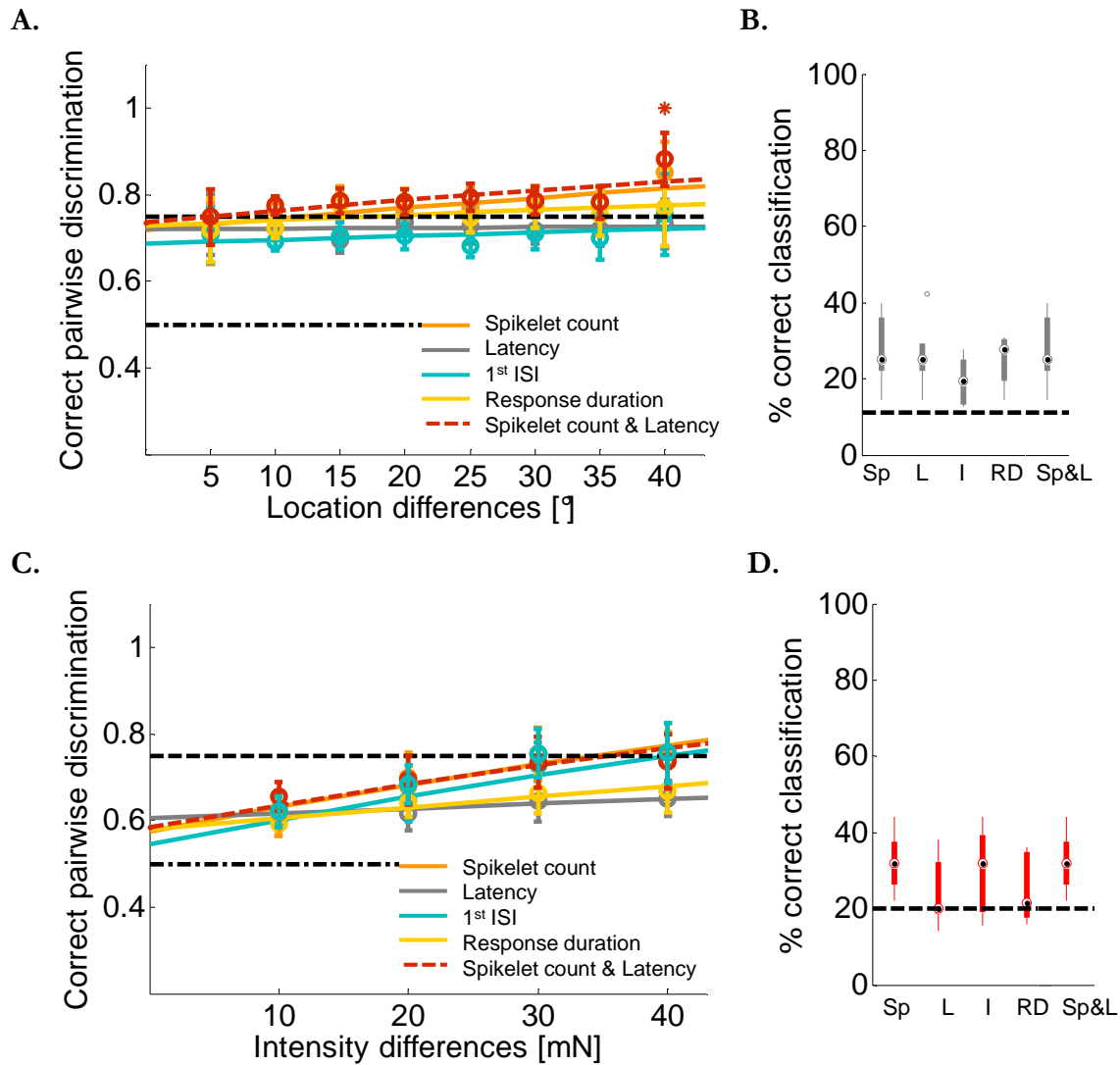
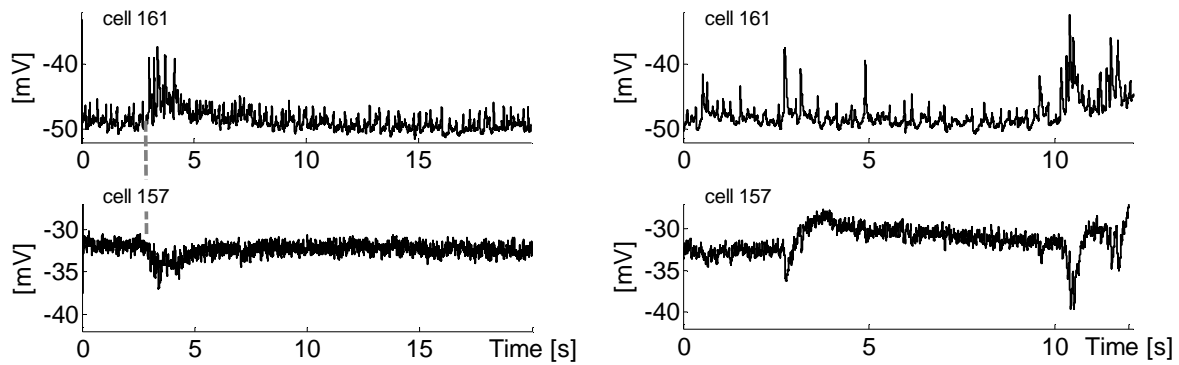


Figure 19: Stimulus estimation results for spikelet features of cell 157. **A.** Pairwise discrimination for location differences 5° to 40° , stimulation center 0° , for 50 mN ($n = 6$). Black dashed lines show chance level and 75% threshold. Asterisks indicate mean values which are significantly ($p < 0.05$, t -test) above threshold. **B.** Classification of 9 locations for 50 mN. Black dashed line show chance level and black dots mark median values. Sp = Spikelet count; L = Latency; I = 1st ISI; RD = Response duration. **C.** Pairwise discrimination for intensity differences between 10 and 40 mN, at 0° ($n = 7$). **D.** Classification of 5 intensities between 10 and 50 mN at 0° .

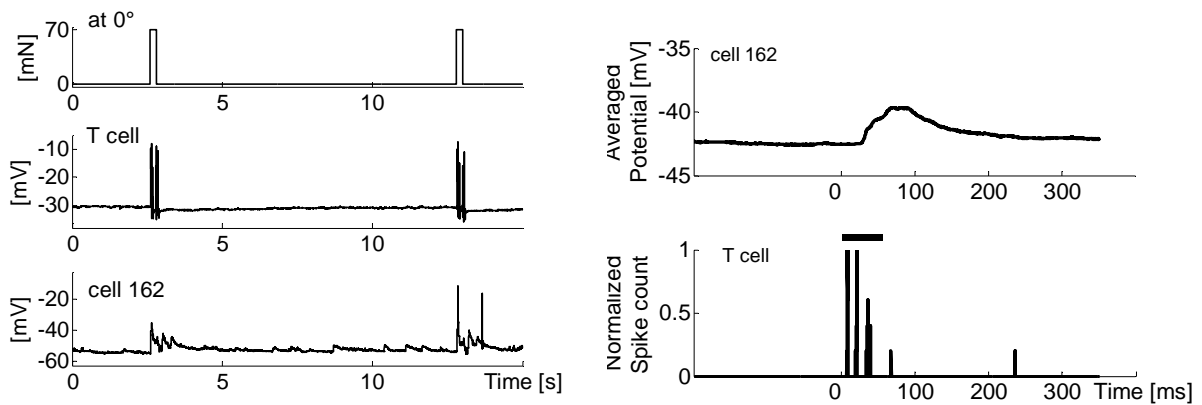
In summary, it is possible to use the responses of one IN type, which received inputs from several types of mechanosensory cells (in this case spike trains of 2 P cells and 2 T cells), for estimating the underlying stimulus properties significantly above chance and even extremely precisely (see Pirschel et al., 2015). The feature which gained the best and most reliable results was the integral of the interneuronal response (see also Kappel et al., 2011). Touch properties also seem to influence the interneuronal response features

differently from the mechanoreceptor response features (e.g., Figs. 18E and 9). This raises the question if the INs accomplish different functions, for instance, as slow integrators or as coincidence detectors and process different information about touch stimuli. That might be emphasized by the distinctly diverse response patterns of different IN types to tactile stimulation (Figs. 14, 20). For instance, cell 162 generated spikes in response to touch (Fig. 20B) and is coupled with T cells (Fig. 20B; according to Gerrit Hilgen, personal communication, the connection is also visible anatomically). Additionally, some INs were observed showing both IPSPs and EPSPs (Fig. 20A). These findings may hint to different specializations of IN types. To characterize these INs and their connections to the mechanoreceptors and to test the coding hypotheses on the level of INs might contribute to the understanding of this small neuronal network.

A.



B.



C.

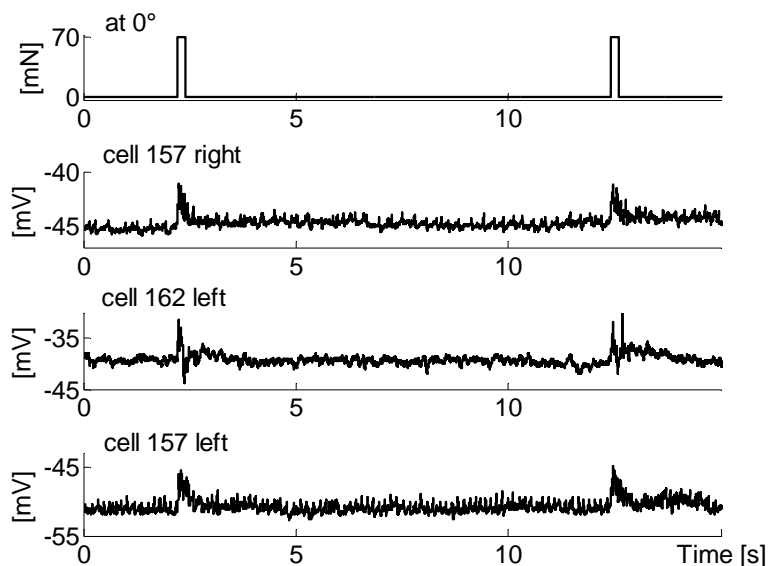


Figure 20: Exemplary neuronal responses of several local bend INs to skin stimulation. **A.** Spontaneous EPSPs of a right cell 161 (upper trace) and as a response IPSPs in a right cell 157 (lower trace). **B.** Stimulation with 70 mN at 0° and the neuronal responses of a T cell and a cell 162 (left). Response of the same cell 162 to current stimulation of the T cell (right). **C.** Recording of three INs, a right cell 157, a left cell 162 and a left cell 157 stimulated at 0° with 70 mN.

5. Discussion

The local bend behavior of the leech shows an extreme precision regarding the touch location (Thomson and Kristan, 2006). Additionally, intensity and duration of the touch influences the magnitude of the behavioral response (Baca et al., 2005). Based on these findings, the present study was designed to investigate how touch stimuli are encoded by neurons of the leech. For all three mechanosensory cell types, neuronal responses depended on touch location and intensity. Furthermore, touch duration affected both P and T cell responses. Stimulus estimation approaches revealed specific response features indicating various possible encoding mechanisms: relative latencies led to the best location estimation performances, while (summed) spike counts and the response duration represented the touch intensities and durations best. These findings may suggest that several coding strategies could be used by the small neuronal network of the leech: temporal as well as rate coding by ensembles of cells.

For the next level of the local bend network, it was found that T cells may play a bigger role than initially thought: not only neuronal responses of this cell type represent the touch location highly accurately, but also synaptic connections between T cells and the interneurons 157 and 159 exist. Touch location can be predicted surprisingly accurately based on graded responses of cell 157. In particular integrals of the interneuronal responses were suited for this task. It was also shown that the interneuronal responses vary strongly across IN types, which may indicate different specialized functions of the INs in this network.

Part of results dealing with the mechanosensory cells have been discussed also in the submitted publication (see chapter 6. for details). Here, a new view on the local bend network and a more comprehensive picture of mechanosensory coding will be discussed as well as technical limitations and future perspectives.

5.1. Technical limitations

The leech possesses in one segment 14 mechanosensory cells of 3 types in total (see *Introduction*; Kristan et al., 2005). Stimulating only the ventral area of the segment activated maximum 6 mechanosensory cells, two of each type. The N cells showed spikes reliably around 100 mN, so lower intensities activated 4 mechanoreceptors: 2 T and 2 P cells. The comprehensive investigation of responses of all three mechanoreceptor types and two types of interneurons due to three touch dimensions (location, intensity, duration) led to numerous combination options. One limitation of this study was that it was not possible to record, for instance, a full set of mechanoreceptors at the same time: the experimental setup allowed recording from up to 3 cells at the same time. This limit constituted primarily of the space available for micromanipulators and electrodes. Another factor that influenced the recording stability, especially of interneurons, and set limits to ranges of touch locations and intensities was the semi-intact preparation: the muscles, which remained connected with the ganglion via the roots, contracted in response to the touch.

An IN recording which showed recording instabilities was shown in figures 15A, B and 17A. It lasted almost 3 hours and covered 15 different touch locations. After a recording time of about 1.5h, the IN generated degraded responses due to stimulation place changes. A sudden change in the integral of the response at plus 30° can be noted (Fig. 15B, p. 56), while changes in amplitude (Fig. 15A) and response latency (Fig. 17A, p. 59) were much smaller.

To enhance the recording stability, it would be possible to use whole cell loose patch recordings for mechanosensory neurons (see Thomson and Kristan, 2006). For interneurons, this method was not a good option, because of their small graded response in the soma. Additionally, for loose patch recordings, the glial sheath had to be removed. The glial sheath regulates the potassium concentration in the space between nerve cells and it could not be ruled out that its function influences the neuronal network activity (Nicholls, 1969; Leite Costa and Moreira Neto, 2015). Furthermore, synaptic connections could be easily damaged by desheating the ganglion.

Nevertheless, the present study gave first insights into response characteristics of several INs and a comprehensive picture of mechanosensory cell responses. The results may constitute an important basis for future studies with more complex tactile stimulations (e.g., moving, rising and vibrating properties or stimulations across adjacent segments, so that receptive fields of cells of neighboring ganglia would be activated), which would further reveal refined coherences between stimulus properties, response features and cell types. Comprehensive decoding experiments (see Thomson and Kristan, 2006) including all mechanosensory cell types and several stimulus properties would additionally provide insights into the behavioral relevance of the found response features. Therefore, findings from this study would help to choose optimal stimulations. Furthermore, the descriptions of interneuron characteristics could be used, for instance, for future studies using voltage sensitive dye recordings which make it possible to record the activity of the neuronal network.

Besides experimental issues, the analysis of the neuronal responses revealed interesting questions. One aspect was statistical differences of response features (the spike count had integer numbers, the latency and interspike intervals were continuous variables and the relative features encompassed also negative numbers) and the resultant influence on the stimulus estimation. Using ranks rather than absolute response feature values solved this problem. But, response feature combinations showed that variances and distributions of the features still had an influence on the stimulus estimation. At first sight, it may be surprising that response feature combinations did not improve the estimation performances. Only when summed spike counts and relative latencies of two P and T cells, respectively, were combined for estimating stimulus property combinations, did coupling of response features add up (Fig. 11). Thomson and Kristan (2006) also found the lack of improvement by feature combinations and suggested the “lack of independence among the measures” (Thomson and Kristan, 2006, p. 8013) as a possible reason. Here, adding features also seemed to enhance redundant information, which may lead to an unfavorable variability of information rather than to a better accuracy. For instance, the summed spike count was maximal around 0° and decreased in both sides of its distribution. In contrast, the relative latency had negative values at negative touch location degrees, was 0 around 0° and became positive at positive touch locations.

Combination of these features did not improve the estimation since the summed spike count did not add information about the touch location. Moreover, the high variance of this feature negatively affected the much more precise relative latencies.

It is not known yet whether INs are able to encode the extremely precise latency differences of the mechanoreceptors and what influence the spike count and bursts of spikes may have on the interneuronal responses. In addition to electrophysiological approaches the relevance of response features (e.g., like latency, spike count or interspike intervals) of mechanosensory cells for interneuronal responses could be addressed in a computational network model, in which connection strength as well as preferred stimulus properties and varied coding strategies could be systematically analyzed. These investigations would give more insights into processing and weighting of the sensory information.

5.2. New view on the local bend network

The neuronal network of the local bend is able to process highly accurate information about touch stimulus properties and thus to elicit a precise behavioral response (Baca et al., 2005; Thomson and Kristan, 2006). Fascinatingly, only a very small number of neurons are involved in this network (Kristan, 2005). The INs form the second layer of the neuronal network of the local bend behavior. Several prior studies examined this behavior (Kristan, 1982; Lockery and Kristan, 1990; Lockery and Sejnowski, 1992; Lewis and Kristan, 1998; Zoccolan and Torre, 2002a; Baca et al., 2005; Thomson and Kristan, 2006), but it was still unknown how the INs process touch properties. Based on these facts, I aimed to reveal how the INs respond to tactile stimulation of the skin, how INs are connected to all types of mechanosensory cells and if it is possible to predict the presented stimulus from interneuronal responses.

Stimulus estimation methods are mainly used for analyses of spike trains (Averbeck et al., 2006; Pouget, 2000). However, in this study, features of graded responses were used to estimate underlying stimulus properties. The results were more than convincing: smallest

location distances and intensity differences could be discriminated based on responses of one IN, which processed in that case spike trains from 4 mechanosensory cells (2 T cells and 2 P cells). The interneuronal responses, which look on first sight quite noisy, seem to decode the spike trains of the mechanosensory cells in a precise manner. The integral of responses led to the best stimulus estimations. This feature was influenced by slope and amplitude of the response and therefore probably led to the most reliable interpretation of the signal. The slope and the response latency, on the other hand, showed the lowest estimation performances. To the latency of interneuronal responses applied that spikelets or other fluctuations of the resting potential strongly influenced the reliability of the computation. Different spikelet frequencies in the INs could be observed depending on membrane potential levels. A study by Lockery and Kristan (1990b), which found the same relation between spontaneous spikelets and the membrane potential, did not find a correlation between these small action potentials and events in motor neurons. Therefore, it is not clear yet how relevant interneuronal spikelets may be for synaptic transmission. Here, the estimation performance of spikelet features like counts and interspike intervals only achieved stimulus estimation results slightly above chance level (Fig. 19, p. 62).

Previous studies on the local bend behavior focused on P cells and synaptic connections between this cell type and local bend INs (Lockery et al., 1989; Lockery and Kristan, 1990a, b; Lockery and Kristan, 1991; Lockery and Sejnowski, 1992; Lockery and Sejnowski, 1993a, b; Lewis and Kristan, 1998a, b, c). In this study, connections between INs and all types of mechanosensory cells were investigated. Staining of multiple cells (kindly provided by Dr. Gerrit Hilgen) showed putative input sites of P and T cells to cell 157 as well as of T cells and cell 159 (Fig. 16A, B, p. 57). Furthermore, N cell spikes were able to elicit PSPs in cell 157 (Fig. 16C). These results suggest that information from all mechanosensory cells could be integrated in cell 157. Lockery and Kristan (1990b) described that synaptic potentials cell 159 did not show time-locking to P cell spikes while other local bend INs did. This finding could be explained by the influence of T cells on the cell 159 found in this study (Figs. 14 and 17, p. 55 and 59).

The experimental sketch of the receptive field of the IN cell 157 (Fig. 15A, p. 56) fit in with the receptive fields of other local bend INs, which Lewis (1999) inferred in his study

using the experimental data of Lockery and Kristan (1990b). IN types exist in pairs, receiving inputs from all mechanosensory types existing in one ganglion (Kristan et al., 2005). This indicates that INs may have a broader receptive field than the mechanosensory cells – depending on their connections to the mechanosensory cells. This hypothesis was confirmed by the results of this study (see Fig. 15A): The cell 157 responded over a range of 140° with still increasing responses, which indicates a receptive field of about 280° or broader, whereas the mechanosensory cells overspan an area of about 180° (Kristan et al., 2005). Additionally, the different response patterns of the IN types (Figs. 14 and 20, p. 55 and 64) lead to the conclusion that IN types with different coding functions should exist in this network.

For instance, cell 157 and 159 showed short response latencies, ranging between the T cell and the P cell response latencies (Figs. 17 and 5, 7, p. 59 and 38,42). Furthermore, previous findings may suggest an involvement of cell 157 and 159 in other behaviors: Briggman and colleagues (2005) used voltage sensitive dye recording to investigate decision-making in the leech and found neurons which discriminated very early in time between the two behaviors of swimming and crawling (Briggman et al., 2005). These neurons were found in the region of the ganglion where cell 157 and 159 are located (Briggman et al., 2005: Fig. 4C). The neuronal system of the leech with its small amount of neurons gains complexity, suggesting that the same INs could switch between behaviors (Shaw and Kristan, 1997; Baca et al., 2005, Briggman et al., 2005).

In conclusion, the local bend network appears to be more complex than a “simple” feed forward network with only input from one mechanosensory cell type (Lockery et al., 1989; Lockery and Kristan, 1990a, b; Lockery and Kristan, 1991; Lockery and Sejnowski, 1992; Lockery and Sejnowski, 1993a, b; Lewis and Kristan, 1998a, b, c). Results of this study outline a network that involves particularly the T cells and possibly N cells in addition to the P cells. Furthermore, the different response patterns of the IN types may indicate different specializations. It might be that INs process as coincidence detectors the relative latencies and consequently decode the touch location, or merge, as slow integrators, the spike counts for decoding the touch intensity. Descending interneurons which showed specialized stimulus property preferences were found in the stick insect antennal mechanosensory pathway (Ache and Dürr, 2013). However, none of these

groups of interneurons were activated by only one stimulus property (Ache and Dürr, 2013).

5.3. Coding strategies

A number of studies examined the local bend behavior and the corresponding mechanosensory cells, but details about encoding of stimulus property combinations and correlations of response features and cell types were still unknown. Different coding mechanisms based on neuronal responses can be employed to solve this question: rate coding as well as temporal coding, single cell and population coding mechanisms and multiplexed encoding with single and combined response features. Here, my aim was to answer questions about fundamental principles of neuronal coding in a simple neuronal network.

5.3.1. Rate coding versus temporal coding

Different coding mechanisms were found to predict best the touch properties: The touch location was represented by a fast temporal code, the duration by a slower temporal feature and the intensity was encoded by a rate code.

These results may answer open questions from previous studies: Thomson and Kristan investigated the encoding of stimulus location based on two P cells with overlapping receptive fields and analyzed response features of spike counts, latencies and their relative combinations (Thomson and Kristan, 2006). The discrepancy between encoding and decoding of relative latencies, combined with the results of this study, may indicate a behaviorally relevant involvement of T cells in decoding of touch locations.

Furthermore, Baca and colleagues found that the ability of leeches to discriminate stimulus intensities is higher for low intensities and falls off linearly with rising intensities. They also found that a longer stimulus duration improves the discriminability (Baca et al., 2005). Similar effects were also described in psychophysical measurements of monkeys (Hernandez et al., 1997). However, the encoding performance for the touch location was not improved by longer stimulus durations (Lewis and Kristan, 1998; Baca et al., 2005).

Hence, the first 100 ms of two P cell responses were concluded to convey the information about the stimulus location (Lewis and Kristan, 1998). Both observations also agree well with the results of this study: If touch location are encoded by the latency difference of a cell pair, additional spikes will not improve the estimation. For the intensity, which was best predicted by a rate code, longer stimulus durations would increase the ability to discriminate behaviorally relevant intensity values (see Baca et al., 2005).

5.3.2. Individual cells versus cell ensembles

The response of each cell type carried information about all stimulus properties. But a more complete and precise image of the stimulus was processed by incorporating several cell types. The results showed that stimulus properties could be predicted based on responses of single cells but combinations of different locations and intensities were almost perfect encoded by responses of four cells of two types.

For leech mechanoreceptors, previous studies claimed specializations for the different mechanoreceptor types: Carlton and McVean (1995) stated that “T cells function more like displacement receptors at low velocities and more like velocity receptors above the transition point” (Carlton and McVean, 1995; p. 790), whereas P cell activation was concluded to be the main trigger of the local bend response (Nicholls and Baylor, 1968; Kristan, 1982; Lewis and Kristan, 1998c; Zoccolan and Torre, 2002b).

I want to merge these results into one hypothesis: the key task of the local bend network is the encoding of the touch location. To perform this task as accurately as possible, the neuronal network is specialized to minimize influences of, for instance, the touch intensity on the response latency by having cells with strongly overlapping intensity ranges. The significant effect of the touch intensity on the response latency attenuates at higher amounts, whereas it influences spike counts more strongly (see Tables 2, 3; p. 37, 41). That applies to P cells in particular. For a broad range of intensities, T cells showed extremely precise latencies, while P cell latencies became more accurate for touch intensities of about 100 mN (Fig. 7C, p. 42). Both cell types were activated at behavioral relevant stimulus intensities (Carlton and McVean, 1997; Baca et al., 2005). Conceivably,

T cells may play an important role in coding touch locations, while P cell responses are able to modulate the strength of the muscle responses and gain more impact on the location coding with higher touch intensities. Assuming that precise encoding of the touch location is the key task, using this combination of extremely precise first spikes and spike counts, lead to a fast encoding, which enables a fast and precise behavioral response adjusted to touch intensities and durations.

5.3.3. Separated coding versus multiplexed coding of stimulus properties

Estimations of individual stimulus properties and their combinations revealed that responses of T and P cells contained information about all stimulus properties. It was possible to associate individual response feature with particular stimulus properties: for instance, relative latencies with touch locations and spike counts with touch intensities.

Moreover, the specific response features found in the analysis suggesting a multiplexing in the sense of Panzeri et al. (2010). The multiplexed code is a “neural code in which complementary information is represented on different temporal scales. For example, when information is represented by the precise timing of individual spikes on the scale of milliseconds and the slow modulation of the spike count on the scale of hundreds of milliseconds.” (Panzeri et al., 2010, p. 111).

The estimation performances of two T and two P cells for location-intensity combinations showed this multiplexing (Fig. 11, p. 49): using the summed spike count for encoding of touch intensities and the relative latency for estimation of locations yielded better results than individual features. Combinations across cell types (summed spike count of P cells and relative latencies of T cells) predicted 3 locations combined with 2 intensities almost perfectly (see Fig. 11B). However, for 5 locations combined with 3 intensities, the estimation based on cells of the same type and across cell types did not differ significantly (see Fig. 11F).

In sum, this small and simple system seems to use the specializations of cell types with different response characteristics and shows an impressive computational strategy of balancing between producing redundant information (neuronal responses contain the

information about all stimulus properties) and uniqueness (the extremely reliable first spikes of T cells or the sustained responses of the P cells).

5.4. Of Worms and Men...

The mechanoreceptors of the leech show similar spiking patterns to human SA1- (P cells; sustained, slowly adapting) and FA1-/ RA- afferents (T cells; rapidly adapting, on- and off-bursts; Figs. 5A, 7A) (leech: Figs. 5A, 7A, 10A and 14; Nicholls and Baylor, 1968; Baca et al., 2005; human: Vallbo and Johansson, 1984; Wheat et al. 1995; Johansson and Flanagan, 2009; Abreira and Ginty, 2013). Furthermore, leech mechanoreceptors could be regarded as afferents (their cell soma) with skin receptors (their nerve endings). Thus, the leech may be, besides investigating of coding in a small neuronal network, also interesting for studying fundamental coding principles of the sense of touch. Studies of the primate sense of touch are discussed here and, in more detail, in the submitted publication (Pirschel and Kretzberg, 2015; see *Publications* for details).

In primate tactile afferents, the temporal structure of mechanosensory spike patterns conveys information about spatio-temporal properties of a tactile stimulation and shapes the perception (Johansson and Briznieks, 2004; Johansson and Flanagan, 2009; Mackevicius et al., 2012; Weber et al., 2013; Harvey et al., 2013), whereas the intensity of a touch is represented in a rate code (Bensmaia, 2008; Harvey et al., 2013). Thus, Muniak et al. hypothesized, in their study on monkeys, that intensity perception is mainly encoded in weighted firing rates of the three main mechanoreceptive afferents and that information of different stimulus properties of these submodalities would all in all give a complete picture of the stimulus intensity (Muniak et al., 2007).

The aforementioned results of the leech mechanosensory system agree with these suggestions: temporal features encode spatial information while spike count features of several cell types convey information about the stimulus intensity. Furthermore, evidence for multiplexed coding is not only found in this study of the leech but is also discussed across various sensory modalities and animal models (Panzeri et al., 2010; Fotowat et al., 2011; Ainsworth et al., 2012; Wohrer et al., 2013) and in particular for the tactile sense of

primates (Harvey et al., 2013; Saal and Bensmaia, 2014). More complex, natural stimulations, such as touching and manipulating objects, always evoke responses in both SA and FA afferents and induce perceptions based on several stimulus properties (Johansson and Flanagan, 2009; Saal and Bensmaia, 2014). Recent studies claim that – contrary to the classical “labeled line” theory (Abreira and Ginty, 2013; Zevke et al., 2013), which assumes that afferent types remain segregated – that neurons of the somatosensory cortex receive inputs from several afferent types and tactile information is integrated already on early stages of processing (Saal and Bensmaia, 2014).

Similarly, although much simpler, the investigated INs of the local bend network integrate responses of several mechanosensory cell types and may process specific features.

In conclusion, despite the simplicity of the neuronal network, this study provides evidence that sensory coding is rather based on combined response features across cell types than on a dichotomy of rate code versus temporal code in separated cell ensembles. The leech with its simple nervous system provides not merely experimental advantages but also insights into integration principles and multiplexed coding of stimulus properties similar to findings in human somatosensation.

6. Publications

1. Multiplexed Encoding of Stimulus Properties by Leech Mechanosensory Cells

Friederice Pirschel¹, Jutta Kretzberg^{1,2}

¹ Computational Neuroscience, Department for Neuroscience, University of Oldenburg, D-26111 Oldenburg, Germany

² Cluster of Excellence "Hearing4all", University of Oldenburg, D-26111 Oldenburg, Germany

Submitted on 5th May 2015 to the Journal of Neuroscience (JN-RM-1753-15), reviews and option for resubmission received on 4th June, 2015.

Submitted manuscript is attached.

2. Decoding of Tactile Stimulus Parameters by Interneurons of the Local Bend Network

Friederice Pirschel¹, Gerrit Hilgen³, Jutta Kretzberg^{1,2}

¹ Computational Neuroscience, Department for Neuroscience, University of Oldenburg, D-26111 Oldenburg, Germany

² Cluster of Excellence "Hearing4all", University of Oldenburg, D-26111 Oldenburg, Germany

³ Institute of Neuroscience, Newcastle University, England, United Kingdom

In preparation, planned submission to the Journal of Neurophysiology in June 2015.

3. Encoding of Tactile Stimuli by Mechanoreceptors and Interneurons of the Leech

In preparation, submission deadline: 31.7.2015.

Frontiers Research Topic “Coding properties in invertebrate sensory systems“ organized by Sylvia Anton, Anders Garm.

Multiplexed Encoding Of Stimulus Properties By Leech Mechanosensory Cells

Friederice Pirschel¹, Jutta Kretzberg^{1,2}

¹ Computational Neuroscience, Department for Neuroscience, University of Oldenburg, D-26111 Oldenburg, Germany

² Cluster of Excellence "Hearing4all", University of Oldenburg, D-26111 Oldenburg, Germany

Abstract

Sensory coding has long been discussed in terms of a dichotomy between spike timing and rate coding. However, recent studies found that in primate mechanoperception and other sensory systems spike rates and timing of cell ensembles complement each other. They simultaneously carry information about different stimulus properties in a multiplexed way. Here, we present evidence for multiplexed encoding in the tiny ensemble of leech mechanoreceptors, consisting of only four individual cells. Each mechanoreceptor neuron of the leech varies spike count and response latency to both touch intensity and location, leading to ambiguous responses to different stimuli. Nevertheless, three different stimulus estimation techniques consistently reveal that the neuronal ensemble allows reliable decoding of both stimulus properties. The relative timing of the first spikes of two mechanoreceptors encodes stimulus location, while summed spike counts represent touch intensity. These results apply to two mechanoreceptor types, the transient responses of T (touch) cells, as well as the sustained responses of P (pressure) cells. Differences between the cell types become evident for the estimation of combined stimulus properties. The best estimation performance is obtained when the relative first spike timing of the faster and temporally more precise T cells for stimulus location. Simultaneously, the sustained responses of P cells indicate touch intensity by summed spike counts and stimulus duration by the duration of spike responses. The striking similarities of these results with previous findings on primate mechanosensory afferents suggest multiplexed encoding as a general principle of somatosensation.

Key words: sensory coding, mechanosensors, latency, spike count, multiplexing, population coding, leech, local bend network

Acknowledgments: We thank Go Ashida and all group members for critically reading the manuscript, Lena Koepcke for mathematical advice and PhD program ‘Neurosenses’ (MWK) for financial support.

Introduction

Encoding of sensory stimuli has been studied intensively across species and sensory systems. Nevertheless, several open questions still remain in particular for encoding of complex stimuli, comprising combined stimulus properties. Traditionally, neural coding has been discussed in terms of dichotomies: 1) Rate encoding versus temporal encoding (Theunissen and Miller, 1995); 2) encoding by individual cells versus cell ensembles (Sakurai, 1996); 3) encoding of single stimulus properties versus multiplexing (Panzeri et al., 2010).

These three pairs of hypotheses have been discussed recently for the somatosensory pathway of the primate hand (Saal and Bensmaia, 2014). They concluded that populations of mixed cell types encode different properties of touch stimuli in a multiplexed way, using both rate coding and temporal response features. In our study, we have tested the three pairs of hypotheses for a much smaller somatosensory system, the tiny ensemble of leech mechanosensory cells.

The skin of the leech is innervated by three different types of mechanoreceptors, which are classically attributed to different intensities of tactile stimuli: T cells for touch, P cells for pressure and N cells for noxious intensities (Nicholls and Baylor, 1968). These individually characterized cells provide the sensory input for a reflex behavior, which we can use to scrutinize their encoding properties. The local bend reflex (Kristan et al., 2005) causes the leech body wall to bend away from tactile stimulation depending on touch intensity, location and duration. Touch locations are discriminated by the leech mechanoreceptors even more finely than by the human finger tip, causing different behavioral reactions for stimuli that are only 500 μm apart (Baca et al. 2005, Thomson and Kristan, 2006).

The goal of this study is to identify the encoding properties of the mechanosensory cell ensemble which form the basis of this surprisingly precise behavior. We have

adopted the approach of Thomson and Kristan (2006), who investigated encoding of touch location by spike count versus response latency of mechanosensory P cells. They have found that relative latency of two P cells encodes touch location precisely enough to explain the behavioral performance. Their results agree with the evidence for latency coding of location-specific information in other systems like the somatosensory cortex of rats (Foffani et al., 2004) and human tactile afferents (Johansson and Briznieks, 2004). However, Thomson and Kristan also have shown that two P cells responding with specific latency differences to electrical stimulation could not trigger local bend movements with the same local precision as touch stimuli applied to the skin. To solve this contradiction, we have introduced three new aspects into the analyses, which allow us to infer a much more complete picture of the sensory coding:

Firstly, we have investigated responses of all three mechanosensory cell types. Since only maximally two cells of each type innervate each patch of the skin, an ensemble of maximally six cells must transmit all tactile information available to the animal.

Secondly, we have extended the list of analyzed neuronal response features. Interspike intervals, burst properties, and combinations of response features have been considered as additional candidate codes. Like Thomson and Kristan (2006), we have compared coding performances of individual cells and cell pairs for all response features.

Thirdly, we have analyzed encoding of three stimulus properties, touch location, intensity and duration, as well as their combinations. While intensity and duration have been shown to shape behavioral responses of the leech (Baca et al. 2005), their encoding by mechanosensory cells have not been studied so far.

When considering combinations of stimulus properties and multiple response features in all cell types, leech tactile encoding strikingly resembles published findings obtained in the

primate fingertip (Saal and Bensmaia, 2014): While each sensory cell responds ambiguously to different combinations of stimulus properties, a tiny ensemble of four cells with mixed cell types encodes stimulus combinations cooperatively. Relative spike timing encodes stimulus location and combined spike counts represent stimulus intensity simultaneously in a multiplexed way.

Materials and Methods

Physiology

We used adult medicinal leeches from Biebertaler Leech Breeding Farm (Biebertal, Germany). The leeches weighed 1 - 2 g and were kept in tanks with Ocean Sea Salt 1:1000 diluted with purified water at room temperature. Animals were anesthetized with ice-cold saline (Muller et al., 1981) before and during dissection. Experiments were done at room temperature. In total, 70 preparations were used for this study. The body-wall preparation (Fig. 1) consisted of mid-body segments 9 to 11 with corresponding ganglia of the ventral nerve cord. Innervations of segment 10 remained unscathed. The body-wall was flattened and pinned out with the epidermal side of the skin facing upwards in a

Table 1: Varied stimulus properties in the different stimulation protocols.

Encoding task	Location [°]	Intensity [mN]	Duration [ms]
Location	-20 to +20 in 5° steps	10, 50, N cells: 100	200
Intensities low	0	10, 20, 30, 40, 50	200
Intensities high	0	10, 20, 50, 70, 100	200
Duration	0	60	50, 200, 500
Duration & Intensity	0	20, 60	50, 200, 500
Location & Intensity	-20, 0°, +20	10, 50	200

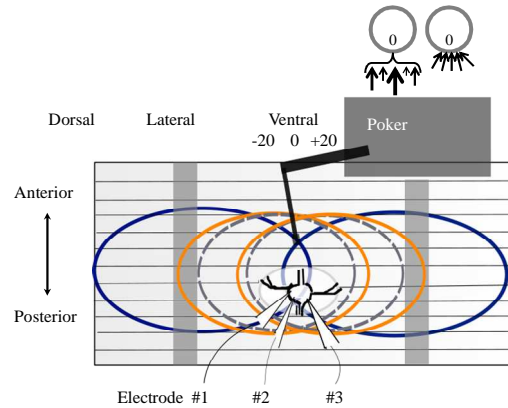


Figure 1: Sketch of the body-wall preparation with receptive fields of T cells (grey), P cells (orange) and N cells (blue). Ventral midline is defined as 0°. Touch locations to the right were stated as plus degrees and to the left as minus degrees. The left end of the preparation marks minus 180°, the right side plus 180°. Responses of 1 to 3 mechanosensory cells were recorded intracellularly while the skin was stimulated mechanically by the poker.

plastic Petri dish, which was coated with a silicone elastomere (Sylgard; Dow Corning Corporation, Midland, MI, USA). In the area of the 5th annulus (counted from anterior) of segment 10, a hole was cut into the skin to provide access to the ventral side of the ganglion, where mechanosensory cell somata are located (Kristan et al., 2005). The skin was stimulated at the middle annulus (3rd annulus of segment 10), which was identified by location of the sensilla (Blackshaw et al., 1982).

The ventral midline of each preparation was defined as 0°. Touch locations to the left are denoted as negative and to the right as positive numbers of degrees (Fig. 1). While stimulating the skin mechanically, we performed single, double or triple intracellular recordings from mechanosensory cells of all types: Pressure (P) cells, Touch (T) cells and Noxious (N) cells (see Nicholls and Baylor, 1968). These cells have been well-studied and are easily identifiable based on their location in the ganglion, their size and electrical properties (Nicholls and Baylor, 1968; Kristan et al., 2005). We used glass electrodes with resistances between 20 and 40 MΩ, filled with potassium-acetate (3M). For numbers of

recorded cells and cell pairs see Tables 2, 3 and 5. The experimental rig consisted of mechanical micromanipulators type MX-1 (Narishige Group, Japan), amplifiers (model SEC-05X and BA1S) from NPI electronic (Tamm, Germany) and the data was acquired by an interface BNC-2090 with NI PCI-6036E board from National Instruments (Austin, TX, USA). Neuronal responses were recorded (sample rate 10 kHz) and analyzed with a custom-developed Matlab software (MathWorks, Natick, MA, USA).

Stimulation

For applying pressure stimuli onto the skin, we used a Dual-Mode Lever Arm System (Aurora Scientific, Ontario, Canada, Model 300B) (see Baca et al. 2005; Thomson and Kristan, 2006) with a poker tip size of 1 mm^2 . The stimulus was varied in intensity (5 to 200 mN) and location (-20° to $+20^\circ$, relative to ventral midline, in 5° steps). Touch lasted 200 ms (see Thomson and Kristan, 2005; Lewis and Kristan, 1998) except for the duration encoding experiments, in which stimulus durations of 50, 200 and 500 ms were combined with intensities of 20 and 60 mN at 0° (Table 1). All combinations of stimulus properties were presented 10 – 15 times in pseudo-randomized order.

Analyzed Response Features

The time of maximum spike amplitude was defined as the spike time. The neuronal responses were quantified by the following response features for single as well as for two simultaneously recorded cells (cell pair):

- A. Spike count: total number of spikes elicited by a single cell during the stimulation.
- B. Relative spike count: difference of spike counts of a cell pair.
- C. Summed spike count: sum of spike counts of a cell pair.
- D. Latency: time between stimulus onset and first spike of one cell.
- E. Relative latency: time difference of the first spikes of a cell pair.

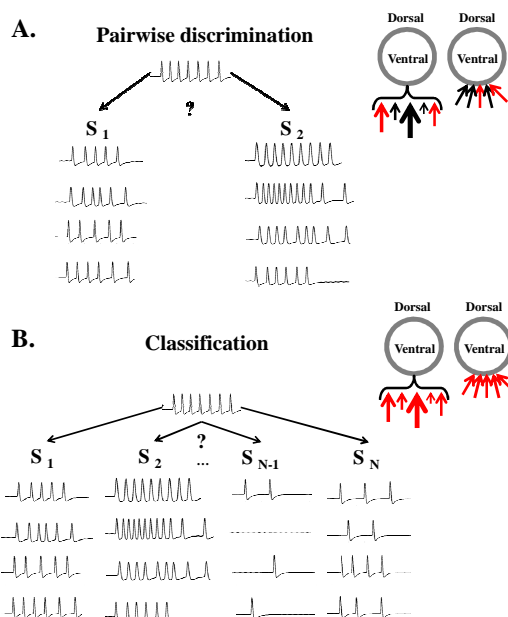


Figure 2: Sketch of the two estimation approaches. **A** Pairwise discrimination task: the stimulus is estimated based on response features evoked by two different stimuli. Red arrows indicate exemplary stimulus intensities (left) or locations (right), for which responses are shown in the figure and used for the shown discrimination task. **B** Classification task: the stimulus is estimated based on response features evoked by a set of N stimuli. Red arrows indicate stimulus intensities (left) or locations (right), for which cell responses were classified.

- F. First interspike interval (1^{st} ISI): time difference between the first and second spike of one cell.
- G. Relative 1^{st} ISI: time difference of the ISIs of a cell pair.
- H. Response duration: time difference between the first spike and the last spike of the elicited neuronal response.
- I. Burst strength: number of spikes in a burst of one cell.
- J. Burst duration: time difference between first and last spike in a burst of one cell.

Bursts were identified based on the distribution of ISIs. If this distribution was bimodal, we defined a threshold separating burst ISIs from longer ISIs (Oswald et al., 2007). The responses of all mechanoreceptor types were tested for occurrence of bursts. Since only T cells were found to generate bursts (see Fig. 4

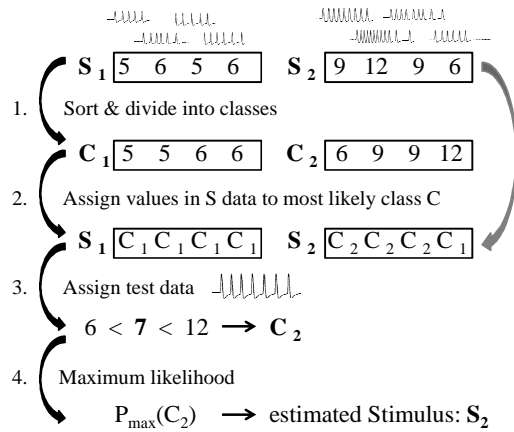


Figure 3: Sketch of the stimulus estimation process. S = Training data set elicited by stimulus number N ; C = Response feature rank class. Top row: 4 example trials for each of two stimulus conditions and their corresponding spike counts (used as example response feature in this figure). 1.: Spike counts are sorted and divided into classes of equal size. 2.: For each response elicited by a specific stimulus the most probable response feature rank class is determined. 3.: The response feature value (here: spike count) is determined for a test trial, compared to the borders of the response feature rank classes, and assigned to one class according to its rank. 4.: For the test trial, the stimulus class with the highest probability of eliciting the calculated response feature rank class is the estimated stimulus.

and 5; Baltzley et al., 2010) burst features of this cell type are shown in Figures 4, 6 and 7.

Stimulus Estimation

The aim of stimulus estimation is to calculate how well the value of a stimulus property can be estimated based on a specific response feature. We used two stimulus estimation approaches based on a maximum likelihood method (Aldrich, 1997): Pairwise discrimination and stimulus classification (see below and Fig. 2). In both approaches a “leave one out” validation was applied (Quiroga and Panzeri, 2009). Each trial was used separately as test data, while the remaining trials comprised the training data set, for which it was known which stimulus elicited which response. This training data set was used to calculate the confusion matrix (see next section) for each response feature. For the test trial, we determined the response feature class (see next paragraph) that was most probable to elicit the observed feature value. The estimated stimulus for each test trial (Fig. 2) was defined as the stimulus value with the highest probability of eliciting a response belonging to the test trial’s response feature class (maximum likelihood). If more than one

Table 2: Number of cells used for stimulus estimation.

Encoding task	T cells		P cells		N cells		NP combined		TP combined	
	Single cells	Cell pairs	Single cells	Cell pairs	Single cells	Cell pairs	Single cells	Cell pairs	Single cells	Cell pairs
Location	10	5	10	5	8	4	-	-	-	-
Intensities low	14	7	24	12	-	-	-	-	-	-
Intensities high	16	8	10	5	-	-	14	7	22	11
Duration	10	-	12	-	-	-	-	-	-	-
Duration & Intensity	10	-	12	-	-	-	-	-	-	-
Location & Intensity	10	5	10	5	-	-	-	-	-	-

stimulus value shared the highest probability, the trial was assigned to all of them to equal parts. Finally, we calculated the percentage of correct estimations by comparing the estimated stimuli with the stimulus values, which experimentally elicited the responses.

Response Feature Classes for Stimulus Estimation

For a fair comparison of the different response features A-J, we processed all of them in the same way even though they differed considerably in their statistical properties (e.g. spike count can only have integer numbers < 20 , while latency is a continuous variable). Therefore, we used response feature ranks rather than absolute values:

1. We determined for each response feature (see Fig. 3), based on the training data set $S_{\{1,\dots,N\}}$, the rank classes $C_{\{1,\dots,N\}}$ where N was the number of different stimuli presented in the experiment (Table 1). The absolute values of S were sorted and divided into commensurate classes C . Consequently, S_i contain all the (unsorted) response feature values which were evoked by stimulus No. 1, whereas C_j could contain values which were evoked by other stimuli $S_{\{1,\dots,N\}}$ (see Fig. 3).

2. Each absolute response feature value of the training data set S was assigned according to its rank to the most likely class C (Fig. 3).

For feature combinations, the class indices $\{1,\dots,N\}$ of each feature were summed after this assignment. Hence, the training data set S could be used for further analysis in the same way as for single feature response classes.

3. In the same way, the test data was assigned to the most probable response feature class C (Fig. 3).

If in step 2 and 3 the same response feature value (e.g. a spike count of 6; Fig. 3) was contained in more than one class contained, this value was assigned to the class with the highest number of occurrence (maximum likelihood; Fig. 3). If two or more classes were equally probable to elicit the specific value, one of them was chosen by chance.

4. The determined class C of the test data was now assigned to the stimulus with the highest probability evoking this class C (Fig. 3).

Finally, we calculated an $N \times N$ confusion matrix showing how often each of the N stimulus values elicited a response belonging to each of the N response feature classes.

This procedure was used for all response features A-H individually and in all possible pairwise combinations for all cells. For T cells, we additionally analyzed burst strength (I.) in combination with burst duration (J.) and with relative latency (E.) as feature pairs.

Pairwise discrimination

The pairwise discrimination (Fig. 2A) deals with the question how well two stimuli can be discriminated based on specific response features. This approach reveals the minimum differences between intensities or locations, which can be discriminated based on the neuronal responses. Results are represented as mean values with standard error of the means (SEM) and fitted with a logistic function. Chance level of pairwise discrimination is 0.5 and discrimination threshold was defined as 0.75 (75% correct estimation) (Johnson and Philips, 1981; Thomson and Kristan, 2006).

Classification

The idea of the classification approach is to quantify how well a set of N stimuli can be estimated based on a specific response feature (Fig. 2B). The test data was assigned to values of the complete stimulus set. Results are given in % correct and displayed in boxplots (Figs. 4, 6, 7), in which black dots mark the median values and box edges the 25th (q_1) and 75th (q_3) percentiles. Whiskers show minimum and maximum data values, which were not considered as outliers. Outliers, determined by the standard Matlab boxplot function as values $x > q_3 + 1.5(q_3 - q_1)$ or $x < q_1 - 1.5(q_3 - q_1)$, are plotted as individual dots. Since in our data set all stimuli were presented equally often, the chance level for this method was defined as $100/N$ %.

With the classification approach, we analyzed the stimulus properties location, intensity and

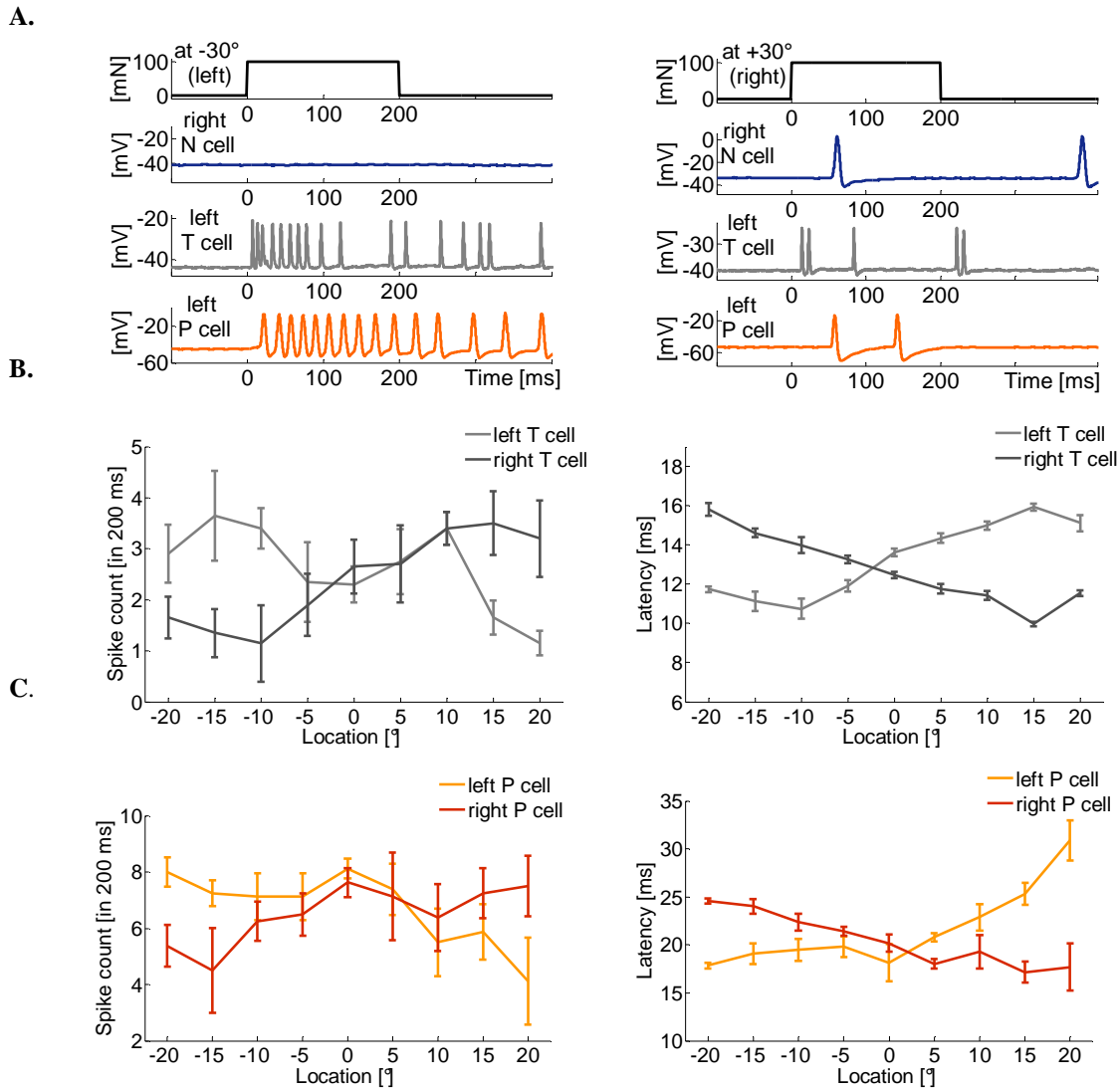


Figure 4: Influences of touch location on neuronal responses of mechanosensors. **A** Representative responses in mV of a right N cell (blue), left T cell (grey) and left P cell (orange) to a touch stimulus of 100 mN for 200 ms at -30° (left) and +30° (right). **B** Spike count and latency (Mean and STD) of a T cell double recording with 10 repeated stimulus presentations and a stimulus intensity of 50 mN. Ventral midline is defined as 0°. Touch locations to the right referred to by positive numbers of degrees, locations to the left by negative numbers. **C** Spike count and latency (Mean and STD) of a P cell double recording with 10 repeated stimulus presentations and a stimulus intensity of 50 mN.

duration (see Table 1), as well as the combination of stimulus properties.

We combined three durations (50, 200 and 500 ms) with two intensities (20 and 60 mN) (Fig. 8). Furthermore, we combined three locations (-20° / 0° / +20°) with two intensities (10 / 50 mN) (Fig. 9). Additional experiments were performed with up to three intensities (10 / 20 / 50 mN) and five locations (-20° / -10° / 0° / +10° / +20°).

For estimation of these location-intensity combinations, we additionally used pooled data of P and T cell double recordings to approximate encoding by the full mechanosensory cell ensemble. Features of the five P cell double recordings were randomly combined across preparations with the five T cell double recordings. Therefore, we also tested whether the estimation results of the pooled groups showed significant differences.

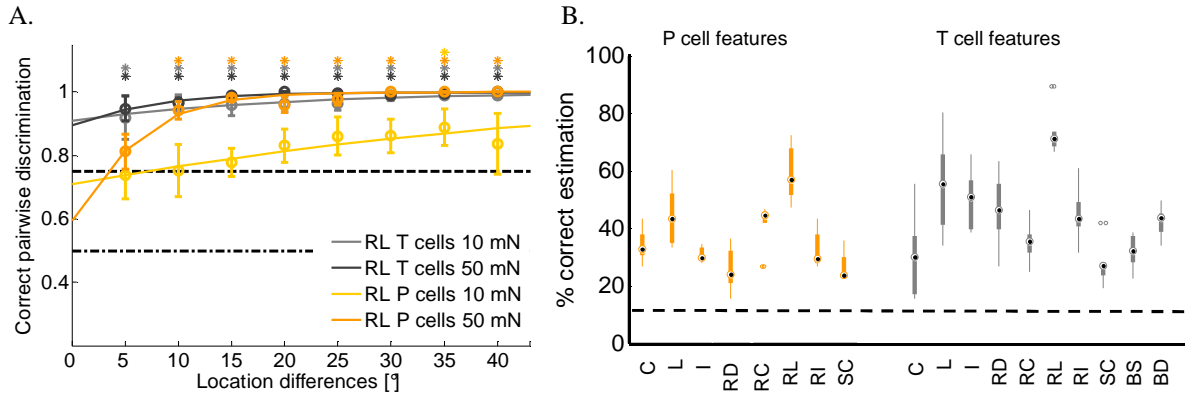


Figure 5: Estimation results for stimulus location. **A** Pairwise discrimination results for location differences between 5° and 40° away from 0°, for T and P cells and two touch intensities (number of cells, see Table 2, for each recording number of stimulus presentations = 10). Black dashed lines show chance level and 75% threshold. Asterisks indicate mean values, which are significantly ($p < 0.05$, t -test) above threshold. **B** Classification result for 9 locations for 50 mN. Black dashed line show chance level and black dots mark the median values (see Material and Methods). Response features: C = spike count; L = latency; I = 1st ISI; RD = response duration; RC = relative spike count; RL = relative latency; RI = relative 1st ISI; SC = summed spike count; BS = burst strength; BD = burst duration.

The results were stable and without significant differences across the pooled data groups.

Mutual information

We computed the mutual information (Quian Quiroga and Panzeri, 2009) of all possible pairs of response features and stimulus properties in bits.

$$I(X, Y) = \sum_{x,y} p(x, y) \log_2 \left(\frac{p(x, y)}{p(x)p(y)} \right),$$

where X denotes the stimulus property and Y the observed neuronal response feature. $p(x, y)$ is the joint probability distribution function of X and Y ; $p(x)$ and $p(y)$ are the marginal probability distribution of X and Y respectively. The values in Table 4 are normalized by the maximal information.

Significance tests

Significant influence of stimulus properties on neuronal response features was identified with the Kruskal-Wallis significance test (Gibbons, 1985; Hollander and Wolfe, 1999), a non-parametric version of the one-way analysis of variance (ANOVA). This test compares medians of independent samples from two or more groups. When not stated otherwise, the significance level for the test was $p < 0.001$ (Table 3 and 5). A significance level of

$p < 0.05$ was used for the features of the N cells (Table 3 and 5), because of the low firing rate of this cell type. We regard $p < 0.05$ as “significant” and $p < 0.001$ as “highly significant”.

Significant differences between classification results were tested with the Kruskal-Wallis test with $p < 0.05$ (Fig. 9). For pairwise discrimination, a one tailed t -test with $p < 0.05$ was applied to define which discrimination results were significantly above the performance threshold of 75 % (see Fig. 5 and 6). All tests were performed with the Matlab Statistics Toolbox (MathWorks, Natick, MA, USA).

Results

We utilized three complementary approaches to compare encoding performances of several response features for specific touch stimulus properties and their combinations. Firstly, pairwise discrimination (Thomson and Kristan, 2006) was used to estimate the minimum difference between touch locations or intensities, which could be discriminated based on a specific neuronal response feature.

Secondly, we applied a classification approach to get a broader perspective on stimulus encoding. This method was used to quantify

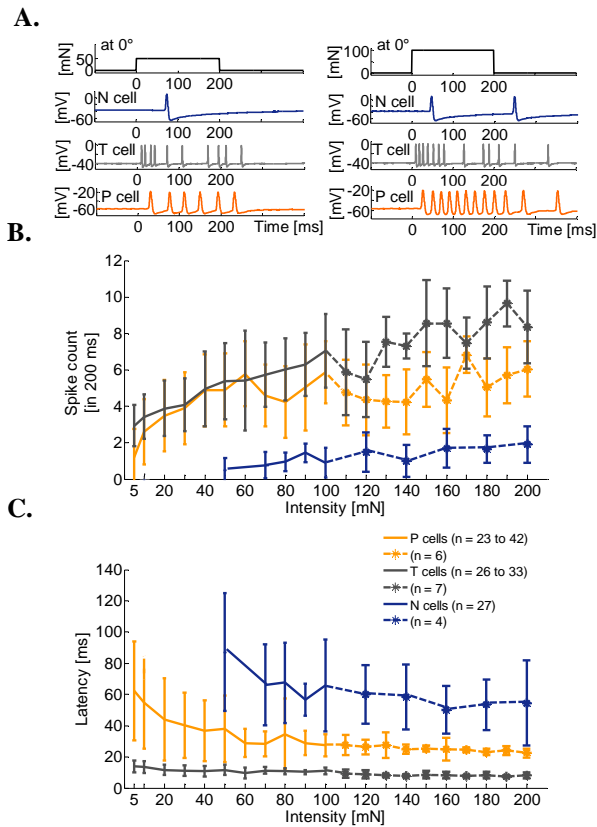


Figure 6: Influences of stimulus intensity on neuronal responses of mechanosensors. **A** Representative responses in mV of a right N cell (blue), left T cell (grey) and P cell (orange) to a touch stimulus of 50 mN (left) and 100 mN (right) for 200 ms at 0° (ventral midline). **B** Spike count and latency (mean and STD) for P cells (orange), T cells (grey) and N cells (blue) for intensities of 5 to 200 mN.

how well all experimentally tested stimulus locations or intensities could be discriminated based on a specific neuronal response feature. Thirdly, the results obtained by both estimation approaches were confirmed by calculating the mutual information between stimulus properties and response features. With these three methods we studied encoding of the stimulus properties touch location, intensity and duration, as well as their combinations.

Encoding of Location

In agreement with Thomson and Kristan (2006) we found that response latency and spike count of P cells depend on touch location (Fig. 4A, C). Qualitatively the same

dependencies were also found for T cell responses (Fig. 4A, B). In both cell types latency increased and spike count decreased significantly with increasing distance to the center of the receptive field, while the 1st ISI was less strongly influenced by touch location (Table 3). Remarkably, both cell types show a small variance across trials in latencies compared to spike counts (Fig. 4B, C). N cells generally needed higher touch intensities for activation and generated smaller numbers of spikes. Nevertheless, dependencies of N cell responses on stimulus location were similar to the other two cell types, despite a lower level of significance (Table 3).

Encoding performances of several P and T cell response features were investigated with two stimulus estimation methods (Fig. 5). For P cells, our results support the finding of Thomson and Kristan (2006) that the relative latency of both cells is the best encoder of touch location. For a stimulus intensity of 50 mN, touch location differences of 10° could significantly be discriminated (Fig. 5A). That means for an average leech with a circumference of 2.5 cm a distance of about 0.7 mm. In the more general task of stimulus estimation, relative P cell latency allowed assigning 60 % of response traces correctly to one of nine classes corresponding to the nine different stimulus locations. Moreover, the mutual information of relative latency and location of a 50 mN stimulus was higher than for any other P cell response features (Table 4).

When comparing cell types, we found that relative latencies of T cell responses encode touch location even more precisely than P cell responses (Fig. 5, Table 4). This finding was particularly evident for very soft touch stimuli of 10 mN, which could not be discriminated based on P cell responses, while T cell responses allowed a significant discrimination of location differences as small as 5° (Fig. 5A). When a higher touch intensity of 50 mN was applied, T cell relative latencies still outperformed P cell responses with a lower discrimination threshold of only 5° location difference (Fig. 5A) and a larger percentage of

about 70% correct estimations of touch location (Fig. 5B).

Combinations of response features did not improve encoding of touch location compared to relative latency of the pair of T cells data (not shown). A smaller set of double recordings of one T and one P cell indicated that location estimation based on the combination of T and P cell features fell short behind relative latencies of two T or two P cells.

We conclude that touch location is most precisely encoded by a temporal ensemble code – relative timing of the first spikes produced by a pair of cells of the same type.

Encoding of Intensity

When varying the force of touch stimuli applied to a constant position of the skin, we found that all three types of mechanosensory cells responded to strongly overlapping intensity ranges (50 – 200 mN) (Fig. 6). P cells, as well as T cells were already activated by extremely light touch of 5 mN.

Elevating stimulus intensity increased spike counts and decreased response latencies of the three cell types (Fig. 6). These effects were most pronounced for P cells and T cells stimulated in the lower intensity range (Table 5). N cells generally responded with a small number of spikes to stimulus intensities up to 200 mN. None of the analyzed N cell response features were found to depend significantly on touch intensity (Table 5).

Stimulus estimation and mutual information

based on single T cell or P cell responses revealed similar results for absolute latencies and spike counts (Fig. 7B, Table 4). Summing spike counts of two cells improved the results slightly, while the performance of relative latencies clearly fell short (Fig. 7, Table 4). Qualitatively the same results were found for a large data set of P and T cells (Tables 1, 2), which were stimulated with a lower range of intensities (results not shown). Since postsynaptic cells are not able to make use of absolute latencies without any further reference point, we conclude that spike rates are the most suitable response feature for intensity encoding.

Concerning the interaction of cell responses, we found that the sum of P cell and T cell spike counts encoded touch intensity at least as good as cell pairs of the same type (Fig. 7). Using the summed spike counts of one P cell and one T cell yielded approximately 70% correct estimations of five different intensities and a pairwise discrimination became significant at 30 mN intensity difference. For the intensity range used in this study, discrimination performance based on single P cell spike counts was improved only marginally by adding N cell spike counts (Fig. 7). However, N cell responses could gain relevance for higher stimulus intensities.

In summary, touch intensity is encoded by a rate code, in which responses of different cell types might be combined.

Encoding of Duration

To analyze the encoding of touch duration, we

Table 3: Significant changes in response features of the mechanosensors due to a location change away from the center of the receptive field ($p < 0.001$ for P and T cells; $p < 0.05$ for N cells, Kruskal-Wallis test). Percentages of cells showing significant changes are color coded, exact numbers of cells are given as 'significant / total' cell numbers.

Intensity [mN]	Spike count [decrease]			Latency [increase]			1 st ISI [increase]		
	10	50	100	10	50	100	10	50	100
T cells	9/ 10	10/ 10	-	10/ 10	10/ 10	-	8/ 10	7/ 10	-
P cells	10/ 10	10/ 10	-	8/ 10	10/ 10	-	1/ 10	5/ 10	-
N cells	-	-	7/ 8	-	-	5/ 8	-	-	-

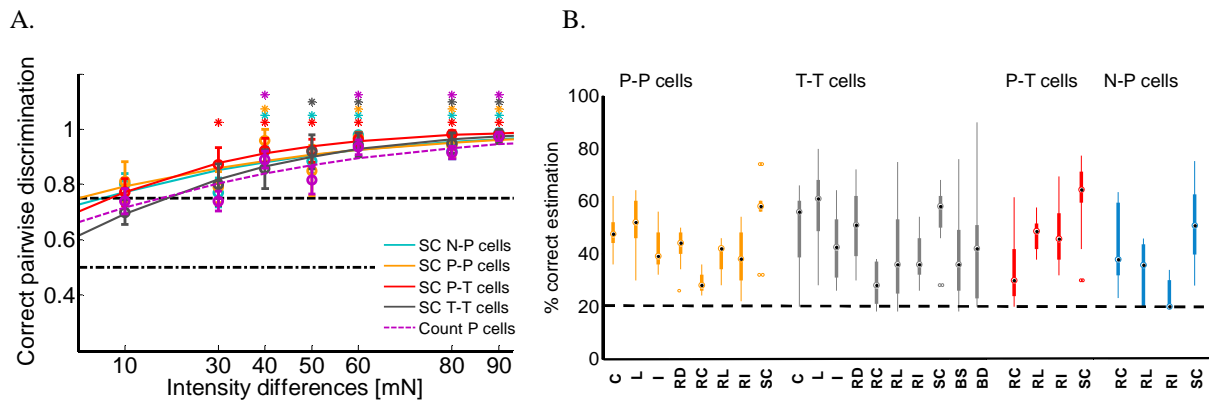


Figure 7: Estimation results for stimulus intensity. **A** Pairwise discrimination of intensity differences between 10 and 90 mN, compared to 10 mN. Black dashed lines show chance level and 75% threshold. Asterisks indicate mean values, which are significantly ($p < 0.05$, t test) above threshold. **B** Classification results. 5 intensities between 10 and 100 mN at 0° . Black dashed line show chance level and black dots mark the median values (see Material and Methods). Response features: C = spike count; L = latency; I = 1^{st} ISI; RD = response duration; RC = relative spike count; RL = relative latency; RI = relative 1^{st} ISI; SC = summed spike count; BS = burst strength; BD = burst duration.

Table 4: Normalized mutual information of response features with stimulus properties. Bold numbers indicate the response feature with the highest mutual information with the stimulus condition. Sum = Summed; Rel = Relative; Resp = Response; Dur = Duration. Stimulus properties for the combined encoding tasks see Table 1.

Location					
Int [mN]	Cells	Count	Latency	Sum Count	Rel Latency
10	T	0.35 ± 0.12	0.49 ± 0.15	0.30 ± 0.11	0.73 ± 0.12
10	P	0.35 ± 0.07	0.36 ± 0.07	0.25 ± 0.07	0.45 ± 0.12
50	T	0.33 ± 0.04	0.51 ± 0.16	0.28 ± 0.08	0.61 ± 0.09
50	P	0.36 ± 0.04	0.49 ± 0.10	0.33 ± 0.06	0.62 ± 0.09
Intensity					
Loc [$^\circ$]	Cells	Count	Latency	Sum Count	Rel Latency
0	T	0.44 ± 0.15	0.46 ± 0.16	0.48 ± 0.15	0.28 ± 0.17
0	P	0.40 ± 0.09	0.39 ± 0.12	0.47 ± 0.11	0.25 ± 0.11
0	N-P			0.41 ± 0.13	0.23 ± 0.17
0	P-T			0.52 ± 0.18	0.38 ± 0.11
Duration					
Int [mN]	Cells	Count	Latency	1^{st} ISI	Resp Dur
60	T	0.60 ± 0.24	0.11 ± 0.15	0.12 ± 0.12	0.59 ± 0.17
60	P	0.84 ± 0.11	0.10 ± 0.08	0.18 ± 0.09	0.72 ± 0.12
Duration & Intensity					
	Cells	Count	Latency	1^{st} ISI	Resp Dur
3 & 2	T	0.42 ± 0.13	0.34 ± 0.21	0.32 ± 0.13	0.49 ± 0.12
3 & 2	P	0.50 ± 0.07	0.30 ± 0.7	0.32 ± 0.09	0.53 ± 0.05
Location & Intensity					
	Cells	Count	Latency	Sum Count	Rel Latency
3 & 2	T	0.38 ± 0.14	0.56 ± 0.07	0.36 ± 0.11	0.71 ± 0.08
3 & 2	P	0.53 ± 0.14	0.49 ± 0.15	0.52 ± 0.13	0.52 ± 0.20

touched the skin with two intensities (20 and 60 mN) for three durations (50, 200, 500 ms). When applying the lower intensity of 20 mN, increase in spike count was highly significant in 11 of 12 P cells and in 5 of 10 T cells ($p < 0.001$, Kruskal-Wallis test). For the higher intensity, all cells of both types showed a highly significant increase in spike count (Fig. 8A).

Since the mechanosensory cells are not spontaneously active, their response duration mimics stimulus duration (Fig. 8B). For both cell types the spike count and response duration yielded best results for stimulus duration estimation (Fig. 8B). The highest mutual information with stimulus duration was

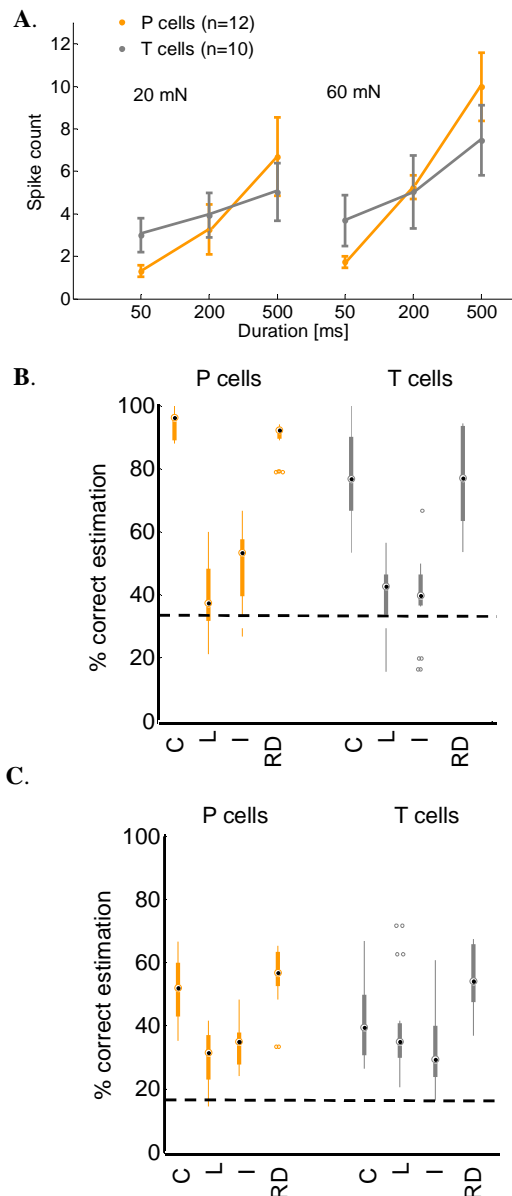


Figure 8: Influences of the stimulus duration on neuronal responses of mechanosensors. **A** Spike count (Mean and STD) for P cells (orange) and T cells (grey) for stimuli of 20 and 60 mN with 50, 200 and 500 ms duration at 0° stimulus location. **B** Classification results for 60 mN stimulus intensity with three durations (Table 1). Black dashed line show chance level and black dots mark the median values (see Material and Methods). Response features: C = spike count; L = latency; I = 1st ISI; RD = response duration. P cell features are shown in orange, T cell features in grey. **C** Classification results for two intensities in combination with three durations (Table 1). Response features and legend see B.

attained by the spike count of P cells (Table 4). Nevertheless, when stimulus duration is varied in combination with intensity, the combination

of stimulus properties (Table 1) can be estimated best based on the response duration of P cells (Fig. 8C). Accordingly, this feature also yielded the highest mutual information with the combination of stimulus intensity and duration (Table 4).

Based on these results, we conclude that the stimulus duration is best encoded by response duration, a slow temporal response feature.

Encoding of Property Combinations

For the estimation of individual stimulus properties location and intensity, we identified two different ensemble codes. A temporal feature – the relative latency of two cells of the same type – was found to be the best encoder for touch location. Touch intensity was encoded best by a spike count code – the summed spike count of cell pairs.

Since touch intensity and location were found to affect the same response features of T and P cells, responses of individual cells to combined stimulus properties must be ambiguous. A response trace with a low latency and a high spike count could be elicited either by a light touch close to the receptive field center, or by a stronger touch farther away. Moreover, estimation of touch depends on stimulus intensity (Fig. 5).

To test how the leech could solve this ambiguity problem, we stimulated the skin with combinations of two intensities and three locations (Table 1), while performing T cell and P cell double recordings (Fig. 9). The resulting 6 stimuli could be estimated above chance level based on responses of each of both cell types (Fig. 9A). Similar results were obtained in additional experiments, with up to 15 different stimuli, also for different values of response feature combinations (data not shown). For T cells, best estimation results for the combined stimulus were attained by relative latency (Fig. 9A, Table 4). For P cells, the combined stimulus features were estimated best based on summed spike counts or a combination of summed counts and relative latencies (Fig. 9A, Table 4). For both cell types, estimation results improved greatly

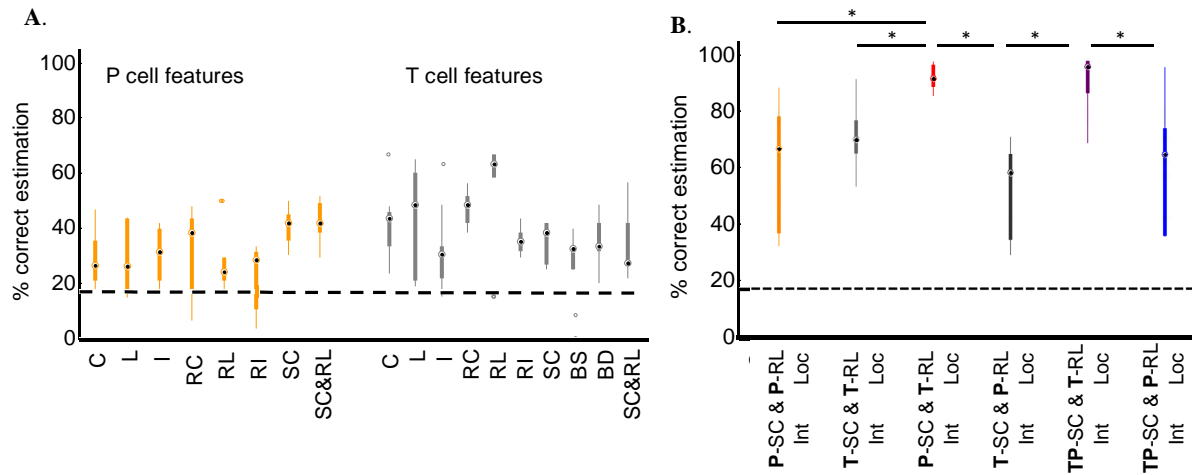


Figure 9: Estimation results for combination of location and intensity. **A** Results for combination of 3 locations (-20 / 0 / 20) and 2 intensities (10, 50 mN). C = spike count; L = latency; I = 1st ISI; RC = relative spike count; RL = relative latency; RI = relative 1st ISI; SC = summed spike count; BS = burst strength; BD = burst duration. Black dashed lines show chance level. **B** Results for combination of summed spike count (SC) for intensity estimation (Int) and relative latency (RL) for location estimation (Loc). P cell pairs in orange, T cell pairs in light grey, pooled data of P cell SC and T cell RL in red and of T cell SC and P cell RL in dark grey; SC of P cell and T cell pooled data with RL of T cells in purple and with RL of P cells in blue. The first response feature is used for intensity estimation, the second one for location estimation. Asterisk: significant difference ($p < 0.05$). The same location-intensity combination like in A is used.

when stimulus properties were estimated separately based on the previously found optimal response features – location with relative latencies and intensity with summed spike counts (Fig. 9B, two left-most box plots). To strictly test if interaction of both cell types improves estimation performance, simultaneous recording of both T together with both P cells would be necessary. However, due to our technical limitation of maximally three intracellular electrodes, we had to approximate full ensemble responses by pooling recordings across preparations. When analyzing all possible pairs of combined experiments we found very consistent results across

preparations. The six different stimuli could be estimated almost perfectly (median 90% correct, Fig. 9B), when P cell spike counts were summed to estimate intensity and T cell relative latencies were used for location estimation. Summing spike counts of all four T and P cells for intensity estimation did not change the result significantly. All other combinations of cell types, response features and stimulus properties led to significantly lower results (Fig. 9B). Qualitatively the same results – albeit on a lower level of correct estimations – were found for more difficult tasks with more stimulus combinations (see methods, results not shown).

Table 5: Significant changes in response features of the mechanosensors due to an intensity increase ($p < 0.001$, Kruskal-Wallis test). Percentages of cells showing significant changes are color coded, exact numbers of cells are given as 'significant / total' cell numbers. Low intensities are < 50 mN; Medium (med) intensities 50 to 100 mN; High intensities 100 up to 200 mN.

Intensity	Spike count [increase]			Latency [decrease]			1 st ISI [decrease]		
	low	med	high	low	med	high	low	med	high
T cells	21/ 33	10/ 26	3/ 7	25/ 33	14/ 26	5/ 7	12/ 33	8/ 26	2/ 7
P cells	36/ 42	14/ 23	3/ 6	38/ 42	9/ 23	1/ 6	20/ 42	8/ 23	1/ 6
N cells	-	1/ 27	0/ 4	-	0/ 27	0/ 4	-	0/ 27	0/ 4

100 %
 80 %
 60 %
 40 %
 20 %
 0 %

In conclusion, we found that individual mechanoreceptors of both types encode different stimulus properties in a multiplexed way and that the optimal strategy for decoding combinations of stimulus properties is to assume cell-type specific tasks and coding strategies. Best stimulus estimation results are obtained when relative latencies of T cells are used for the estimation of touch location in combination with summed spike counts of P cells for the estimation of stimulus intensity.

Discussion

The leech is able to react surprisingly precisely to touch stimuli, despite its small nervous system and low numbers of mechanosensory neurons (Kristan et al., 2005; Baca et al., 2005; Thomson and Kristan, 2006). Several prior studies examined leech mechanosensory cells and local bend behavior (Kristan, 1982; Lockery and Kristan, 1990; Lockery and Sejnowski, 1992; Lewis and Kristan, 1998; Zoccolan and Torre, 2002; Baca et al., 2005; Thomson and Kristan, 2006), but neither encoding of stimulus property combinations nor the interaction of mechanosensory cell types have been examined so far. In this study, we present evidence that multiplexed encoding of touch properties by two mechanoreceptor types provides the basis for the excellent behavioral performance of stimulus discrimination.

Regarding the literature on leech mechanoreception, these results could provide the solution to an open question left by the study of Thomson and Kristan (2006). Analyzing P cell responses, they found, in agreement with our study, relative latency to be the best encoder for stimulus location. Nevertheless, electric stimulation of P cells simulating their responses to tactile stimuli did not elicit local bend muscle contractions with the same spatial precision as tactile stimuli themselves. Our results suggest that the extremely precisely timed T cell spikes are required to achieve this behavioral goal.

In a broader perspective, we discuss our results in the context of primate mechanoreception

and identify common principles of somatosensory encoding.

Rate coding versus temporal coding

While rate and temporal coding traditionally were discussed controversially (Theunissen and Miller, 1995; Shadlen and Newsome, 1998; deCharms and Zador, 2000), recent studies found in several sensory systems evidence for simultaneous usage of both types of encoding representing different stimulus aspects (Panzeri et al., 2010; Ainsworth et al., 2012; Wohrer et al., 2013). In particular the somatosensory system was found to rely on both spike rates and timing simultaneously (Harvey et al., 2013; Saal and Bensmaia, 2014). Mechanoreceptors of the primate glabrous skin and their downstream cortical targets seem to represent spatio-temporal features of tactile stimuli with temporal response properties (Johansson and Birznieks, 2004; Mackevicius et al., 2012, Weber et al. 2013, Harvey et al., 2013), while touch intensity is represented by a rate code (Bensmaia, 2008; Harvey et al., 2013). In good accordance with these results, we found evidence that the leech mechanosensory system also uses both types of encoding simultaneously. By means of stimulus estimation methods, we identified a temporal feature – relative latencies – to be the best encoder for touch location. At the same time a rate code – summed spike counts – encoded touch intensity best. Spike counts also allowed estimation of stimulus duration. Hence, this study provides additional evidence that sensory coding should be discussed in terms of the general principles of response feature combinations rather than a dichotomy of spike count versus spike timing code.

Individual cells versus cell ensembles

The classical hypothesis about mechanoreception of the primate glabrous skin is a labeled line code (Abreira and Ginty, 2013; Zeveke et al., 2013), which assumes that different receptor types provide input to isolated channels of information transmission for different modalities. However, several

recent studies found evidence, that signals from different mechanoreceptor types participate in shaping cortical response patterns, causing an integrated perception of several aspects of cutaneous stimulation (Bensmaia 2008; Abreira and Ginty, 2013; Zeveke et al., 2013; Saal and Bensmaia, 2014). These findings are particularly relevant for natural tactile stimulation in behavioral contexts, because touching and manipulating objects always cause perception shaped by several combined stimulus properties (Johansson and Flanagan, 2009; Saal and Bensmaia, 2014). In particular, SA-I (slowly adapting) and FA-I/RA (rapidly adapting) afferents were shown to provide input to the same target cells in the somatosensory cortex (Saal and Bensmaia, 2014) and both to be involved in overlapping sensory tasks like perception of intensity (Bensmaia, 2008), stimulus shape (Johansson and Birznieks, 2004) and texture (Weber et al., 2013) of tactile stimuli.

The mechanoreceptors of the leech serve the same function as mammalian mechanosensory afferents, i.e. transmitting mechanically induced action potentials to the central nervous system. They respond strikingly similarly to the afferents of the mammalian glabrous skin, e.g. the human fingertip and rodent paws (Zimmermann et al., 2014). P cells resemble SA-I afferents in their sustained, slowly adapting responses to constant touch stimulation, while T cells share with FA-I afferents the rapidly adapting bursts after stimulus onset and also tend to produce a short off-response at stimulus offset (leech: see Fig. 4A; Nicholls and Baylor, 1968; Baca et al., 2005; human: Vallbo and Johansson, 1984; Johansson and Flanagan, 2009; Abreira and Ginty, 2013).

Remarkably, these two leech receptor types seem to play very similar functional roles in encoding tactile stimulus properties like their primate counterparts. For humans and monkeys it was found that estimation of touch intensity requires the integration of several afferents (Johnson 1974; Muniak et al., 2007; Bensmaia, 2008; but see Arabazadeh et al., 2014). SA-I afferents are essential for intensity

estimation of constant touch stimuli, but the perceived intensity of vibrating stimuli is approximated best by the weighted sum of activities of all afferent types (Muniak et al., 2007; Bensmaia, 2008). In agreement, we found summed spike counts of two or more leech mechanoreceptors to allow best touch intensity estimation, in particular if responses of at least one P cell were included.

Primates and leeches also share a common ensemble coding principle for spatial properties of touch stimuli, the relative timing of first spikes. In humans, the relative timing of first spikes represents the shape of tactile stimuli, with RA afferents allowing faster decoding than SA-I (Johansson and Birznieks, 2004). In leeches, the location of a small touch stimulus can be estimated very precisely based on the relative latency of two mechanosensory cells, in particular a pair of T cells.

Encoding of single stimulus properties versus multiplexing of stimulus properties

Leech mechanosensory cells and primate mechanosensory afferents clearly encode multiple properties of tactile stimuli in a multiplexed way. As already discussed, each slowly adapting (SA-I and P), as well as each rapidly adapting (RA and T) cell tunes its spike rate to stimulus intensity and at the same time its first spike latency to spatial aspects of tactile stimuli. Hence, response features on different temporal scales simultaneously represent complementary information on two different stimulus properties. This finding exactly matches the definition of multiplexing given by Panzeri et al. (2010).

However, our estimation of stimulus property combinations, i.e. stimulus location and intensity, suggests specialization of cell types for encoding one of the stimulus properties with a single response feature. The relative timing of the fast and temporally precise first spikes of T cells provide the information about stimulus location, while the summed spike counts of sustained P cell responses indicate stimulus intensity (Fig. 9). In particular combinations of response features can be predicted much better when responses of both

mechanoreceptor types are considered than for each cell type separately. Hence, our results of stimulus encoding on the sensor cell level suggest that their multiplexed signals may be split for decoding. Nevertheless, this hypothesis needs to be tested experimentally on the next level of sensory signal processing, the responses of postsynaptic interneurons in the leech local bend network. If the leech uses the strategy we identified, we would expect to find coincidence detector interneurons sensitive to relative spike timing on the one hand and temporal integrator interneurons summing inputs over time on the other hand. Further experiments will reveal if these distinct types of interneurons exist or whether multiplexed coding of stimulus properties is carried onto the next network layer.

Studies on the primate sensory system so far usually focused on one stimulus property. To the best of our knowledge, no results were published yet on the encoding of combined intensity and spatial properties of tactile stimuli. Anyhow, very good evidence exists that neurons in the somatosensory cortex receive inputs from both SA-I and RA afferents and tune their responses to several (individually analyzed) properties of tactile stimuli, including intensity and spatial features (Saal and Bensmaia, 2014).

Conclusion

Leech mechanoreceptors and afferents of the primate glabrous skin share not only their response patterns to tactile stimulation, but also several mechanisms of encoding. Despite the great difference in numbers of participating cells, both systems seem to use the same stimulus property-specific ensemble encoding strategies. Since these encoding strategies are shared by two systems as different as the human fingertip and the leech body wall, they might be general mechanisms underlying somatosensation in general. Though, the question of combined encoding of multiple stimulus properties requires further analyses, particularly in the context of natural tactile stimuli. When an object is touched by the hand of a primate or by the body wall of a moving

leech, it induces complex, temporally and spatially dynamic mechanical stimulation (Johansson and Flanagan, 2009), comprising several stimulus properties. The experimentally easily approachable, minimalistic system of the leech might help to understand how various stimulus features are integrated into one consistent perception representing an object touched by a human finger tip.

References

- Abraira VE, Ginty DD (2013) The sensory neurons of touch. *Neuron* 79: 618-639.
- Ainsworth M, Lee S, Cunnigham MO, Traub RO, Kopell NJ, Whittington MA (2012) Rates and rhythms: A synergistic view of frequency and temporal coding in neuronal networks. *Neuron* 75: 572-583.
- Aldrich J (1997) R. A. Fisher and the making of Maximum Likelihood 1912 – 1922. *Stat Sci* 12: 162-176.
- Arabzadeh E, Clifford CWG, Harris JA, Mahns DA, Macefield VG, Birznieks I (2014) Single tactile afferents outperform human subject in a vibrotactile discrimination task. *J Neurophysiol* 112: 2382-2387.
- Baca SM, Thomson EE, Kristan WB (2005) Location and intensity discrimination in the leech local bend response quantified using optic flow and principal components analysis. *J Neurophysiol* 93: 3560–3572.
- Baltzley MJ, Gaudry Q, Kristan WB (2010) Species-specific behavioral patterns correlate with differences in synaptic connections between homologous mechanosensory neurons. *J Comp Physiol A* 196: 181-197.
- Bensmaia SJ (2008) Tactile intensity and population codes. *Behav Brain Res* 190: 165-173.
- Blackshaw SE, Nicholls JG and Parnas I (1982) Physiological responses, receptive fields and terminal arborizations of nociceptive cells in the leech. *J Physiol* 326: 251-260.

- deCharms RC, Zador A (2000) Neural representation and the cortical code. *Ann Rev Neurosci* 23: 613-647.
- Foffani G, Tutunculer B, Moxon KA (2004) Role of spike timing in the forelimb somatosensory cortex of the rat. *J Neurosci* 24: 7266–7271.
- Gibbons JD (1985) *Nonparametric Statistical Inference*. New York: Marcel Dekker, 1985.
- Harvey MA, Saal HP, Dammann JF III, Bensmaia SJ (2013) Multiplexing Stimulus information through rate and temporal codes in primate somatosensory cortex. *PLOS Biol* 11: e1001558
- Hollander M, Wolfe DA (1999) *Nonparametric Statistical Methods*. Hoboken, NJ: John Wiley & Sons, Inc.
- Johansson RS, Birznieks I (2004) First spikes in ensembles of human tactile afferents code complex spatial fingertip events. *Nat Neurosci* 7: 170-177.
- Johansson RS, Flanagan JR (2009) Coding and use of tactile signals from the fingertips in object manipulation tasks. *Nat Rev Neurosci* 10: 345-359.
- Johnson KO (1974) Reconstruction of population response to a vibratory stimulus in quickly adapting mechanoreceptive afferent fiber population innervating glabrous skin of the monkey. *J Neurophysiol* 37: 48-72.
- Johnson KO, Philips JR (1981) Tactile spatial resolution. I. Two-point discrimination, gap detection, grating resolution, and letter recognition. *J Neurophysiol* 46: 1177-1191.
- Kristan WB (1982) Sensory and motor neurons responsible for the local bending response in leeches. *J Exp Biol* 96: 161–180.
- Kristan WB, Calabrese RL, Friesen WO (2005) Neuronal control of leech behavior. *Prog Neurobiol* 76: 279-327.
- Lewis JE, Kristan WB (1998) Representation of touch location by a population of leech sensory neurons. *J Neurophysiol* 80: 2584–2592.
- Lockery SR, Kristan WB (1990) Distributed processing of sensory information in the leech. II. Identification of interneurons contributing to the local bending reflex. *J Neurosci* 10: 1816–1829.
- Lockery SR, Sejnowski TJ (1992) Distributed processing of sensory information in the leech. III. A dynamical neural network model of the local bending reflex. *J Neurosci* 12: 3877–3895.
- Mackevicius EL, Best MD, Saal HP, Bensmaia SJ (2012) Millisecond precision spike timing shapes tactile perception. *J Neurosci* 32: 15309-15317.
- Muller KJ, Nicholls JG, Stent GS (1981) Appendix C: The nervous system of the leech: a laboratory manual. In: *Neurobiology of the leech*. New York: Cold Spring Harbor Laboratory, p. 249-275.
- Muniak MA, Ray S, Hsiao S, Dammann JF, Bensmaia SJ (2007) The neural coding of stimulus intensity: Linking the population response of mechanoreceptive afferents with psychophysical behavior. *J Neurosci* 27: 11687-11699.
- Nicholls JG, Baylor DA (1968) Specific modalities and receptive fields of sensory neurons in CNS of the leech. *J Neurophysiol* 31: 740–756.
- Oswald A-MM, Doiron B, Maler L (2007) Interval coding. I. Burst interspike intervals as indicators of stimulus intensity. *J Neurophysiol* 97: 2731–2743.
- Panzeri S, Brunel N, Logothetis NK, Kaiser C (2010) Sensory neural codes using multiplexed temporal scales. *Trends Neurosci* 33: 111-120.
- Quiñero Quiroga R, Panzeri S (2009) Extracting information from neuronal populations: information theory and decoding approaches. *Nat Rev Neurosci* 10: 173-185.
- Saal HP, Bensmaia SJ (2014) Touch is a team effort: interplay of submodalities in cutaneous sensibility. *Trends Neurosci* 37: 689-697.
- Sakurai Y (1996) Population coding by cell assemblies – what it really is in the brain. *Neurosci Res* 26: 1-16.

- Shadlen MN, Newsome WT (1998) The variable discharge of cortical neurons: Implications for connectivity, computation, and information coding. *J Neurosci* 18: 3870-3896.
- Theunissen F, Miller JP (1995) Temporal encoding in nervous systems: A rigorous definition. *J Comput Neurosci* 2: 149-162.
- Thomson EE, Kristan WB (2006) Encoding and decoding touch location in the leech CNS. *J Neurosci* 26: 8009–8016.
- Vallbo A, Johansson R (1984) Properties of cutaneous mechanoreceptors in the human hand related to touch sensation. *Hum Neurobiol* 3: 3–14.
- Weber AI, Saal HP, Lieber JD, Cheng JW, Manfredi LR, Dammann JF III, Bensmaia SJ (2013) Spatial and temporal codes mediate the tactile perception of natural textures. *PNAS* 110: 17107–17112.
- Wohrer A, Humphries MD, Machens CK (2013) Population-wide distributions of neural activity during perceptual decision-making. *Prog Neurobiol* 103: 156-193.
- Zeveke AV, Efes ED, Polevaya SA (2013) An integrative framework of the skin receptors activation: Mechanoreceptors activity patterns versus “labeled lines“. *J Integr Neurosci* 12: 47-56.
- Zimmermann A, Bai L, Ginty DD (2014) The gentle touch receptors of mammalian skin. *Science* 346: 950-954.
- Zoccolan D, Torre V (2002) Using optical flow to characterize sensory-motor interactions in a segment of the medicinal leech. *J Neurosci* 22: 2283–2298.

7. References

- Abraira VE, Ginty DD (2013) The sensory neurons of touch. *Neuron* 79: 618–639.
- Ache JM, Dürr V (2013) Encoding of near-range spatial information by descending interneurons in the stick insect antennal mechanosensory pathway. *J Neurophysiol* 110: 2099–2112.
- Adrian ED (1926) The impulses produced by sensory nerveendings. Part 4. Impulses from pain receptors. *J Physiol* 62: 33–51.
- Adrian ED, Matthews R (1927a) The action of light on the eye. Part I. The discharge of impulses in the optic nerve and its relation to the electric changes in the retina. *J Physiol* 63: 378–414.
- Adrian ED, Matthews R (1927b) The action of light on the eye. Part II. The processes involved in retinal excitation. *J Physiol* 64: 279–301.
- Adrian ED, Matthews R (1928) The action of light on the eye. Part III. The interaction of retinal neurones. *J Physiol* 65: 273–298.
- Adrian ED, Zotterman Y (1926a) The impulses produced by sensory nerve-endings. Part II. The response of a single end-organ. *J Physiol* 61: 151–171
- Adrian ED, Zotterman Y (1926b) The impulses produced by sensory nerve endings. Part III. Impulses set up by touch and pressure. *J Physiol* 61: 465–483.
- Ainsworth M, Lee S, Cunnigham MO, Traub RO, Kopell NJ, Whittington MA (2012) Rates and rhythms: A synergistic view of frequency and temporal coding in neuronal networks. *Neuron* 75: 572–583.
- Akam T, Kullmann DM (2014) Oscillatory multiplexing of population codes for selective communication in the mammalian brain. *Nat Rev Neurosci* 15: 111–122.
- Aldrich J (1997) R. A. Fisher and the making of Maximum Likelihood 1912 – 1922. *Stat Sci* 12: 162–176.
- Averbeck BB, Latham PE, Pouget A (2006) Neural correlations, population coding and computation. *Nat Rev Neurosci* 7: 358–366.
- Baca SM, Marin-Burgin A, Wagenaar DA, Kristan WB (2008) Widespread inhibition proportional to excitation controls the gain of a leech behavioral circuit. *Neuron* 57: 276–289

- Baca SM, Thomson EE, Kristan WB (2005) Location and intensity discrimination in the leech local bend response quantified using optic flow and principal components analysis. *J Neurophysiol* 93: 3560–3572.
- Baltzley MJ, Gaudry Q, Kristan WB (2010) Species-specific behavioral patterns correlate with differences in synaptic connections between homologous mechanosensory neurons. *J Comp Physiol A* 196: 181–197.
- Baylor DA, Nicholls JG (1969) Chemical and electrical synaptic connections between cutaneous mechanoreceptor neurones in the central nervous system of the leech. *J Physiol* 203: 591–609.
- Bensmaia SJ (2008) Tactile intensity and population codes. *Behav Brain Res* 190: 165–173.
- Birznieks I, Macefield VG, Westling G, Johansson RS (2009) Slowly adapting mechanoreceptors in the borders of the human fingernail encode fingertip forces. *J Neurosci* 29: 9370–9379.
- Blackshaw SE (1981) Morphology and distribution of touch cell terminals in the skin of the leech. *J Physiol* 320: 219–228.
- Blackshaw SE, Nicholls JG and Parnas I (1982) Physiological responses, receptive fields and terminal arborizations of nociceptive cells in the leech. *J Physiol* 326: 251–260.
- Briggman KL, Abarbanel HDI, Kristan WB (2005) Optical imaging of neuronal populations during decision-making. *Science* 307: 896–901.
- Brodfoehr PD, Friesen WO (1986a) Control of leech swimming activity by the cephalic ganglia. *J Neurobiol* 17: 697–705.
- Brodfoehr PD, Friesen WO (1986b) From stimulation to undulation: an identified pathway for the control of swimming activity in the leech. *Science* 234: 1002–1004.
- Brodfoehr PD, Kogelnik AM, Friesen WO, Cohen AH (1993) Effect of the tail ganglion on swimming activity in the leech. *Behav Neural Biol* 59: 162–166.
- Bullmore E, Sporns O (2009) Complex brain networks: graph theoretical analysis of structural and functional systems. *Nat Rev Neurosci* 10: 186–198.
- Burgin AM, Szczupak L (2003) Network interactions among sensory neurons in the leech. *J Comp Physiol A* 189: 59–67
- Calabrese R (1980) Control of multiple impulse-initiation sites in a leech interneuron. *J Neurophysiol* 44: 878–896.

- Carlton T, McVean A (1995) The role of touch, pressure and nociceptive mechanoreceptors of the leech in unrestrained behavior. *J Comp Physiol A* 177: 781–791.
- Cover TM, Thomas JA (2006) *Elements of Information Theory* 2nd edition. Wiley-Interscience Publication, John Wiley & Sons, Inc., NJ, USA, ISBN-13 978-0-471-24195-9
- deCharms RC, Zador A (2000) Neural representation and the cortical code. *Annu Rev Neurosci* 23: 613–647.
- Di Lorenzo PM, Victor JD (2003) Taste response variability and temporal coding in the nucleus of the solitary tract of the rat. *J Neurophysiol* 90:1418–1431.
- Di Lorenzo PM, Victor JD (2007) Neural coding mechanisms for flow rate in taste-responsive cells in the nucleus of the solitary tract of the rat. *J Neurophysiol* 97:1857–1861.
- Di Lorenzo PM, Chen J-Y, Victor JD (2009) Quality time: Representation of a multidimensional sensory domain through temporal coding. *J Neurosci* 29: 9227–9238.
- Du Bois-Reymond, E (1849) *Untersuchungen über thierische Elektrizität, Zweiter Band, Erste Abtheilung*. Berlin: Georg Reimer
- Dykes RW (1975) Nociception. *Brain Research* 99: 229–245.
- Eggermont JJ (1998) Azimuth coding in primary auditory cortex of the cat. II. Relative latency and interspike interval representation. *J Neurophysiol* 80: 2151–2161.
- Eisenhart FJ, Cacciatore TW, Kristan WB (2000) A central pattern generator underlies crawling in the medicinal leech. *J Comp Physiol* 186:631–643.
- Engel AK, Fries P, Singer W (2001) Dynamic predictions: Oscillations and synchrony in top-down processing. *Nat Rev Neurosci* 2: 704–716.
- Foffani G, Tutunculer B, Moxon KA (2004) Role of spike timing in the forelimb somatosensory cortex of the rat. *J Neurosci* 24: 7266–7277.
- Fotowat H, Harrison RR, Gabbiani F (2011) Multiplexing of motor information in the discharge of a collision detecting neuron during escape behaviors. *Neuron* 69: 147–158.

- Friesen WO (1985) Neuronal control of leech swimming movements: interactions between cell 60 and previously described oscillator neurons. *J Comp Physiol A* 156: 231–242.
- Friesen WO, Kristan WB (2007) Leech locomotion: Swimming, crawling, and decisions. *Curr Opin Neurobiol* 17: 704–711.
- Friesen WO, Poon M, Stent GS (1978) Neuronal control of swimming in the medicinal leech. IV. Identification of a network of oscillatory interneurons. *J Exp Biol* 75: 25–43.
- Gibbons JD (1985) *Nonparametric Statistical Inference*. New York: Marcel Dekker, 1985.
- Gire DH, Whitesell JD, Doucette W, Restrepo D (2013) Information for decision-making and stimulus identification is multiplexed in sensory cortex. *Nat Neurosci* 16: 991–994.
- Harvey MA, Saal HP, Dammann JF III, Bensmaia SJ (2013) Multiplexing stimulus information through rate and temporal codes in primate somatosensory cortex. *PLoS Biol* 11: e1001558.
- Hernandez H, Salinas E, Garcia R, Romo R (1997) Discrimination in the sense of flutter: new psychophysical measurements in monkeys. *J Neurosci* 17: 6391–6400.
- Hollander M, Wolfe DA (1999) *Nonparametric Statistical Methods*. Hoboken, NJ: John Wiley & Sons, Inc.
- Huk AC (2012) Multiplexing in the primate motion pathway. *Vis Res* 62: 173–180
- Johansson RS, Birznieks I (2004) First spikes in ensembles of human tactile afferents code complex spatial fingertip events. *Nat Neurosci* 7: 170–177.
- Johansson RS, Flanagan JR (2009) Coding and use of tactile signals from the fingertips in object manipulation tasks. *Nat Rev Neurosci* 10: 345–359.
- Johnson KO (2001) The roles and functions of cutaneous mechanoreceptors. *Curr Opin Neurobiol* 11: 455–461.
- Johnson KO, Philips JR (1981) Tactile spatial resolution. I. Two-point discrimination, gap detection, grating resolution, and letter recognition. *J Neurophysiol* 46: 1177–1191.
- Juusola M, Robinson HPC, de Polavieja GG (2007) Coding with spike shapes and graded potentials in cortical networks. *BioEssays* 29:178–187.
- Kandel ER (2001) The molecular biology of memory storage: A dialogue between genes and synapses. *Science* 294: 1030–1038.

- Kandel ER, Dudai Y and Mayford MR (2014) The molecular and systems biology of memory. *Cell* 157: 163–186.
- Kappel M, Pirschel F, Kretzberg J (2011) Stimulus reconstruction based on postsynaptic potentials of leech interneurons. *BMC Neurosci* 2011, 12: P179.
- Kettenmann H (1997) Alexander von Humboldt and the concept of animal electricity. *Trends Neurosci* 20: 239–242
- King AJ, Walker KMM (2012) Integrating information from different senses in the auditory cortex. *Biol Cybern* 106:617–625.
- Kretzberg J, Pirschel F, Fathiazar E (2015) Minimal ensemble coding of combined stimulus properties in the leech CNS. *Cosyne Abstracts 2015, Salt Lake City USA*.
- Kristan WB (1982) Sensory and motor neurons responsible for the local bending response in leeches. *J Exp Biol* 96: 161–180.
- Kristan WB, Calabrese RL, Friesen WO (2005) Neuronal control of leech behavior. *Prog Neurobiol* 76: 279–327.
- Kristan WB, McGirr SJ, Simpson GV (1982) Behavioral and mechanosensory neurone responses to skin stimulation in leeches. *J exp Biol* 96: 143–160.
- Leite Costa, FA, Moreira Neto, FL (2015) Satellite glial cells in sensory ganglia: its role in pain. *Brazilian J Anesthesiol (English Edition)* 65: 73–81.
- Lewis JE (1999) Sensory processing and the network mechanisms for reading neuronal population codes. *J Comp Physiol* 185a: 373–378.
- Lewis JE, Kristan WB (1998a) A neuronal network for computing population vectors in the leech. *Nature* 391: 76–79.
- Lewis JE, Kristan WB (1998b) Quantitative analysis of a directed behavior in the medicinal leech; implications for organizing motor output. *J Neurosci* 18: 1571–1582.
- Lewis JE, Kristan WB (1998c) Representation of touch location by a population of leech sensory neurons. *J Neurophysiol* 80: 2584–2592.
- Lockery SR, Kristan WB (1990a) Distributed processing of sensory information in the leech. I. Input-output relations of the local bending reflex. *J Neurosci* 10: 1811–1815.
- Lockery SR, Kristan WB (1990b) Distributed processing of sensory information in the leech. II. Identification of interneurons contributing to the local bending reflex. *J Neurosci* 10: 1816–1829.

- Lockery SR, Kristan WB (1991) Two forms of sensitization of the local bending reflex of the medicinal leech. *J Comp Physiol A* 168: 165–177.
- Lockery SR, Sejnowski TJ (1992) Distributed processing of sensory information in the leech. III. A dynamical neural network model of the local bending reflex. *J Neurosci* 12: 3877–3895.
- Lockery SR, Sejnowski TJ (1993a) A lower bound on the delectability of nonassociative learning in the local bending reflex on the medicinal leech. *Behav Neural Biol* 59: 208–224.
- Lockery SR, Sejnowski TJ (1993b) The computational leech. *Trends Neurosci* 16: 283–290.
- Lockery SR, Wittenberg G, Kristan WB, Cottrell GW (1989) Function of identified interneurons in the leech elucidated using networks trained by back-propagation. *Nature* 340: 468–471.
- Luna R, Hernández A, Brody CD, Romo R (2005) Neural codes for perceptual discrimination in primary somatosensory cortex. *Nat Neurosci* 8: 1210–1219.
- Mackevicius EL, Best MD, Saal HP, Bensmaia SJ (2012) Millisecond precision spike timing shapes tactile perception. *J Neurosci* 32: 15309–15317.
- Meister MLR, Hennig JA, Huk AC (2013) Signal multiplexing and single-neuron computations in lateral intraparietal area during decision-making. *J Neurosci* 33: 2254–2267.
- Muller KJ, Nicholls JG, Stent GS (1981) Appendix C: The nervous system of the leech: a laboratory manual. In: *Neurobiology of the leech*. New York: Cold Spring Harbor Laboratory, p. 249–275.
- Muniak MA, Ray S, Hsiao S, Dammann JF, Bensmaia SJ (2007) The neural coding of stimulus intensity: Linking the population response of mechanoreceptive afferents with psychophysical behavior. *J Neurosci* 27: 11687–11699.
- Nicholls JG (1969) Slow changes in the membrane potentials of glial cells and neurons following nerve impulses. *Electroencephalogr Clin Neurophysiol* 27: 702.
- Nicholls JG, Baylor DA (1968) Specific modalities and receptive fields of sensory neurons in CNS of the leech. *J Neurophysiol* 31: 740–756.
- Nicholls JG, Martin AR, Wallace BG, Fuchs PA (2001) *From neuron to brain*. 4th edition. Sinauer Associates, Inc. Sunderland, MA, USA. ISBN 978-0-87893-439-3.

- Nicholls JG, Purves D (1970) Monosynaptic chemical and electrical connexions between sensory and motor cells in the central nervous system of the leech. *J Physiol* 209: 647–667.
- Oswald A-M, Doiron B, Maler L (2007) Interval coding. I. Burst interspike intervals as indicators of stimulus intensity. *J Neurophysiol* 97: 2731–2743.
- Panzeri S, Brunel N, Logothetis NK, Kaiser C (2010) Sensory neural codes using multiplexed temporal scales. *Trends Neurosci* 33: 111–120.
- Panzeri S, Petersen RS, Schultz SR, Lebedev M, Diamond ME (2001) The role of spike timing in the coding of stimulus location in rat somatosensory cortex. *Neuron* 29: 769–777.
- Parent A (2004) Giovanni Aldini: From animal electricity to human brain stimulation. *Can J Neurol Sci* 31: 576–584.
- Pearce JMS (2001) Emil Heinrich Du Bois-Reymond (1818-96). *J Neurol Neurosurg Psych* 71: 620.
- Perkel DH, Gerstein GL, Moore GP (1967) Neuronal spike trains and stochastic point processes. I. The single spike train. *Biophys J* 7: 391–418.
- Petersen RS, Panzeri S, Diamond ME (2001) Population coding of stimulus location in rat somatosensory cortex. *Neuron* 32: 503–514.
- Petersen RS, Panzeri S, Diamond ME (2002a) The role of individual spikes and spike patterns in population coding of stimulus location in rat somatosensory cortex. *BioSystems* 67: 187–193.
- Petersen RS, Panzeri S, Diamond ME (2002b) Population coding in somatosensory cortex. *Curr Opin Neurobiol* 12: 441–447.
- Piccolino M (1997) Luigi Galvani and animal electricity: two centuries after the foundation of electrophysiology. *Trends Neurosci* 20: 443–448.
- Pirschel F, Kuehn O, Kretzberg J (2015) The role of mechanosensory T cells for stimulus encoding in the local bend network of the leech. *BMC Neurosci* 2015, 16.
- Pirschel F, Kretzberg J (2013) Coding of touch properties by three types of mechanosensory cells of the leech *Hirudo medicinalis*. *BMC Neurosci* 2013, 14: P224.
- Pirschel F, Kretzberg J (2012) Encoding of touch location and intensity by neurons of the medicinal leech *Hirudo medicinalis*. *BMC Neurosci* 2012, 13: P103.

- Pirschel F, Kretzberg J (2011) Encoding of tactile stimulus parameters by mechanosensory P cells of the medicinal leech *Hirudo medicinalis*. *BMC Neurosci* 2011, 12: P180.
- Pirschel F, Kretzberg J (2015) Multiplexed Encoding Of Stimulus Properties By Leech Mechanosensory Cells. Submitted to *Journal of Neuroscience* (details see *Publications*).
- Pouget A, Dayan P, Zemel R (2000) Information processing with population codes. *Nat Rev Neurosci* 1: 125–132.
- Puhl JG, Mesce KA (2010) Keeping it together: Mechanisms of intersegmental coordination for a flexible locomotor behavior. *J Neurosci* 30: 2373–2383.
- Quiñ Quiroga R, Panzeri S (2009) Extracting information from neuronal populations: information theory and decoding approaches. *Nat Rev Neurosci* 10: 173–185.
- Reich DS, Mechler F, Victor JD (2001) Temporal coding of contrast in primary visual cortex: when, what, and why? *J Neurophysiol* 85: 1039–1050.
- Saal HP, Bensmaia SJ (2014) Touch is a team effort: interplay of submodalities in cutaneous sensibility. *Trends Neurosci* 37: 689–697.
- Sakurai Y (1996) Population coding by cell assemblies – what it really is in the brain. *Neurosci Res* 26: 1–16.
- Shadlen MN, Newsome WT (1998) The variable discharge of cortical neurons: Implications for connectivity, computation, and information coding. *J Neurosci* 18: 3870–3896.
- Shaw BK, Kristan WB (1995) The whole–body shortening reflex of the medicinal leech: motor pattern, sensory basis, and interneuronal pathways. *J Comp Physiol A* 177: 667–681.
- Shaw BK, Kristan WB (1997) The neuronal basis of the behavioral choice between swimming and shortening in the leech: Control is not selectively exercised at higher circuit levels. *J Neurosci* 17: 786–795.
- Shu Y, Hasenstaub A, Duque A, Yu Y, McCormick DA (2006) Modulation of intracortical synaptic potentials by presynaptic somatic membrane potential. *Nature* 441: 761–765.
- Stuart AE (1970) Physiological and morphological properties of motoneurons in the central nervous system of the leech. *J Physiol* 209: 627–646.

- Theunissen F, Miller JP (1995) Temporal encoding in nervous systems: A rigorous definition. *J Comput Neurosci* 2: 149–162.
- Thompson WJ, Stent GS (1976) Neuronal control of heartbeat in the medicinal leech. II. Intersegmental coordination of heart motor neuron activity by heart interneurons. *J Comp Physiol* 111: 281–307.
- Thomson EE, Kristan WB (2006) Encoding and decoding touch location in the leech CNS. *J Neurosci* 26: 8009–8016.
- Vallbo A, Johansson R (1984) Properties of cutaneous mechanoreceptors in the human hand related to touch sensation. *Hum Neurobiol* 3: 3–14.
- Weber AI, Saal HP, Lieber JD, Cheng JW, Manfredi LR, Dammann JF III, Bensmaia SJ (2013) Spatial and temporal codes mediate the tactile perception of natural textures. *Proc Natl Acad Sci USA* 110: 17107–17112.
- Weeks JC (1982a) Synaptic basis of swim initiation in the leech. I. Connections of a swim-initiating neuron cell 204 with motor neurons and pattern generating “oscillator” neurons. *J Comp Physiol A* 148: 253–263.
- Weeks JC (1982b) Synaptic basis of swim initiation in the leech. II. A pattern generating neuron cell 208 which mediates motor effects of swim-initiating neurons. *J Comp Physiol* 148: 265–279.
- Weeks JC (1982c) Segmental specialization of a leech swim-initiating interneuron, cell 205. *J Neurosci* 2: 972–985.
- Wheat H, Goodwin A, Browning A (1995) Tactile resolution: peripheral neural mechanisms underlying the human capacity to determine positions of objects contacting the fingerpad. *J Neurosci* 15: 5582–5595.
- Wilson RJ, Kleinhaus AL (2000) Segmental control of midbody peristalsis during the consummatory phase of feeding in the medicinal leech, *Hirudo medicinalis*. *Behav Neurosci* 114: 635–646.
- Wohrer A, Humphries MD, Machens CK (2013) Population-wide distributions of neural activity during perceptual decision-making. *Prog Neurobiol* 103: 156–193.
- Yau KW (1976) Receptive fields, geometry and conduction block of sensory neurones in the central nervous system of the leech. *J Physiol* 263: 513–538.
- Zeveke AV, Efes ED, Polevaya SA (2013) An integrative framework of the skin receptors

- activation: Mechanoreceptors activity patterns versus “labeled lines”. *J Intgr Neurosci* 12: 47–56.
- Zhang X, Wilson RJ, Li Y, Kleinhaus AL (2000) Chemical and thermal stimuli have short-lived effects on the Retzius cell in the medicinal leech. *J Neurobiol* 43: 304–311.
- Zimmermann A, Bai L, Ginty DD (2014) The gentle touch receptors of mammalian skin. *Science* 346: 950–954.
- Zipser B (1979) Identifiable neurons controlling penile eversion in the leech. *J Neurophysiol* 42: 455–464.
- Zoccolan D, Torre V (2002a) Using optical flow to characterize sensory-motor interactions in a segment of the medicinal leech. *J Neurosci* 22: 2283–2298.
- Zoccolan D, Torre V (2002b) Highly variable spike trains underlie reproducible sensorimotor responses in the medicinal leech. *J Neurosci* 22: 10790–10800.

Contributions of collaborators

Study 3: Processing of touch stimuli in the local bend network

The cell staining of interneurons and mechanosensory neurons (Fig. 17A and B) were done by Dr. Gerrit Hilgen (2012-2013 member of the Computational Neuroscience group, University of Oldenburg, Germany; presently: Institute of Neuroscience, Newcastle University, England, United Kingdom).

Curriculum Vitae

Personal information

Name: Friederice Pirschel
Birth Date: August 2nd, 1984
Birth Place: Wilhelmshaven, Germany
Gender: Female
Marital Status: Single
Nationality: German
Mail: friederice.pirschel@uni-oldenburg.de

Education

1990 – 1994 Primary school Osterstraße, Varel
1994 – 2002 Jade-Gymnasium, Jaderberg, University entrance qualification
Oct 2003 – May 2010 Studies of Biology at the University of Oldenburg

May 2010 Diploma thesis: “Encoding of tactile stimuli in sensory neurons of the leech *Hirudo medicinalis*”, supervised by Prof. Dr. Jutta Kretzberg (Computational Neuroscience) and Dr. Karin Dedek (Neurobiology)

2nd July 2010 Awarded for an outstanding Diploma thesis from the Faculty of Mathematics and Sciences, University of Oldenburg

June 2010 – present PhD-student of Prof. Dr. Jutta Kretzberg, Computational Neuroscience, University of Oldenburg
Fellowship: PhD-Program “Neurosenses”, 2011 – 2014

Erklärung

Hiermit erkläre ich, dass ich die vorliegende Dissertation selbstständig angefertigt, nur die angegebenen Hilfsmittel und Quellen verwendet und sie in dieser oder ähnlicher Form noch nicht anderweitig eingereicht habe.

Oldenburg, den

Friederice Pirschel